

Aus der

Klinik und Poliklinik für Herzchirurgie am Universitätsklinikum Rostock
Direktor: Prof. Dr. med. habil. Gustav Steinhoff

Entwicklung und Evaluation von biotechnologischen Techniken für myokardiale Angiogenese und funktionale Genesung

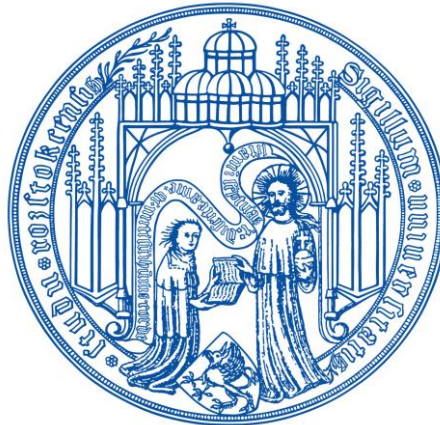
Dissertation

zur Erlangung des akademischen Grades

Doctor rerum naturalium (Dr. rer. nat.)

der Mathematisch-Naturwissenschaftlichen Fakultät

der Universität Rostock



Vorgelegt von

Yue Zhang

geboren am 28.07.1982 in Tianjin, V. R. China

Rostock, October 2012

From the
Clinic and Policlinic for Cardiac Surgery at the University of Rostock
Director: Prof. Dr. med. habil. Gustav Steinhoff

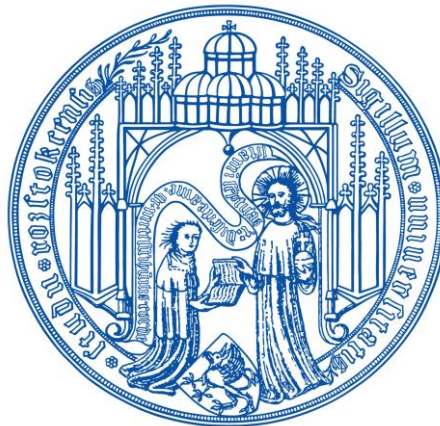
**Development and evaluation of biotechnological
techniques for myocardial angiogenesis
and functional recovery**

Dissertation

to obtain the academic degree

Doctor rerum naturalium (Dr. rer. nat.)

at the Faculty of Mathematics, Physics and Natural Sciences,
University of Rostock



Submitted by

Yue Zhang

born on July 28, 1982 in Tianjin, P. R. China

Rostock, October 2012

Dekan: Prof. Dr. Martin Köckerling

1. Gutachter:

Prof. Dr. med. Gustav Steinhoff

Universitätsklinikum Rostock, Klinik und Poliklinik für Herzchirurgie.

Schillingallee 35, 18057 Rostock, Deutschland

2. Gutachter:

Prof. Dr. rer. nat. Jan Gimsa

Mathematisch-Naturwissenschaftliche Fakultät, Institut für Biowissenschaften

Gertrudenstr. 11A, 18057 Rostock, Deutschland

3. Gutachter:

Prof. Dr. rer. nat. Hubert Bahl

Mathematisch-Naturwissenschaftliche Fakultät, Institut für Biowissenschaften

Albert-Einstein-Str. 3, 18051 Rostock, Deutschland

Date of submission: April 8th, 2013

Date of defense: April 4th, 2014.

Table of contents

Abbreviations	v
Summary.....	xii
1 Introduction.....	1
1.1 Ischemic heart disease	1
1.1.1 Myocardial infarction.....	1
1.1.2 The inflammatory response after MI	4
1.1.3 The pathophysiology and mechanisms of left ventricular remodelling after MI.....	13
1.2 Approaches in the regenerative medicine.....	16
1.2.1 Angiogenic gene therapy and methods of gene delivery	16
1.2.2 Tissue engineering combined stem cells for cardiac regeneration	22
1.2.3 Goal of the thesis.....	24
2 Material & methods.....	25
2.1 HUVECs isolation and culture	25
2.2 MSCs isolation and culture.....	26
2.3 Viral vector amplification and purification	27
2.4 MNBs/Ad complexes formation.....	27
2.5 HUVECs network formation to evaluate VEGF function.....	28
2.6 <i>In vitro</i> transduction.....	28
2.7 MTT cytotoxicity	29
2.8 Characterization of MNBs/Ad complexes.....	30
2.9 Magnetic field guided <i>in vitro</i> transduction	30
2.10 Experimental design of MNBs/hVEGF for cardiac regeneration ..	31
2.11 FACS analysis for inflammatory response	33
2.12 Quantitative Real-Time PCR and immunohistochemical staining analysis for Ad distribution.....	34
2.13 Immunohistochemical staining analysis of hVEGF expression in the heart.....	35
2.14 Immunohistochemical analysis for GFP distribution and expression <i>in vivo</i>	36
2.15 Prussian blue staining for MNBs distribution <i>in vivo</i>	37
2.16 Left Ventricular Catheterization for heart function evaluation	37
2.17 Determination of functional perfusion and capillary density	38
2.18 Immunohistochemical staining of CD31 for determination of capillary density	39
2.19 Infarct size and wall thickness analysis	39
2.20 Fibrosis analysis.....	40

2.21 Determination of arteriole density	40
2.22 Experimental design of matrigel for cardiac repair	41
2.23 MI and local matrigel administration	43
2.24 Immunohistochemical staining for c-kit+ cells	43
2.25 Immunohistochemical staining for CD34+ cells	43
2.26 Statistical analyses	44
3 Results	45
3.1 HUVECs vascular network formation.....	45
3.2 HUVECs transduction efficiency and cytotoxicity of MNBs/Ad complexes <i>in vitro</i>	47
3.3 MNBs/Ad complexes characterization	46
3.4 Magnetic field guidance <i>in vitro</i>	49
3.5 Distribution and expression of hVEGF <i>in vivo</i>	52
3.6 Prussian blue staining of MNBs in infarcted rat heart	53
3.7 Expression of GFP in infarcted rat heart	54
3.8 Localization of hVEGF expression in infarcted rat heart.....	54
3.9 Inflammatory response analysis after injection of MNBs/Ad _{hVEGF} complexes	57
3.10 MNBs/AdhVEGF complexes injection improved cardiac function	58
3.11 MNBs/AdhVEGF complexes injection increased infarct wall thickness and reduced fibrosis	62
3.12 MNBs/AdhVEGF complexes injection enhanced capillary density	64
3.13 MNBs/AdhVEGF complexes injection increased arteriole density	67
3.14 AdhVEGF expression in the host connective tissue.....	68
3.15 Matrigel injection improved cardiac function	73
3.16 Matrigel injection increased infarct wall thickness	69
3.17 Matrigel injection enhanced capillary density	71
3.18 Matrigel injection increased CD34+ and c-kit+ cell recruitment...	72
4 Discussion.....	75
4.1 MNBs/AdhVEGF complexes for cardiac repair	75
4.2 Matrigel for cardiac repair	84
4.3 Biotechnological techniques for myocardial angiogenesis and functional recovery	87
5 Conclusions	89
References.....	91
Declaration.....	xi

Abbreviations

Adeno-associated viral vectors	AAV
Adenoviral vectors	Ad
Ad encoded GFP gene	Ad _{GFP}
Ad encoded human VEGF gene	Ad _{hVEGF}
Ad encoded LacZ gene	Ad _{LacZ}
Ad encoded luciferase gene	Ad _{luc}
Angiotensin II	Ang II
Basic fibroblast growth factor	bFGF
Cardiac output	CO
Coronary artery disease	CAD
Coronary artery bypass graft	CABG
Deoxyribonucleic acid	DNA
Dulbecco's modified eagle medium	DMEM
Ejection fraction	EF
End diastolic volume	EDV
End systolic volume	ESV
Extracellular matrix	ECM
Fluorescence-activated cell sorting	FACS
Green fluoresce protein	GFP
Heart rate	HR
High power field	HPF
Human umbilical vein endothelial cells	HUVECs
Insulin-like growth factor	IGF
Intercellular adhesion molecule-1	ICAM-1
Lentiviral vectors	LVs
Left anterior descending coronary artery	LAD
Left ventricle	LV
Magnetic nanobeads	MNBs
Magnetic nanoparticles	MNPs
Matrix metalloproteinase	MMP

Maximum pressure	P max
Mitogen-activated protein kinase	MAPK
Mesenchymal stem cells	MSCs
Myocardial infarction	MI
[3-(4,5-dimethylthiazol-2-yl)-2,5-diphenyl tetrazolium bromide]	MTT
Nuclear factor kappa-light-chain-enhancer of activated B cells	NF-κB
Peak rate of maximum pressure decline	-dp/dt max
Peak rate of maximum pressure rise	dp/dt max
Percutaneous coronary intervention	PCI
Phosphatidylinositol 3-kinase	PI3K
Phosphate-buffered solution	PBS
Phosphoinositide phospholipase C- γ	PLC- γ
Plague-forming unit	PFU
Polymerase chain reaction	PCR
Pressure-volume	PV
Protein kinase B	PKB
Platelet derived growth factor	PDGF
Reactive oxygen species	ROS
Renin-angiotensin-aldosterone system	RAAS
Ribonucleic acid	RNA
Roswell park memorial institute medium	RPMI
Revolution(s) per minute (rpm)	RPM
Src homology region 2 domain-containing phosphatase	SHP
Standard deviation	SD
Standard error of the mean	SEM
Stem cell factor	SCF
Stroke volume	SV
Systemic vascular resistance	SVR

α -Smooth muscle actin	α -SMA
Tissue inhibitor of metalloproteinases	TIMP
Transforming growth factor- β	TGF- β
Tumour necrosis factor- α	TNF α
TNF receptor	TNFR
Vascular endothelial growth factor	VEGF
VEGF receptor	VEGFR

Abbreviations for experimental settings

MI-Magnet⁺MNBs/Ad: in a rat MI model, a cylindrical magnet was placed in the chest of the rat closely adjacent to the infarcted area of the heart and MNBs/Ad complexes were injected intravenously.

MI-Magnet⁻MNBs/Ad: in a rat MI model, a similar size ceramic bar was placed in the chest of the rat closely adjacent to the infarcted area of the heart and MNBs/Ad complexes were injected intravenously.

MI-MNBs: in a rat MI model, a cylindrical magnet was placed in the chest of the rat closely adjacent to the infarcted area of the heart and MNBs were injected intravenously.

MI-PBS: in a rat MI model, PBS was injected at five injection sites into anterior and lateral regions of the border zone between viable myocardium.

MI-M: in a rat MI model, matrigel was injected at five injection sites into anterior and lateral aspects of the border zone between viable and infarcted myocardium.

Physiological Saline: in a rat MI model, 0.9% NaCl was injected intravenously.

Sham: in a rat MI surgical procedure without LAD ligation.

Structure of the thesis

The present work is organized as follows. As my thesis consists of 2 parts of work with distinct foci, I chose to describe the use of MNBs/AdhVEGF complexes for cardiac regeneration first, whereas my work on the application of matrigel for cardiac regeneration forms the content of a second part. The introduction gives an overview on the pathology of ischemic heart disease as well as the approaches of regenerative medicine, thus providing the link between both parts of my work. In material & methods, 2.1-2.21, and 2.26, describe experiments of the first part (MNBs/AdhVEGF complexes for cardiac regeneration), while in 2.16, 2.18, 2.19, and 2.22-2.26, the second part (matrigel for cardiac regeneration) is described. Results of the first part are included in chapter 3.1-3.14, and results from the second part are described in chapter 3.15-3.18. The discussion of MNBs/AdhVEGF complexes for cardiac regeneration can be found in chapter 4.1, and chapter 4.2 contains the discussion of matrigel for cardiac regeneration. Finally, conclusions are drawn from the entire body of work and, again, an overview is given on the whole subject of my work.

Zusammenfassung

Der Herzinfarkt stellt eine irreversible Schädigung des Herzmuskels dar. Große Infarkte bewirken komplexe Umbauprozesse im Gewebe der Ventrikel. Diese Veränderungen können die ventrikuläre Funktion beeinträchtigen und werden als ventrikuläres Remodelling bezeichnet. Das Remodelling führt schließlich zur progressiven Dilatation des linken Ventrikels und zum Herzversagen. Daher stellen die Begrenzung und Regeneration der myokardialen Schädigung eine große Herausforderung in der klinischen Forschung dar. Ansätze, die auf Gentherapie und Tissue Engineering basieren, spielen für die regenerative Therapie nach Myokardinfarkt eine wichtige Rolle.

Die Gentherapie des Myokardinfarkts wird in Grundlagenforschung sowie präklinischen Forschungsprojekten bereits häufig genutzt. Insbesondere der vaskuläre endotheliale Wachstumsfaktor (vascular endothelial growth factor, VEGF) spielt eine wichtige Rolle bei der Regeneration des Herzens nach Myokardinfarkt. Diesbezüglich könnte die intravenöse Applikation therapeutischen Genmaterials eine für die Klinik besser geeignete Option darstellen als die gängige intramyokardiale Applikation. Erstere Methode weist jedoch Limitationen auf - es lassen sich beispielsweise nur geringe Konzentrationen des Genmaterials im Herzgewebe erreichen. Daher kam in der vorliegenden Arbeit eine neue Technik zum Einsatz, nämlich der magnetfeldverstärkte Gentransfer in das kardiovaskuläre System, der ein hohes Potential für rasche und effiziente Gentransduktion zeigte. Die Kopplung magnetischer Nanopartikel (magnetic nanobeads, MNBs) an adenovirale Vektoren, die für humanes VEGF kodieren (Ad_{hVEGF}), erhöhte die Genexpression nach systemischer Gabe und gleichzeitigem Targeting auf das infarzierte Myokard durch einen extern aufgesetzten Magneten deutlich. Dies führte zu Neovaskularisierung und verbesserter Erholung der Funktion des linken Ventrikels nach dem Infarkt.

Die intravenöse Applikation von Genmaterial mit Hilfe von Magnetnanopartikeln könnte somit eine wichtige, nicht-invasive Strategie für die Gentherapie zur Heilung der

ischämischen Herzerkrankung darstellen und zukünftig in der klinischen Anwendung eine bedeutende Rolle spielen.

Die extrazelluläre Matrix (ECM) spielt eine wesentliche Rolle bei der Regulation zellulärer Prozesse wie etwa der Proliferation und Differenzierung von Stammzellen. Matrigel, eine künstliche ECM, die neben einer Anzahl extrazellulärer Matrixkomponenten auch Wachstumsfaktoren enthält, zeigte eine vielversprechende Wirkung bei der Behandlung des Herzinfarktes. Die vorliegende Arbeit belegt, dass Matrigel die Angiogenese im Myokard nach ischämischer Schädigung anregt und das Remodelling des Myokards vermindert.

Intrakardiale Injektion von Matrigel milderte den Verlust an Wandstärke und verstärkte die Neovaskularisierung in der Infarktzone, zudem vermittelte sie eine Rekrutierung von c-kit⁺ und CD34⁺ Stammzellen in das ischämische Herzgewebe und verbesserte so schließlich die linksventrikuläre Funktion.

Summary

Myocardial infarction (MI) is an irreversible injury of the heart muscle leading to complex changes in ventricular construction. These changes can affect ventricular function in a process called ventricular remodelling. Ultimately, ventricular remodelling causes the progressive dilatation of the **left ventricle (LV)** resulting in heart failure. Hence, the reduction and repair of myocardial damage are great challenges in clinical research. Therapeutic gene based approaches and tissue engineering play important roles in regenerative therapy after MI.

Gene therapy for treatment of MI has been widely used in basic and preclinical research. Especially **vascular endothelial growth factor (VEGF)** plays an important role in cardiac regeneration after MI. Intravenous delivery of therapeutic genes as a non-invasive way of administration has been considered for clinical therapy. However, this method has drawbacks such as low gene concentration at the target area. In the present study, a novel technique of magnetic force-enhanced gene delivery to the cardiovascular system showed great potential for rapid and efficient transduction. In a rat MI model, systemic delivery of **magnetic nanobeads (MNBs)/adenoviral vectors (Ad) encoding human VEGF (Ad_{hVEGF})** complexes under external magnetic guidance could increase VEGF expression in the infarcted myocardium, leading to neovascularization and improving post-infarction recovery of LV function. Intravenous MNB based delivery of therapeutic genes may be a useful, non-invasive gene therapy strategy for ischemic heart disease healing in patients bearing great potential for clinical application.

The **extracellular matrix (ECM)** plays a dominant role in regulating cellular processes, such as proliferation and differentiation of stem cells. Matrigel as an engineered ECM contains a considerable amount of ECM components as well as growth factors and showed great promise in the treatment of MI. My research proves that matrigel promotes angiogenesis in the myocardium after ischemic injury and prevents remodelling of the myocardium. Intracardiac matrigel injection attenuated the decrease of infarct wall thickness, promoted neovascularization in the infarct area, mediating c-kit⁺ and CD34⁺

stem cell recruitment to the ischemic myocardium, and finally improved left ventricular function.

1 Introduction

1.1 Ischemic heart disease

1.1.1 Myocardial infarction

The clinical and diagnostic establishment the term MI took place about 100 years ago and was published almost simultaneously by two Russian scientists, Obratsov and Strazhesko in a German journal (1910) ¹. MI is the irreversible injury and subsequent necrosis along a transmural wavefront from subendocardium to subepicardium due to severe and accentuated reduction in coronary perfusion. This specific pattern of cardiomyocyte death was named the wave-front phenomenon ². Transmural MI of the anterior wall leads to complex changes in ventricular construction including both necrotic and non-necrotic areas. These changes can affect ventricular function by the so-called ventricular remodelling. Ventricular remodelling and dilatation caused by MI occur in a continuum that starts with ventricular expansion of the necrotic area alone. Dilatation then continues at the expense of the contractile segment by volume overload hypertrophy in response to increased wall tension. In the chronic phase, this remodelling progress of the infarction area will persist for a prolonged time period. Whereas there is no further expansion during the scar-forming process, the contractile segment elongates because of the hypertrophy. Finally, ventricular remodelling causes the progressive dilatation of the LV and heart failure. Ventricular aneurysm is another complication which may arise from the progression of infarction. An aneurysm can accentuate LV dysfunction, as it is “a systolic or diastolic deformation of the ventricular wall, including the akinetic-dyskinetic necrotic area.” ³ The aneurysm aggravates the systolic dysfunction and in some cases worsens the secondary mitral failure.

MI causes the ischemic zone to change from a state of active systolic shortening to one of passive diastolic lengthening in only 60 seconds ⁴. If coronary occlusion is removed less than 20 minutes after onset, tissue viability is preserved and the resulting cellular damage and depression of cell function are transient. Furthermore, reperfusion of the infarcted area allows for the salvage of variable amounts of myocardium ⁵. After 40 minutes of ischemia followed

by reperfusion, 60%-70% of the ultimate infarct is salvageable. However, after 3 hours of occlusion, this phenomenon decreases significantly to 10%.

Acute coronary occlusion can cause three states of impaired myocardium: infarcted, hibernating, and stunned (**Figure 1**). MI can cause irreversible myocardial cell death resulting from prolonged ischemia. Hibernating myocardium shows persistent LV dysfunction due to a reduced coronary blood flow, but myocardial viability can be preserved. Because of the lowered metabolism and hypoperfusion, hibernating myocardium has compromised contractility. This down-regulation of LV function at rest is a protective mechanism resulting from decreased oxygen consumption in the heart to secure myocyte survival. It has been proven that the hibernating myocardium may recover to normal if a normal myocardial oxygen supply-demand relationship is re-established^{6, 7}. Stunned myocardium is a syndrome of contractile dysfunction, but myocardial cells retain viability following revascularization after an ischemic episode. The most likely mechanism of myocardial stunning includes the generation of free oxygen radicals, calcium overload, structure changes of contractile protein⁸, extracellular collagen matrix damage and reduced sensitivity of myofilaments to calcium⁹⁻¹¹. In summary, infarcted myocardium may develop if the ischemia is severe and prolonged; if a chronic LV dysfunction leads to a reduced blood supply but myocytes, still receive enough oxygen to remain viable, then the myocardium is described as hibernating myocardium. The stunned myocardium consists of viable cells that are acutely dysfunctional after reperfusion⁴.

Myocardial reperfusion is the restoration of coronary blood flow, either spontaneously or therapeutically induced, after a period of coronary occlusion⁵. Restoration of blood flow to the ischemic myocardium offers the best chance for salvage following MI. Thrombolytic, percutaneous transluminal coronary artery bypass surgery, and coronary angioplasty have reduced the morbidity and mortality associated with MI significantly. Although reperfusion has the potential to salvage ischemic myocardium, a wide range of side effects may result from reperfusion including not only reversible, functional changes, but also irreversible injury.

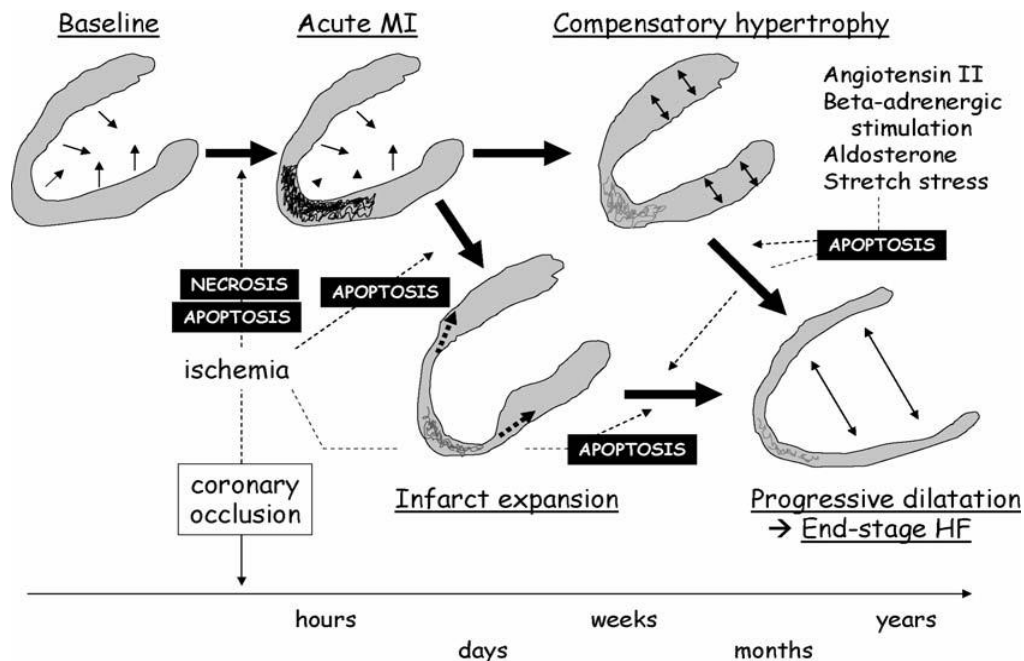


Figure 1: Cardiac remodelling following MI: Hyperkinesia and hypertrophy of the non-infarcted myocardium are early and late compensatory mechanisms in MI, respectively. The infarct region (exemplified as a dark staining of the myocardium) is characterized by reduced contractility (arrowheads vs. full arrows), and then wall thinning. The compensatory hyperkinesia (full arrows) in the non-infarcted myocardium stimulates hypertrophy (exemplified by thickening of the wall and double-headed arrows in the myocardial wall). Thick arrows highlight the potential evolution of the remodelling process over time. In the early and late phase after MI, the major inducers of apoptosis are listed. Neurohormones (angiotensin II, norepinephrine, and others) and stretch stress are major inducers of apoptosis not in the peri-infarct region but in the remote unaffected areas ¹².

At the pathophysiological level, myocardial reperfusion induces an intense inflammatory condition with activation of multiple cell types, including leucocytes and endothelial cells, and reduced nitric oxide bio-availability, leading to leucocyte adherence and transmigration of mononuclear cells ⁵. At the cellular level at least three major pathways may contribute to lethal reperfusion injury. Firstly, myocardial reperfusion results in massive intracellular calcium overload via Na^+/H^+ and $\text{Na}^+/\text{Ca}^{2+}$ exchange, which leads to mitochondrial calcification and contraction band necrosis. Secondly, when reperfusion provides exposure of the injured cardiomyocytes to a large amount of extracellular fluid, the ischemia may cause intracellular accumulation of osmotically active catabolites that may induce massive cellular sarcolemmal rupture and necrosis. Thirdly, when oxygen is reintroduced into the ischemia region, more cells will experience accelerated death due to oxygen free radical generation.

Cellular swelling and contracture lead to a “no-reflow phenomenon” that limits the recovery of some myocytes and possibly add to irreversible injury of other myocytes^{3,4}.

In general, although restoration of blood flow to ischemic regions is essential, the accompanying reperfusion injury can initially worsen, rather than improve myocardial dysfunction. The three basic types of reperfusion injury are: stunned myocardium, reperfusion arrhythmias, and vascular injury⁴.

1.1.2 The inflammatory response after MI

The systemic inflammatory response consists of a humoral as well as a cell-mediated reaction. After MI, apoptosis of cardiomyocytes can initiate an inflammatory response to clear the matrix debris and necrotic cells. Finally, this phenomenon may result in the replacement of infarct tissue with scar tissue¹³. Dead cells release their contents and cause an intense inflammatory reaction by activating the innate immune cascade and stimulating the complement system. On the other hand, the release of cell contents play a critical role in triggering the post-infarction inflammatory response by initiating the **nuclear factor kappa-light-chain-enhancer of activated B cells (NF-κB)** system. This mechanism results in an increased infiltration of leukocytes into the infarcted myocardium: The infiltrated leukocytes clear necrotic cells and the matrix debris and regulate metabolism by inducing growth factors and cytokines. The complement system can stimulate secretion of the inhibitory mediators such as **transforming growth factor- β (TGF-β)** to suppress inflammatory cytokine and chemokine synthesis and to remove apoptotic inflammatory leukocytes from the infarcted area. Furthermore, activation of TGF-β signalling promotes ECM deposition and fibroblast to myofibroblast transdifferentiation¹⁴. Finally, neovessels acquire a muscular coat¹⁵. A mature scar is formed including cross-linked collagen and a small cellular fraction¹⁶⁻¹⁸.

1.1.2.1 Humoral inflammatory response to MI

Impact of the complement system in MI: The complement cascade is one essential part of the immune system and a major effector in a variety of immunopathological diseases. Over

30 proteins form this complex protein system, which may trigger a variety of biological activities essential for a correct immunological response.

Three biochemical pathways activate the complement system: the classical complement pathway, the alternative complement pathway, and the mannose-binding lectin pathway^{18, 19} (**Figure2**). Research has proven that MI may initiate the complement cascade²⁰. Hill and his colleagues were the first researchers who have shown that leukotactic activity in the ischemic rat heart can be explained by the C3 cleavage product²¹. Further studies^{20, 22} have suggested that during MI, mitochondria, extruded through breaks in the sarcolemma, unfold and release membrane fragments which are rich of cardiolipin and protein. The subcellular fragments provide the components to disseminate the complement-mediated inflammatory response to ischemic injury by binding C1 and supplying sites for the assembly of later acting complement components. Messenger **ribonucleic acid (RNA)** and proteins for all the components of the classical complement pathway are up-regulated in MI²³. However, a strong local inflammatory response has some side effects and the complement activation may play an important role in vascular permeability, leukocytes and mononuclear-cell chemotaxis, and several phagocytic processes^{24, 25}.

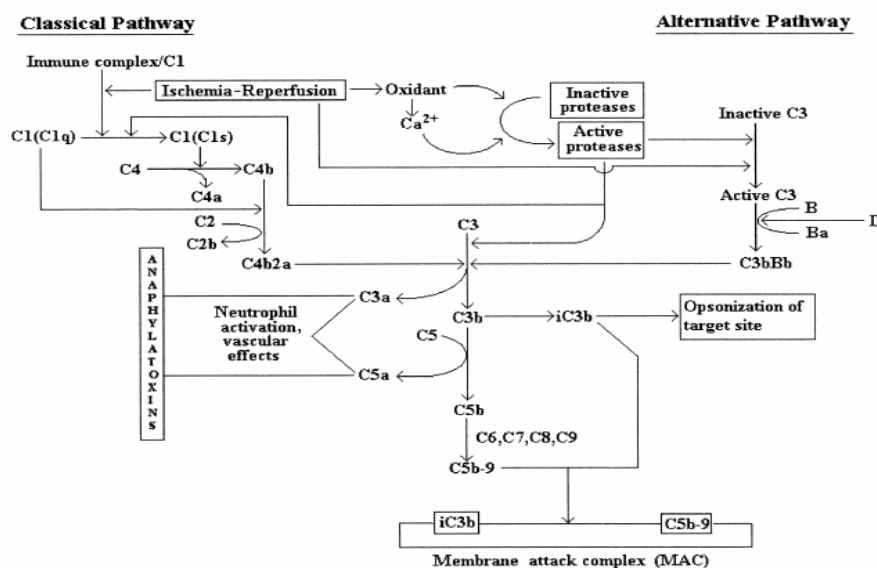


Figure 2: Proposed scheme of the classical and alternative pathways of complement activation under oxidation stress caused by ischemia in the myocardium. Activation via the classical pathway occurs primarily as a result of immune complex formation. Immune complex interaction with the C1 molecule confers enzymatic activity to the C1s subunit of

C1. The C1 molecule cleaves C4, releasing C4a, and forms C4b, which binds to the surface of the target cell. C2, in association with C4b, is also cleaved by C1q, releasing C2b and leaving the bound C4b2a complex that possesses proteolytic activity for C3 convertase ²⁶.

Generation of reactive oxygen species (ROS) and the post-inflammatory response: ROS are chemically reactive molecules containing oxygen in the form of oxygen ions and peroxides. ROS are highly reactive because of the unpaired valence shell electrons. ROS are a byproduct of the normal metabolism of oxygen and play an important role in cell signalling and homeostasis ²⁷. They also have harmful effects on the cells such as damage of **deoxyribonucleic acid (DNA)**, oxidation reactions of polyunsaturated fatty acids (lipid peroxidation), oxidation reactions of amino acids in proteins and oxidative inactivation specific enzymes by oxidation of co-factors. Under normal circumstances, cells possess a substantial ability to counterbalance the generation of ROS with enzymes. Examples include catalases, peroxisomes and lactoperoxidases. However, during stress condition such as MI, the ROS level may increase significantly. A series of scientific studies have shown that after MI/reperfusion, ROS may trigger leukotactic stimuli including complement activation ^{28, 29}, induction of P-selectin ³⁰, chemokines and cytokines upregulation through NF- κ B activation ^{31, 32} and an increase of endothelial **intercellular adhesion molecule (ICAM)-1** to bind to neutrophils ³³. Meanwhile, it has been proven that ROS exert an inhibitory effect on myocardial function *in vivo* and play an important role in the pathogenesis of myocardial stunning ^{24, 34-36}.

Cytokines in MI: Cytokines are small cell signalling proteins that can be secreted by ischemic myocardium, liver and numerous cells of the immune system. A large number of studies ³⁷⁻³⁹ have proven that MI is associated with the coordinated activation of many cytokines such as **tumor necrosis factor-alpha (TNF- α)** ⁴⁰, interleukin-1 ³⁷ and interleukin-6 ⁴¹. Complement cascade, NF- κ B activation and ROS generation potently stimulate cytokine secretion in a series of cells including resident and blood derived cells. Especially NF- κ B activation plays a vital role in the induction of pro-inflammatory mediators in MI/reperfusion. The genes regulated by NF- κ B are diverse and include inflammatory, cell adhesion and growth factors. Under normal condition, there are very few cytokines expressed in the heart ²⁵. However, they may increase up to 50 fold in the ischemic and border zone during the MI.

Usually, in the case of severe MI, cytokines may persist for a very long time and at high level in the normal adjacent myocardium. This phenomenon can cause an unfavorable contractile dysfunction²⁵.

TNF- α : TNF- α is a cytokine involved in systemic inflammation and belongs to the group of cytokines that stimulate the acute phase response as in case of MI. Several studies found that TNF- α enhances cardiomyocyte apoptosis⁴² and suppresses cardiac contractility^{40, 43}. Furthermore, Siwik and his colleagues⁴⁴ have proven that by stimulating TNF- α , leukocytes and endothelial cells can express pro-inflammatory cytokines, adhesion molecules and chemokines. And TNF- α regulates ECM metabolism by reducing collagen synthesis and by enhancing **matrix metalloproteinase (MMP)** activity in cardiac fibroblasts. However, some groups showed that TNF- α signalling has positive effects in the infarcted myocardium⁴⁵. Normally, TNF- α may exert distinct biological effects through the **TNF receptor (TNFR) 1** and TNFR2. Recently, investigations showed that TNFR1 medication are deleterious, inducing contractile dysfunction, but TNFR2 mediated action may be protective by attenuating adverse remodelling⁴⁶. Obviously, TNF- α plays a much more complex role in MI and may explain the unpredictable effects of cytokine-targeted therapeutic strategies in clinical trials²⁴.

The interleukin family of cytokines: Interleukins, a group of cytokines, are synthesized by CD4+ T lymphocytes, as well as by macrophages, monocytes and endothelial cells that participate in the regulation of immune responses and inflammation reactions⁴⁷. In the early phase of MI, interleukins such as interleukin-1 and interleukin-6 may activate a series of inflammatory proteins such as cytokines, chemokines⁴⁸, adhesion molecules⁴⁹ and colony-stimulating factors¹⁷. Through expression of chemokines and adhesion molecules, interleukins can infiltrate the infarcted myocardium in a targeted manner. Also, the interleukin signalling cascade regulates ECM metabolism and alters the **MMP/tissue inhibitor of metalloproteinases (TIMP)** balance during MI¹⁷. Some research showed that cardiac transduction with interleukin-1Ra, an inhibitor specific for interleukin-1, significantly decreased infarct size and reduced the inflammatory reaction in a rat MI/ reperfusion model

⁵⁰, proving a side-effect role for interleukin-1 in the injured heart tissue. In contrast, another group demonstrated that interleukin-1 neutralization resulted in a significant increase of ischemic heart tissue remodelling and enhanced contractile dysfunction ⁵¹. Also, Wollert and Drexler showed that the interleukin-6 family has an attenuating effect on cardiomyocytes by promoting cardiac hypertrophy. Furthermore the interleukin-6 family may protect cardiomyocytes from apoptosis oppositely ⁵². The complete characteristic features of cytokines, such as overlapping or even contradictory functions, are still hampering us to understand their effects in MI injury and repair ²⁴.

1.1.1.2 The cellular inflammatory response to MI

The neutrophil: Neutrophils are the most abundant type of white blood cells of mammals and play an important role in immune reactions. Neutrophils are recruited at the early stage after ischemia. Significant migration and infiltration of neutrophils may occur after MI/reperfusion. Endothelial adhesion molecules are induced and the permeability of the microvasculature is enhanced after activating inflammation response. Subsequently, a series of chemokines and cytokines such as interleukin-8, C5a, and leukotriene B4 are secreted by injured cardiac tissue. Then a variety of subsets recruit neutrophils to infiltrate the myocardium. Transmigration of neutrophils into infarcted myocardium requires adhesive molecular interactions between neutrophils and endothelium. The selectin family of adhesion molecules mediates the initial capture of neutrophils from the rapidly flowing blood stream to the blood vessel. There are three selectin molecules involved in leukocyte entry into myocardium, namely E-selectin (CD62E), L-selectin (CD62L), and P-selectin (GMF140, CD62P) ²⁴.

Upon activation, the majority of circulating neutrophils express L-selectin which plays a role in regulating neutrophil recruitment and rolling velocity ⁵³. E-selectin is expressed by the cytokine-induced endothelial cells. In addition, P-selectin, stored in Weibel-Palade bodies of endothelial cells, can be transferred to the surface of endothelial cells rapidly mediated by inflammatory cytokines and chemokines. Experimental studies suggested that antibodies neutralizing L-selectin ⁵⁴ and P-selectin ⁵⁵ successfully reduced neutrophil accumulation,

attenuated cardiac myocyte necrosis and enhanced contractile function. In contrast, some experiments suggested ⁵⁶ that P-selectin deficiency may impair neutrophil trafficking. Current concepts suggest that selectin may support neutrophil margination under shear stress, but the effects of selectin-related interventions for myocardial infarction were inconsistent ^{24, 56}.

Obviously, rolling of neutrophils appears to be a prerequisite for stable adherence to the luminal endothelial cells under condition of flow, but selectin mediated adhesion of neutrophils necessitates another set of adhesion molecules, namely the integrins, to take part in and finally form a firm adhesion. Integrins are obligatory heterodimers containing two chains, named α (alpha) and β (beta) subunits. Neutrophil adhesion to the luminal endothelial cells and their transendothelial migration are dependent on β 12 (CD18) subunits which are transported to the surface of endothelial cells as a complex ⁵⁷. The β 12 (CD18) linked to one of four integrin α subunits indicated as CD11a (LFA-1), CD11b, or CD11c (p150, 95). CD11a/CD18 is constitutively expressed on the neutrophil membrane. The physiological counter ligand of the CD18 complex on the neutrophil is the **intercellular adhesion molecule-1 (ICAM-1)** which is expressed on the endothelial cell. ICAM-1 is upregulated by pro-inflammatory mediators such as ROS, interleukin-1, and TNF α ^{58, 59}. Constitutive moderate expression of ICAM-1 levels on endothelial cells may support CD18 mediated adhesion and subsequent transendothelial migration.

The neutrophil-mediated cardiomyocyte injury: Infiltrating neutrophils generate ROS and release enzymes contributing to the removal of dead cells and debris in the infarcted area. Furthermore, they can secrete chemokines including interleukin-8 and TNF α ⁶⁰ to amplify cell recruitment. Experiments have proven that neutrophils may mediate tissue damage directly by the release of proteolytic enzymes ⁶¹. Neutrophil accumulation on the injured area might lead to secretion of serine proteases and release of proteinases ⁶² which are highly positively charged, and their cationic nature may directly alter the membrane charge distribution ⁶³ of the injured tissue. Moreover, elastase may act by hydrolysing proteins of the ECM such as elastin and fibronectin ^{57, 62, 64}. It has been proven that neutrophils play a significant role in wound healing not only through clearing dead cells and debris from

ischemic tissue, but also by mediating a large number of cytokines and chemokines ⁵⁷. However, it has been found that neutrophils have no effects on granulation tissue formation, and neither do they contribute to the deposition of fibrous tissue during the healing of the infarcted heart ⁶⁵. The main contribution of neutrophils to the healing response is apoptosis and subsequent clearance by macrophages which then secrete TGF- β ²⁴.

Mononuclear cell infiltration: Mononuclear cells are one type of white blood cells and are part of the innate immune system of vertebrates. Mononuclear cells may infiltrate in infarcted myocardium rapidly after activation of inflammatory pathways. Research has proven that at an early phase after reperfusion C5a plays an important role in monocyte recruitment in the ischemic myocardium ⁶⁶. At the late phase (normally 3 hours after perfusion), monocyte chemotactic activity largely depends on monocyte chemoattractant protein-1 and TGF- β . Other mediators including ROS and other CC chemokines may also play distinct roles in regulating monocyte infiltration. These blood derived cells will differentiate and mature to macrophages after recruitment into the infarcted myocardium. Macrophage-colony stimulating factor and granulocyte macrophage-colony stimulating factor are crucial for providing the milieu necessary for monocyte differentiation ³⁹. Mature macrophages play multiple roles in the healing process of scar formation. Firstly, they can phagocytose and clean debris, dead neutrophils and cardiomyocytes. Secondly, they serve as a source of cytokines and growth factors regulating fibroblast growth and angiogenesis ⁶⁷. Last but not least, they are responsible for regulating ECM metabolism by producing MMPs and their inhibitors, TIMPs ^{24, 68}.

The mast cell: Mast cells are resident cells and may secrete abundant pro-inflammatory and pro-fibrotic mediators involved in wound healing. Furthermore, resident mast cells were detected in large numbers in the mammalian heart, mainly located in close proximity to vessels ⁶⁹. Frangogiannis *et al.* ⁷⁰ showed that in its early stages, mast cells may secrete histamine and TNF- α to regulate the inflammatory response. In the later stages, mast cells play a critical role in the orchestrated interaction of cytokines, growth factors and ECM proteins to mediate injured tissue repair. In addition, mast cells can provide a rich source of

cytokines and growth factors to support fibroblast proliferation⁶⁸. The factors responsible for mast cell accumulation in areas of fibrosis remain to be elucidated. **Stem cell factor (SCF)** is a potent mast cell chemoattractant that stimulates directional motility of both mucosal- and connective tissue type-mast cells⁶⁸. In addition, SCF may recruit and mediate the homing of bone marrow derived progenitor cells, and these cells have the ability to differentiate to cardiomyocytes and endothelial cells⁷¹⁻⁷⁴. Thus, SCF may be a useful cytokine for heart regeneration.

Mast cell degranulation leads to the secretion of a wide range of mediators. Mast cell derived histamine stimulates fibroblasts and collagen synthesis⁷⁵. Tryptase, the most abundant of the proteases found in mast cell granules, induces granulocytes⁷⁶, stimulates fibroblast differentiation⁷⁷ and chemotaxis and upregulates type I collagen synthesis⁷⁸. In addition, mast cells are a rich source of **basic fibroblast growth factor (bFGF)**, VEGF and TGF- β , which can regulate ECM metabolism, modulate endothelial cell proliferation and stimulate fibroblast differentiation²⁴.

The cardiac fibroblast and myofibroblast: Fibroblasts are widely distributed connective tissue cells that are found in all vertebrate organisms. These mesenchymal derived cells can secrete a variety of ECM components such as collagen and fibronectin. Cardiac fibroblasts play an important role in cardiac development and remodelling as well as defining cardiac structure and function⁷⁹. Under normal conditions, resident cardiac fibroblasts have no contractile microfilaments or stress fibers, and secrete only minimal amounts of ECM components⁸⁰. After MI, the inflammatory milieu stimulates fibroblasts to proliferate and differentiate into myofibroblasts. Myofibroblasts may cover the ischemic area, accelerate the synthesis of ECM, and replace necrotic cardiomyocytes forming a scar. Differentiated myofibroblasts may be identified through their expression of **α -smooth muscle actin (α -SMA)**⁸¹. However, myofibroblasts express comparatively low amounts of smooth muscle myosin heavy chain⁸². In contrast, during the proliferative phase, myofibroblasts produce interstitial collagen I and collagen III for ECM construction, and TGF β markedly increases ECM protein synthesis and enhances TIMP expression which promotes matrix preservation

²⁴. After reconstruction of the damage, infarcted myofibroblasts undergo apoptosis. However, mechanisms responsible for myofibroblast apoptosis remain obscure.

Vascular cell and pericyte: Angiogenesis is an important mechanism of blood vessel formation and it is an integral part of wound healing. Neovascularisation is essential for supplying necessary oxygen and nutrients to the highly dynamic and metabolically active cells of a healing wound ²⁴. In the local environment, ECM, endothelial cells, and pericytes are all responsible for sustaining the balance between angiogenic factors and angiostasis ^{52, 83-86}. After MI, angiogenic growth factors including VEGF, interleukin-8 and bFGF are rapidly induced in the injured heart tissue ⁸⁷⁻⁸⁹, and play a role in increasing infarct region neovascularisation. The mechanisms of infarct angiogenesis remain undetermined. Angiogenesis starts with vasodilatation, a process involving nitric oxide. In addition, hypoxia-inducible factor, one of the earliest effectors of the response to ischemia, can activate VEGF induction and release ⁹⁰. Vascular permeability increases in response to VEGF, thus allowing extravasation of plasma proteins that lay down a provisional scaffold for endothelial cell migration. The enhancement of permeability is mediated by the formation of fenestrations, vesiculo-vacuolar organelles and the redistribution of platelet endothelial cell adhesion molecule-1 as well as vascular endothelial cadherin ⁹¹. Although permeability is positive for angiogenesis, excessive vascular leakage has side effects such as circulation collapse. Angiopoietin-1, a ligand for the endothelial Tie2 receptor, is a natural inhibitor of vascular permeability and it can tighten pre-existing vessels. Angiopoietin-1-Tie2 signalling plays an important role in impeding endothelial cell activation and inhibiting the initiation of the angiogenic response. Furthermore, Angiopoietin-1 protects against plasma leakage without profoundly affecting vascular morphology ⁹². Angiopoietin-2, an endogenous antagonist, acts in concert with VEGF as angiogenic factors in the earliest stages of infarct angiogenesis through inhibiting Angiopoietin-1-Tie2 signalling. Other cytokines, including bFGF, TGF β , and the ECM are important for modulating angiogenesis and take part in the complex process of new vessel formation after MI ^{24, 93} (**Figure 3**).

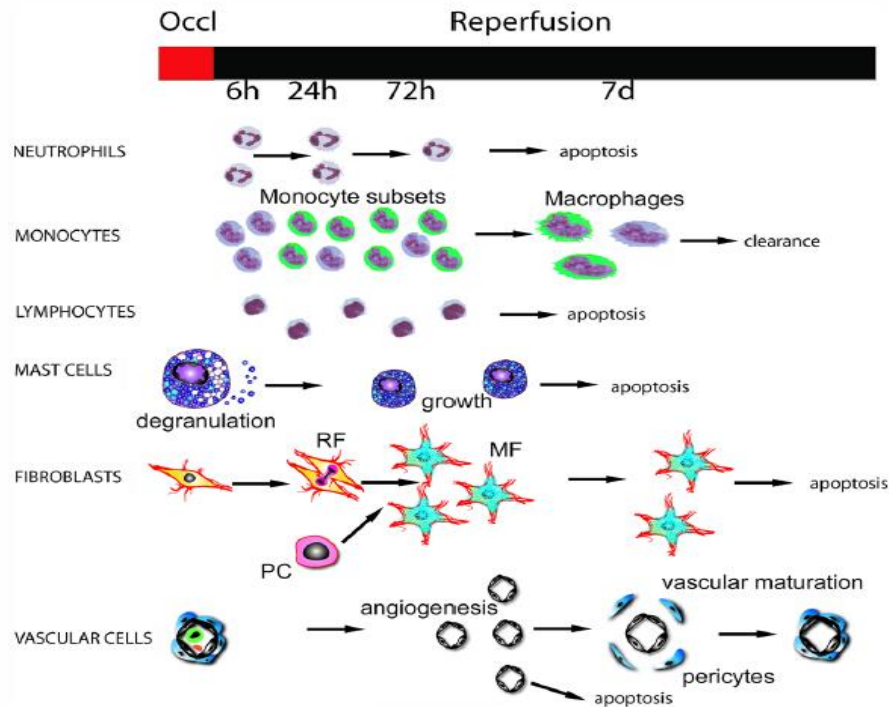


Figure 3: The cell biology of MI healing. Infarct healing is dependent on the sequential infiltration of the ischemic cardiac tissue with mononuclear cells, lymphocytes, neutrophils, mast cells, fibroblasts and vascular cells. This is a dynamic orchestrated process: proliferation of each cell type is followed by activation. Various cell populations have distinct but overlapping functions. Orchestration of the sequence of cellular events in the healing infarct is dependent on timely apoptosis of specific cell types. The time course presented here is based on a reperfused murine MI⁶⁸.

1.1.3 The pathophysiology and mechanisms of left ventricular remodelling after MI

Cardiac remodelling is a physiologic and pathologic circumstance that may occur after MI. Cardiac remodelling encompasses many changes including molecular, cellular and interstitial changes that are clinically manifested as changes in size, shape and function of the ischemic heart⁹⁴. This process is regulated by mechanical, neurohormonal, and genetic factors^{95,96}.

Due to MI, the acute loss of myocardium can result in an abrupt overload condition. This phenomenon may activate a pattern of remodelling including the infarcted border zone and remote non-infarcted areas. Cardiac myocyte necrosis and the resultant enhancement in load trigger a series of intracellular signalling pathways to modulate repair processes including

dilatation, hypertrophy and collagen scar formation. Cardiac remodelling can continue for weeks till the distending forces are counter-balanced by the tensile strength of the collagen scar⁹⁷.

Early remodelling: Postinfarction remodelling has been divided in an early phase (within 72 hours) and a late phase (beyond 72 hours). In the early phase, infarct expansion results from the degradation of the inter-myocyte collagen struts by serine proteases and the activation of MMP released from the neutrophils⁹⁸ and myofibroblasts⁴⁴. This phase of remodelling, due to infarct expansion, includes cardiomyocyte lengthening, infarct zone wall thinning, ventricular dilatation and elevation of diastolic and systolic wall stresses. The initial compensatory responses are invoked to maintain **stroke volume (SV)** after loss of contractile tissue in which the non-infarcted remote myocardium is involved⁹⁹. Infarct expansion causes deformation of the border and remote myocardium which augments shortening. Perturbations in circulatory hemodynamics stimulate the sympathetic adrenergic system, which triggers catecholamine synthesis by the adrenals and spillover from sympathetic nerve terminals, and stimulates the **renin-angiotensin-aldosterone system (RAAS)**⁹⁷.

Late remodelling and hypertrophy: Research of global LV chamber volumes and muscle mass proves that early remodelling may continue progressively. The late remodelling involves myocyte hypertrophy as well as alterations of ventricular geometry and architecture. The LV becomes less elliptical and more spherical, and ECM forms a collagen scar to stabilize the distending forces and to prevent further deformation^{94, 97}.

Cardiac hypertrophy is an adaptive response during late remodelling that offsets the enhanced load, progressively decreases dilatation and stabilizes contractile ability⁹⁵. Cardiac hypertrophy stimulates and regulates a diversity of transcriptional factors, enzymes and growth factors including natriuretic peptides, angiotensin-converting enzyme, and endothelin-1¹⁰⁰⁻¹⁰². Myocyte hypertrophy is triggered by neurohormonal activation, myocardial stretching, activation of local tissue RAAS, and paracrine/autocrine factors. Hypotension after MI triggers the sympathetic adrenergic system, which activates the RAAS

and stimulates the secretion of natriuretic peptides. Increasing secretion of norepinephrine, released from the sympathetic neurons, regulates myocyte hypertrophy directly and indirectly. Norepinephrine may activate $\alpha 1$ adrenoreceptors and causes myocyte hypertrophy through a $G_{\alpha q}$ -dependent signalling pathway. In addition, the stimulation of $\beta 1$ adrenoreceptors in the juxtaglomerular apparatus, which is located in the kidney and regulates blood volume and pressure, induces renin release. Thereby, the production of **angiotensin (Ang) II** is increased¹⁰³. Furthermore, endothelin-1, another stimulus for myocyte hypertrophy, augments the release through stimulation of Ang II and norepinephrine. Serine proteases stimulate the local RAAS in the noninfarcted cardiac tissue, resulting in an increased expression of angiotensinogen. Renin then catalyzes the conversion of angiotensinogen to the decapeptide angiotensin I, which is subsequently hydrolyzed by angiotensin-converting enzyme to form Ang II^{104, 105}. These changes enhance local Ang II production, which is responsible for hypertrophy in noninfarcted myocardium⁹⁷ (**Figure 4**).

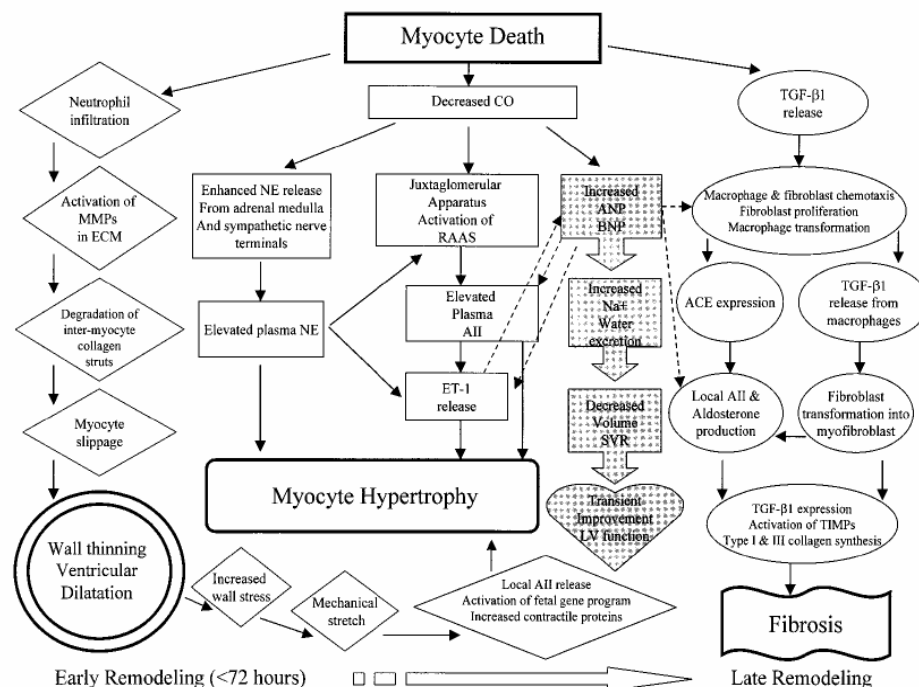


Figure 4: Diagrammatic representation of the numerous factors involved in the pathophysiology of ventricular remodelling. RAAS, renin-angiotensin-aldosterone system; CO, cardiac output; SVR, systemic vascular resistance; and AII, angiotensin II⁹⁷.

Mechanical stretch is another way to induce hypertrophy in cardiomyocytes. Stretch induced hypertrophy mimics hemodynamic load-induced hypertrophy^{104, 106}. Mechanical stretch results in the secretion of Ang II from cytoplasmic granules of cardiomyocytes. It has been demonstrated that Ang II binding to its angiotensin type1 receptor induces hypertrophy and apoptosis of cardiomyocytes¹⁰⁷. Fortuno *et al.*¹⁰⁸ pointed out that apoptotic signals have the potential to produce an enlargement of cardiomyocytes. Subsequently, growth signals produce a contradictory genetic demand and trigger the apoptotic response when they persist chronically in terminally differentiated cells^{109, 110}. A molecular explanation for this double response may be the persistence of growth stimuli driving hypertrophied cardiomyocytes to lose intracellular survival signals that normally suppress the development of the apoptotic process¹¹¹. Hence, late remodelling is accompanied by hypertrophy and apoptosis of cardiomyocytes, defective vascular development, and fibrosis. Finally, this phenomenon is followed by transition to cardiac failure and progressive contractile dysfunction^{108, 112}.

1.2 Approaches in regenerative medicine

1.2.1 Angiogenic gene therapy and methods of gene delivery

1.2.1.1 Mechanism of angiogenesis

Normal tissue formation depends on adequate supply of oxygen and nutrition through blood vessels. In embryos, blood vessels are formed through two distinct pathways, vasculogenesis⁹³ and angiogenesis. Vasculogenesis takes place during embryonic development and leads to the formation of a primary vascular plexus. The term angiogenesis is used to describe the growth and remodelling process which then transforms the primitive capillary network into a complex network. This consists of an enlargement of venules, which sprout from pillars of peri-endothelial cells or from trans-endothelial cell bridges whose mother vessel split in turn into individual capillaries⁹³. In adults, angiogenesis plays an essential role for repair and regeneration of tissues for example during wounding healing¹¹³. Bauters's group and Takeshita's group have proven that a large number of factors such as VEGF, granulocyte-monocyte colony-stimulating factor, bFGF and **insulin-like growth factor (IGF)-1** are

essential for development and differentiation of the vascular system^{114, 115}. Especially VEGF is thought to play a key role in *de novo* angiogenesis and wound healing.

All members of the **VEGF** family activate cellular responses by binding to tyrosine kinase **receptors (VEGFRs)** on the cell surface, causing them to dimerize and to become activated by phosphorylation. Three specific receptor tyrosine kinases have been identified for VEGF, namely, VEGFR1, VEGFR2, and VEGFR3. A large number of studies^{116, 117} have proven that cellular VEGF signalling is mainly mediated via VEGFR2. After VEGF binding to VEGFR2, endothelial cells may express endothelial nitric oxide synthase¹¹⁸, produce nitric oxide¹¹⁷, mobilize Ca^{2+} ¹¹⁹, migrate, and proliferate¹²⁰. VEGF inhibits endothelial cell apoptosis by activating a **phosphatidylinositol 3-kinase (PI3K)**-dependent anti-apoptosis kinase pathway. Besides triggering the anti-apoptotic signalling pathway of endothelial cells, VEGF may promote the formation of new vessels and help maintain their integrity. Thereby, VEGF may mediate DNA synthesis and endothelial cell proliferation via VEGFR2. Furthermore, VEGF strongly induces the activity of the intracellular **mitogen-activated protein kinase (MAPK)**. The activation of this pathway plays an important role in the stimulation of endothelial cell proliferation^{116, 121}. Also, VEGF may stimulate **phosphoinositide phospholipase C (PLC) - γ** tyrosine phosphorylation and then trigger protein kinase C and Ca^{2+} mobilization. Studies indicated that the activation of protein kinase C plays a vital role in endothelial cell proliferation¹²²⁻¹²⁵. It has been proven that VEGF stimulates endothelial production of nitric oxide and prostacyclin¹²⁶⁻¹³⁰. Normally, nitric oxide production is stimulated by VEGF via the activation of a constitutive endothelial nitric oxide synthase isoform, in part through VEGF-induced Ca^{2+} mobilization. It is well known that nitric oxide is crucial for vasodilation, however, it also has some vascular protective effects, such as anti-platelet, anti-thrombotic effects, as well as inhibition of leukocyte adhesion¹³¹. Concerning the functions of promoting angiogenesis and protecting vasculum, VEGF may have the potential for promoting therapeutic angiogenesis and consequently enhancing heart function¹³² (**Figure 5**).

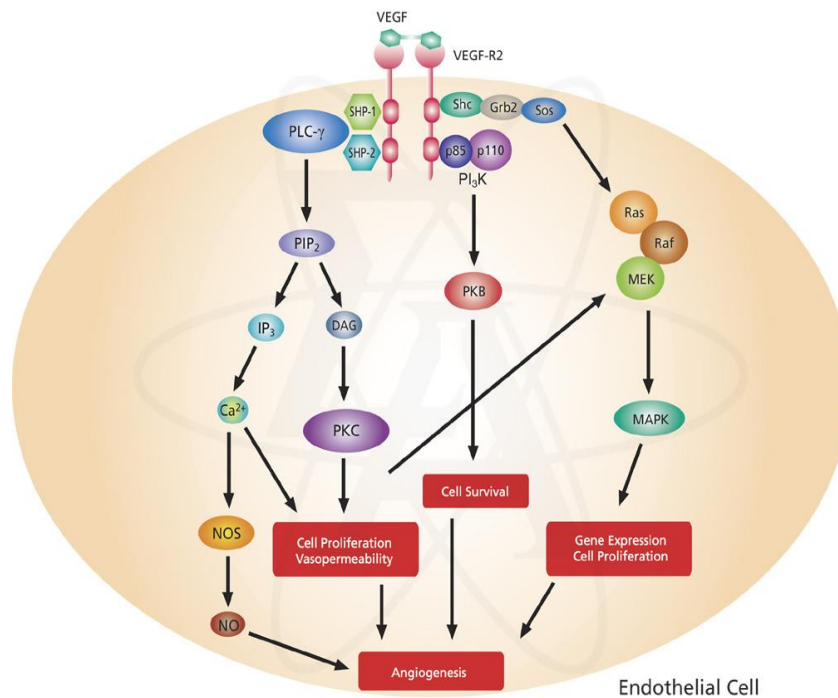


Figure 5: Signaling pathways activated by VEGF: VEGF regulates several endothelial cell functions, including differentiation, proliferation, permeability, and the production of vasoactive molecules. Upon ligand binding, the receptor is phosphorylated, allowing the receptor to stimulate a range of signaling molecules, such as the SHP-1 and SHP-2, and PI3K. VEGF receptor activation can induce activation of the MAPK cascade leading to gene expression and cell proliferation, stimulation of PI3K leading to PKB activation and cell survival, stimulation of PLC-γ leading to cell proliferation, vasopermeability, and angiogenesis. Src homology region 2 domain-containing phosphatase (SHP); protein kinase B (PKB). (Picture is from www.sigmaaldrich.com/life-science/cell-biology/learning-center.)

1.2.1.2 Clinical trials investigating therapeutic angiogenesis

Although conventional mechanical revascularisation by **percutaneous coronary intervention (PCI)** and **coronary artery bypass graft (CABG)** have reduced the morbidity and mortality significantly, some patients are unsuitable for these surgical techniques and a substantial proportion of PCI and CABG patients experience incomplete revascularization. Therefore, there is an important clinical need for additional treatment options of ischemic heart disease. The aim of therapeutic angiogenesis is the use of angiogenic factors to induce the formation of a collateral blood supply, suitable to transport sufficient amounts of oxygen and nutrients, and to thereby reduce and repair myocardial damage. In animal studies, several

families of proteins have been shown to have angiogenic potential in ischemic heart tissue^{133, 134}. However, in pre-clinical trials, VEGF had the highest potential to induce angiogenesis. To date, there are more than 25 phase II and phase III clinical trials including 2300 patients, assessing the functions of recombinant angiogenic growth factors or therapeutic genes encoding for these growth factors including VEGF as well as fibroblast growth factors in patients with ischemic heart disease^{135, 136}.

VEGF gene therapy: Gene therapy is one optional way of delivering therapeutic cytokines to achieve a more steady biological effect. Preclinical and clinical studies of VEGF gene delivery encoded in plasmids or Ad proved an impressive enhancement of cardiac function in diverse animal models^{137, 138}. The methods employed in clinical trials to deliver genes to cardiac tissue have included direct intracoronary infusion and direct intramyocardial injection during bypass surgery. Plasmids encoding the VEGF gene have been used as naked plasmid DNA or in transfection formulations such as a liposome plasmid DNA complex. The first group to perform cardiac VEGF gene therapy, Orlic's group¹³⁹, investigated VEGF A encoded in plasmid DNA for patients with severe **coronary artery disease (CAD)**. Their results demonstrated that the clinical use of plasmids is therapeutically safe and shows promising signs of clinical benefit. However, in two randomised, double-blind, placebo-controlled trials of VEGF therapy, no significant difference between the VEGF treated group and the placebo group were detected concerning the primary end point, amelioration of myocardial perfusion. Meanwhile, most phase II/III trials of therapeutic angiogenesis in CAD using plasmid vectors have negative results. Even though plasmid vectors have many advantages such as being simple to manufacture and comparatively safe, the main drawback is the low transfection efficacy of pure plasmid vectors.

Although mainly secreted diffusible proteins such as VEGF have been used for therapeutic angiogenesis, which could theoretically achieve a widespread effect even if relatively few cells are transfected, it has been argued that viral vectors which can transduce a much larger proportion of cells in the target tissue are able to achieve a sufficient expression level for a therapeutic effect^{135, 136}. Even though several types of viral vectors are available including

vectors of retroviral, lentiviral and adenoviral type, so far, adenoviruses have been the best candidates for cardiovascular disease therapy, because they display a high transduction efficacy in many proliferating and non-proliferating cell types. Although concern has been raised about the safety of adenoviruses, their genomes have not been found to integrate into host genome at high frequency, and episomal viral genomes are rapidly lost from dividing cells. Furthermore, many adenoviral serotypes are only mildly pathological. Intramyocardial Ad_{VEGF} injection via thoracotomy was proven to be safe and well tolerated by 21 patients in a phase I study¹⁴⁰. In the Kuopio angiogenesis phase II trial, 103 patients with untreated angina were randomised to receive either Ad_{VEGF} or placebo. Vectors were infused by an infusion-perfusion catheter during the stent placement. A significant enhancement of heart perfusion was shown in the treatment group compared to the placebo¹⁴¹.

1.2.1.3 Delivery techniques in experimental and clinical use

Systemic intravenous injection and magnetically guided intravenous injection: In experimental and clinical practice, many therapies are applied by venous delivery. In general, systemic injection is a cornerstone of medical therapy. However, lack of targeting specificity leads to the presence of therapeutical agents in organs such as liver, lungs, spleen, and kidney and thus limits systemic injection due to the resulting poor cardiac uptake. Therefore, in the context of intravenous gene therapy, increasing cardiac specificity, for instance by using cardiac specific promoters and viral vectors that lead to relative cardiac tropism, is a possible solution for this problem.

Magnetic nanoparticles (MNPs) based transfection was first established in the 1970s for magnetically targeted drug delivery. Cathryn Mah and her colleagues¹⁴² were the first to successfully use **adeno-associated viral vectors (AAV)** linked to magnetic microspheres via heparin for *in vitro* and *in vivo* transduction. Since this initial study, the term ‘magnetofection’ has been established. This technique is based on the binding of genetic material such as a viral vector to magnetic nano or micro particles. For *in vitro* transfection, the MNPs/genetic construct complex is incubated with cultured cells in a cell culture plate and a magnetic field gradient is produced by magnets positioned beneath the plate. The

external magnetic field gradient increases sedimentation of the complex as well as speed and efficacy of transfection. *In vivo*, a magnetic field focused over the target site has the potential not only to enhance transfection efficacy, but also to target therapeutic genes towards a specific organ or site of the body ¹⁴².

The physical principles of magnetofection are based on the attractive force exerted on MNPs by a magnetic field source according to the **Equation 1**.

$$F_{\text{mag}} = (\chi_2 - \chi_1)V \frac{1}{\mu_0} B(\nabla B)$$

Equation 1: F_{mag} is the force on the magnetic particle, χ_2 is the volume magnetic susceptibility of the magnetic particle, χ_1 is the volume magnetic susceptibility of the surrounding medium, μ_0 is the magnetic permeability of free space, V is the particle volume, B is the magnetic flux density in Tesla (T), ∇B is the field gradient and can be reduced to $\delta B/\delta x$, $\delta B/\delta y$, $\delta B/\delta z$ ¹⁴³.

From **Equation 1** I can deduce that high gradient, rare-earth magnets are highly preferable for magnetofection. Meanwhile, the magnetic field must have a high gradient in order to generate an appreciable force on the magnetic particles. In the presence of a homogeneous field, the particle will not be subjected to any force. **Equation 1** also indicates that several other parameters can influence the force on the magnetic particles including particle number, magnetic field strength and the magnetic properties of the particles.

The technique of MNB-based gene therapy is widely applied and a series of studies have proven that *in vitro* MNB based infection increased sedimentation of the complex as well as speed and efficiency of transfection. *In vivo*, the therapeutic gene may be specifically expressed in a target site or organ of the body and transduction efficiency can be enhanced by additional guiding by a magnetic field. Pandori and colleagues ¹⁴⁴ utilized streptavidin and its ligand biotin to associate Ad to silica beads which resulted in higher infection efficiency for a variety of cell lines and an improved localization by magnetic force. Moreover, Hofmann *et al.* ¹⁴⁵ used charge to couple MNPs to **lentiviral vectors (LVs)** and applied MNPs to combine cell transduction and positioning in the vascular system. Additionally, *in vivo*

MNPs/LVs biodistribution was proven to be significantly changed by external magnetic field intervention in a murine model ¹⁴⁵.

Generally, MNPs/therapeutic gene complexes can be injected intravenously and external magnets are used to guide and attract complexes as they flow through the blood stream. Once captured by the magnetic field, the complexes will be held within the target area and taken up by the tissue. Furthermore, therapeutic genes may be released and expressed in the targeted zone ^{146, 147}.

1.2.2 Tissue engineering combined stem cells for cardiac regeneration

Heart disease is the leading cause of death worldwide, due to the fact, among other aspects, that the heart is one of the least regenerative organs in the human body. Stem cell therapy has been proposed as a promising strategy for cardiac repair following myocardial damage because of the plasticity of stem cells. Direct myocardial cellular therapy and/or cytokine mobilization are undergoing investigation for the treatment of MI ¹⁴⁸. Evidence suggests that cell therapy employing bone marrow-derived or circulating progenitor cells for MI can improve cardiac function ¹⁴⁹⁻¹⁵¹, no matter if the differentiation of the stem cells to myocyte-like cells occurs ^{139, 152, 153, 154}. However, the use of stem cells for myocardial repair remains controversial ^{155, 156}. This suggests that the rate and type of cellular regeneration in the injured myocardium may rely not only on the ability of stem cells to transdifferentiate into myocytes or endothelial cells, but also on surrounding factors that play essential roles in creating conditions conducive to stem cell-mediated cardiac repair.

C-kit is a receptor tyrosine kinase ¹⁵⁷, which constitutes a type III protein tyrosine kinase superfamily with the receptors for **platelet-derived growth factor (PDGF)** ¹⁵⁸, colony-stimulating factor 1 and flt-3 ligand ^{159, 160}. Upon ligand binding, the tyrosine kinase subunit of c-kit is enabled to bind src homology domain-containing proteins, including proteins of the p21 MAPK pathway and the p85 subunit of PI3K. Subsequently, those proteins are activated and trigger signalling cascades that cause various cellular responses including migration, survival, and proliferation ¹⁶¹. In addition, it has been proven that haematopoietic

derived c-kit⁺ stem cells have the function to improve cardiac performance after MI^{152, 153, 162}. Fazel *et al.*¹⁶² showed that coronary ligation leads to a significant recruitment of c-kit⁺ cells from peripheral blood. After MI, c-kit⁺ cells could be found in the injured heart tissue that is subtended after the ligated coronary artery. However, c-kit⁺ stem cell therapy for myocardial repair is thought to be partly limited by the number of stem cells that bear insufficient potential for migration, survival, and, differentiation into the cardiac cell types.

Tissue engineering materials such as bio-artificial tissue have a great potential for regenerating heart function, which is, nevertheless, associated with significant limitations. The bio-artificial tissue needs to be robust enough to endure high ventricular wall stress during the heartbeat. The heart constitutes a complex helical structure with significant local asymmetry and anisotropy¹⁶³. Different parts of the heart display a distinct mechanical performance and microstructure. The contractions of particular elements in all areas of the ventricle have to be coordinated to guarantee maximal hemodynamic output¹⁶⁴. The majority of previously used biodegradable rigid materials which were designed for implantation into the injured ventricular wall cannot achieve this goal.

Matrigel is a basement membrane extract containing collagen that is secreted by a mouse sarcoma cell line¹⁶⁵. Additionally, matrigel contains a large number of growth factors and cytokines such as IGF-1, PDGF, bFGF, and VEGF¹⁶⁶. It is well known that IGF-1 promotes cytoprotection¹⁶⁷ and PDGF has been shown to prevent cardiac cell apoptosis post-MI¹⁶⁸. Meanwhile, bFGF and VEGF as pro-angiogenic factors may promote neovascularization, increase capillary and arteriole densities. Therefore, these factors may preserve cardiac cell survival after MI by promoting the restoration of blood flow to the ischemic cardiac tissue¹⁶⁹⁻¹⁷³. In addition, matrigel constitutes a functional platform to reduce the rate of diffusion and prolong the half-life of the therapeutic factors which it contains¹⁷⁴.

After MI, the mobilization of c-kit⁺ stem/progenitor cells into the peripheral blood and the significant recruitment of c-kit⁺ stem cells to the infarcted heart are associated with a short term, temporally, and spatially distributed up-regulation of SCF. Matrigel could reinforce

stem cell homing by the release of various therapeutic molecules promoting anti-apoptosis and pro-angiogenesis. Moreover, matrigel may provide an appropriate environment by secreting the therapeutic molecules to support c-kit⁺ cell survival and proliferation via the growth factors mentioned above^{164, 175-179}.

1.2.3 Goal of the thesis

Based on these studies, I hypothesized that in a rat MI model, intravenous MNB based delivery of therapeutic genes/VEGF complexes could be targeted towards the ischemic area of the heart via externally applied magnetic force. Thereby, targeted VEGF expression in the heart may promote neovascularization and improve cardiac function. Overall, MNB based VEGF delivery and therapy may be a useful, non-invasive therapeutic strategy with good potential for treatment of MI.

On the other hand, the technique of local matrigel injection may provide several advantages for MI therapy. Firstly, matrigel delivery by catheterization has the benefit of minimal invasion. Secondly, Matrigel, as bio-artificial ECM, may support a series of growth factors in enhancing the recruitment of c-kit⁺ cells and in regulating their survival and proliferation. Last but not the least, matrigel may provide three-dimensional support to reduce negative remodeling processes of the infarcted area. Therefore, matrigel combined with c-kit⁺ stem cell therapy can be expected to become a promising strategy to treat MI.

2 Material & methods¹

2.1 HUVECs isolation and culture

Human umbilical vein endothelial cells (HUVECs) were isolated from umbilical cord, and expanded. Firstly, the fresh umbilical cord was placed in a 25 cm dish. Then it was washed with **phosphate-buffered solution (PBS)** to clear the blood away. The cord was checked for clamp damage, and the damage part was removed. Using PBS, the vein of the cord was washed until it ran clear. *Then umbilical cords were washed with 0.2-mm-filtered cord buffer (140 mM NaCl, 4 mM KCl, 2 mM MgCl₂, 11 mM glucose, 10 mM HEPES [pH 7.4]) and reperfed with 0.2-mm-filtered cord buffer containing 1% bovine serum albumin (Sigma Aldrich, St. Louis, USA) and 0.05% Clostridium histolyticum collagenase (Sigma Aldrich, St. Louis, USA). The cord was clamped and incubated at 37 °C for exactly 13 minutes.* Every 3 minutes, the cord was gently flushed with the collagenase solution back and forth. After incubation, the collagenase solution was removed and transferred to a 50ml tube. The vein was flushed with **Roswell park memorial institute medium (RPMI) 1640** (Lonza, Basel, Switzerland), collecting the flow-through in a 50ml tube. The RPMI 1640 containing the HUVECs was subsequently pelleted by centrifugation for 6 minutes at 1000 **revolution(s) per minute (rpm)**. The supernatant was aspirated carefully and the cell pellets were re-suspended in 1ml RPMI 1640. Finally, 10 µl aliquots were taken for mononuclear cell count. Cells were then plated in 60 mm plastic culture dishes at a cell density of 2.5×10^6 cells/cm² in RPMI 1640 containing 20% fetal calf serum (PAN Biotech, Aidenbach, Germany), 5% endothelial mitogen (Biomedical Technologies, Stoughton, USA), 100 µg/ml of streptomycin (PAA, Pasching, Germany) at 100 units/ml of penicillin (PAA, Pasching, Germany), 14 mM HEPES (pH 7.4) and 2 mM L-glutamine and the cells were grown at 37 °C and 5% CO₂ atmosphere, and the medium was changed every 2 days. After 80% confluence was achieved, adherent cells were defined as passage 0. *Cells were harvested using trypsin and subsequently replated in endothelial medium (Lonza, Basel, Switzerland) for continued*

¹ Parts material & methods are described in ^[173], ^[180]. Please see the list of own publications. In the following, the text printed in italics is a citation of the text from these papers.

passaging. Medium was changed three times per week. After HUVECs became confluent to 90%, cells were kept in liquid nitrogen for long-term storage. After third passage, cells can be used for subsequent in vitro experiments.

2.2 MSCs isolation and culture

Rat **mesenchymal stem cells (MSCs)** were isolated from rat bone marrow, and expanded. Firstly, the femur and tibia of rat hind legs were harvested and cut open. A 23-gauge needle was inserted into the bone to flush the bone marrow out using 30 ml **Dulbecco's modified eagle medium (DMEM)** (PAN Biotech, Aidenbach, Germany) with 10% fetal bovine serum (PAN Biotech, Aidenbach, Germany). The medium with the bone marrow was collected in a 50 ml tube. For density gradient centrifugation, a fresh 50 ml tube with 15 ml Ficoll (Sigma Aldrich, St. Louis, USA) was prepared and 30 ml DMEM including the rat bone marrow cells was overlaid onto the Ficoll carefully. The tube was centrifuged at 2000 rpm for 30 minutes at 20 °C. The mesenchymal stem cell-enriched mononuclear cell population was then aspirated with a Pasteur pipette (Sigma Aldrich, St. Louis, USA) (approximately 1 ml) and washed with PBS by further centrifugation at 1600 rpm for 10 minutes at 20 °C. The pellets were re-suspended in 10 ml of DMEM. 10 µl aliquots were taken for mononuclear cell count. Mononuclear cells were then plated in 100 mm plastic culture dishes at a cell density of $1 \times 10^7/\text{cm}^2$. Cells were grown at 37 °C and 5% CO₂ atmosphere, and the DMEM was changed every 2 days. After 80% confluence was achieved, adherent cells were defined as passage 0. *Cells were harvested using trypsin and subsequently replated for continued passage. Medium was changed once every two days. After MSCs became 80% confluent, cells were harvested by trypsinization and subsequently kept in liquid nitrogen for long-term storage. After third passage, cells have been used for in vitro experiments.*

2.3 Viral vector amplification and purification

Ad5. cytomegalovirus (Vector Biolabs, Philadelphia, USA) is derived from adenovirus serotype 5 with the deletion of the viral E1 and E3 genes. These Ad could carry LacZ, green fluorescent protein (GFP), luciferase and human VEGF gene separately under the control of the human cytomegalovirus immediate-early promoter with a polyadenylation site. These viral vectors were produced by using the 293A cell line (Invitrogen, Carlsbad, USA), a subline of 293 cells (human embryonal kidney cells transformed by sheared adenovirus serotype 5 genome), and purified by adenovirus purification kit (Clontech, Shiga, Japan). Firstly, low passage 293a cells were seeded on several 15 cm dishes with a density of 1.5×10^7 cells/dish. Subsequently, the adenoviral stock solution was used to infect the 293a cells. The infected cells were incubated at 37 °C and a humidified atmosphere containing 5% CO₂ for 3-5 days until the cytopathic effect was complete. The pellets of 293a cells were centrifuged at 1500 rpm for 10 minutes. The supernatant was discarded. The cell pellets were re-suspended in 5 ml of fresh DMEM. Three consecutive freeze-thaw cycles were performed to lyse the cells. After the final thawing, the lysate was centrifuged at 3000 rpm for 5 minutes. The supernatant was collected in a sterile centrifuge tube and the pellets were discarded. Then 5 µl nuclease (Clontech, Shiga, Japan) was added to the supernatant and the mixture was incubated for 30 minutes at 37 °C. After that, 5 ml dilution buffer were added to the tube and the lysate was clarified by filtering it through a 0.45 µm filter (Millipore, Billerica, USA). The lysate was passed through an adeno-purification filter (Clontech, Shiga, Japan) to load the Ad onto the purification filter. For the final step, 3 ml 1 × elution buffer (Clontech, Shiga, Japan) was passed through the adeno-purification filter to elute the Ad. The original preparation of Ad was aliquoted and stored frozen at -80 °C.

2.4 MNBs/Ad complexes formation

Firstly, an appropriate amount of 100 nm average effective diameter Streptavidin MagneSphere® MNBs (Promega, Fitchburg, USA) were washed two times using PBS and re-suspended in PBS. *For the next step, Sulfo-NHS-LC-biotin (Pierce Chemical, Rockford,*

USA) was used as the biotinylation reagent. 5 mg Sulfo-NHS-LC-biotin was diluted in 1 ml PBS to a final concentration of 5 mg/ml. 50 μ l of diluted Sulfo-NHS-LC biotin solution was mixed with 0.5×10^{10} **plague-forming unit (pfu)** Ad in 450 μ l PBS (pH 7.6) to a final concentration of 500 ng/ml. *The mixtures were placed on ice, in the dark, for 2 hours, and subsequently, 90 mM glycine in PBS was added to each reaction mixture to absorb excess sulfo-NHS-LC-biotin.* Next, a desalting column (Promega, Fitchburg, USA) was used for the removal of the remaining free biotinylation reagent. *Finally, MNBs were added to biotinylated Ad and the complexes were provided by vortexing for 30 seconds and followed by incubation at room temperature for 30 minutes.* The biotinylated Ad were coupled to MNBs via the Streptavidin linker. The original preparation of MNBs/Ad complexes was stable in aqueous solution and was stored at -80 °C.

2.5 HUVECs network formation to evaluate VEGF function

HUVECs were seeded 2×10^4 per well of a 6 well plate and incubated overnight at 37 °C and 5 % CO₂. Before transduction, Ad_{hVEGF} were added to 250 μ l endothelial medium (without VEGF). After incubation for 5 minutes, medium including Ad_{hVEGF} was added to HUVECs. Then HUVECs were incubated with Ad_{hVEGF} for 24 hours (untransduced HUVECs were used as the control group). Before network formation experiments, 200 μ l matrigel was pipetted per well of a 12 well plate with pre-cooled tips. The plate with matrigel was incubated at 37 °C for 30 minutes. Subsequently, transduced HUVECs were carefully seeded on the matrigel-coated plate and incubated overnight. Computer-assisted Zeiss microscopy (Carl Zeiss, Jena, Germany) was used to analyze network formation.

2.6 *In vitro* transduction

In vitro transduction efficiency of Ad or MNBs/Ad **encoded luciferase (Ad_{luc})** complexes was evaluated by the luciferase reporter gene in HUVECs. The HUVECs were maintained in endothelial medium with 100 μ g/ml of streptomycin at 100 units/ml of penicillin, at 37 °C, in

a humidified 5% CO₂ incubator. HUVECs were seeded in 48-well plates at a density of 5×10^4 cells per well 24 hours prior to the transduction. Before the transduction, the cells were allowed to achieve 50%-60% confluence. Throughout the transduction, the culture medium was aspirated and replaced with 0.5 ml fresh medium, meanwhile MNBs/Ad_{luc} complexes were added to the fresh medium. *The cells receiving Ad_{luc} alone were taken as control. Cell culture dishes were kept with a magnet placed underneath for 30 minutes. The size of the cylindrical sintered neodymium-iron-boron magnet (NeoDelta; remanence Br: 1080–1120 mT) (IBS, Berlin, Germany) was 6×5 mm (diameter \times height). Cells were incubated with complexes for 24 hours at 37 °C, in a in a humidified 5% CO₂ incubator. Following the incubation, the cells were washed with PBS and lysed with 100 μ l of cell lysis buffer (Promega, Fitchburg, USA). Luciferase activity in cell extracts was measured by using the luciferase reporter assay kit (Promega, Fitchburg, USA) on a 96-well microplate luminometer (EG&G Berthold, Stuttgart, Germany). The relative light units were normalized against protein concentration. Protein concentration was measured by a microplate reader using the bicinchoninic acid protein assay kit (Pierce Chemical, Rockford, USA).*

2.7 MTT cytotoxicity

Cytotoxicity of MNBs/Ad was evaluated by performing [3-(4,5-dimethylthiazol-2-yl)-2,5-diphenyl tetrazolium bromide] (MTT) (Sigma Aldrich, St. Louis, USA) assay. HUVECs (1×10^4 cells/well) were seeded into the 96-well plates. *The MNBs/Ad_{luc} complexes were added 24 hours after seeding.* The cells were incubated in 200 μ l medium containing different doses of MNBs and Ad. After 40 hours of incubation at 37 °C, in a humidified 5% CO₂ incubator, the metabolic activity of the HUVECs was analyzed. Firstly, 15 μ l of 5 mg/ml MTT stock solution in 1 \times PBS was added into each well. After 4 hours of incubation at 37 °C, in a humidified 5% CO₂ incubator, the medium was removed and 100 μ l of extraction buffer (20 μ g purple crystals (Sigma Aldrich, St. Louis, USA) were dissolved in 100 μ l dimethylsulfoxide (Sigma Aldrich, St. Louis, USA) was added to each well and the plates were incubated for 2 hours in the dark at 37 °C, in a humidified 5% CO₂ incubator. *Finally absorbance was measured at a wavelength of 550 nm and a reference wavelength of*

655 nm using a microplate reader (Bio-Rad, Hercules, USA). The results were expressed as the percentage of viability relative to the control cells, which were cultured without complexes treatment. Cell viability was calculated using the **Equation 2**.

Equation 2: Cell Viability (%) = (OD550-OD655) samples / (OD550-OD655) control × 100%.

2.8 Characterization of MNBs/Ad complexes

The solution containing the Ad complexes was diluted with PBS to the final amount of Ad of 8×10^7 pfu. Subsequently, different doses of MNBs were added to prepare complexes with different MNB/Ad ratios. MNBs/Ad complex size was measured with ZetaPALS analyzer (Brookhaven Instruments, Älvsjö, Sweden) by dynamic light scattering at 25 °C.

2.9 Magnetic field guided *in vitro* transduction

HUVECs were incubated for 24 hours with MNBs/Ad **encoded lacZ** (Ad_{lacZ}) complexes by the reporter gene LacZ in the presence of three cylindrical magnets (each 6 mm in diameter) affixed to the bottom of a 10 cm culture dish. Three cylindrical magnets were evenly attached to the bottom of the dish to form a three-point magnetic field pattern prior to the application of MNBs/ Ad_{lacZ} complexes. The positions of three magnets were adjusted to exclude the possibility of passive accumulation of complexes in the center or along the peripheral edge of the dish. The dish was subjected to gentle agitation at room temperature for 30 minutes and further cultured for 48 hours without the magnets. MSCs were transduced by Ad_{lacZ} complexes as described above. MSCs were incubated for 24 hours with Ad_{lacZ} complexes by the reporter gene LacZ in the presence of one rectangular magnet (20 × 10 × 5 mm (length × width × height)) affixed to the bottom of one well of a 6 well dish. β-gal staining kit (Invitrogen, Carlsbad, USA) was used to evaluate LacZ gene expression. MSCs were also transduced by MNBs/Ad **encoded GFP** (Ad_{GFP}) complexes as described above. MSCs were incubated for 24 hours with MNBs/ Ad_{GFP} in the presence of one cylindrical magnet (6 mm in

diameter) affixed to the bottom of one well of a 24 well dish. Finally, gene expression was observed using a Leica SP2 Confocal Microscope (Leica, Solms, Germany).

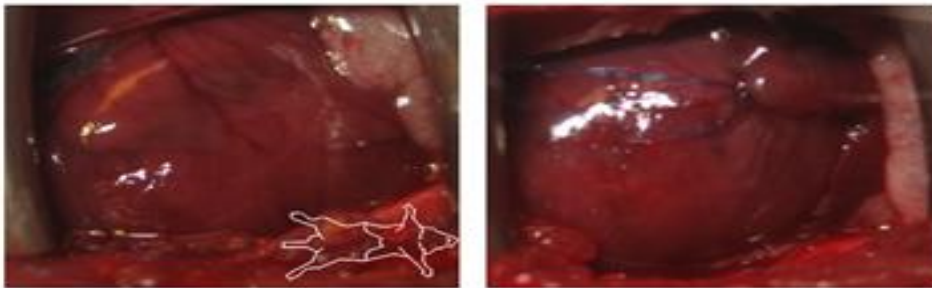
2.10 Experimental design of MNBs/hVEGF for cardiac regeneration

For this study, Lewis rats (male, 250 ± 5 g), which were purchased from Charles River Laboratories (Sulzfeld, Germany) were used. The federal animal care committee of the Landesamt für Landwirtschaft, Lebensmittelsicherheit und Fischerei (Mecklenburg-Vorpommern, Germany) approved the study protocol (approval number M-V/TSD/7221.3-1.1-080/11). All animal procedures were performed in accordance with requirements of the “Animal Care and Use Committee” of the Medical Faculty, University of Rostock. During the surgery, the body temperature of the rat was maintained at 37.5 degree ± 0.5 using a heating table. In the first postoperative days, rats were offered NovaMin sulfone (Metamizol, Frankfurt, Germany) (10 drops/300 ml water) to mitigate pain the drinking water was replaced daily. Furthermore, the animals` conditions such as activity, behaviour, lethargy, lack of appetite, and hair texture were assessed each day. The rats were euthanized, when they exhibited significant impairments of their conditions.

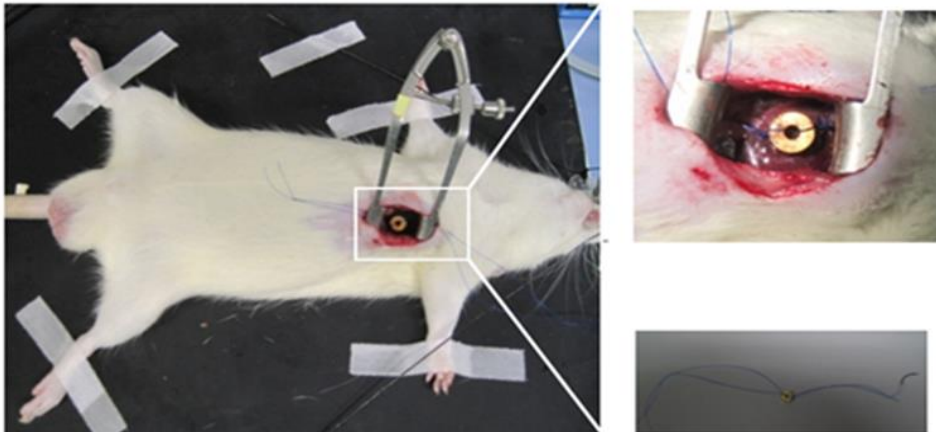
*Rats were randomly assigned to 7 groups as follows: MI-Magnet⁺ MNBs/Ad_{hVEGF} n = 18; MI-Magnet MNBs/Ad_{hVEGF}, n = 18; MI-MNBs, n = 18; MI-Saline, n = 18; sham-operation, n = 13; MI-Magnet⁺ MNBs/Ad_{GFP}, n = 8; and MI-Magnet MNBs/Ad_{GFP}, n = 8. Usually, three methods can be used to induce MI: The surgical ligation model, the cryo-injury model, or the pharmacologically-induced model. In this experiment, the surgical ligation method was used to induce MI. The surgical procedure consists of three steps. Firstly, the rat was anesthetized intraperitoneally with Ketamine (60 mg/kg body weight)/Xylazin (10 mg/kg body weight) (Sigma Aldrich, St. Louis, USA) and its heart was exposed following a left thoracotomy between the third and fourth intercostal space. Secondly, the **left anterior descending coronary artery (LAD)** was ligated by a 6-0 surgical suture permanently (**Figure 6 A**). After the anterior wall of LV blanched, the procedure was considered successful. Finally, the chest was closed by a 4-0 surgical suture. This ligation technique of LAD is simply, well-*

reproducible, and may cause permanent ischemia to the cardiac tissue of the LV. After the surgery, a $6 \times 2 \times 2$ mm cylindrical NdFeB magnet (Br: ≈ 1000 m Tesla) (IBS, Berlin, Germany) was placed in the chest of the rat closely adjacent to the blanched area of the heart, then the magnet was fixed between the third and the fourth rib of the rat by a 4-0 suture (**Figure 6 B**). In the MI-Magnet MNBs/ Ad_{hVEGF} group, the operation procedure was identical except for magnet placement. The saline group underwent the identical surgery procedure of LAD ligation. A sham operation was performed on another group of rats by passing a suture around the LAD without ligation. 24 hours after infarction, Ad encoded hVEGF (1×10^{10} pfu/ml) or GFP (1×10^{10} pfu/ml) coupling to 500 μ l MNBs, MNBs alone, or saline were injected into the rat body in a total volume of 1 ml through the tail vein. Animals from each groups (n = 4) were sacrificed 48 hours and 7 days after systemic administration and transgene expression was evaluated by immunohistochemical staining and Real-Time **polymerase chain reaction (PCR)** in different organs (kidney, heart, lung, liver, and, spleen). The remaining animals were used for histopathological analysis and heart functional evaluation (**Figure 6 C**).

A



B



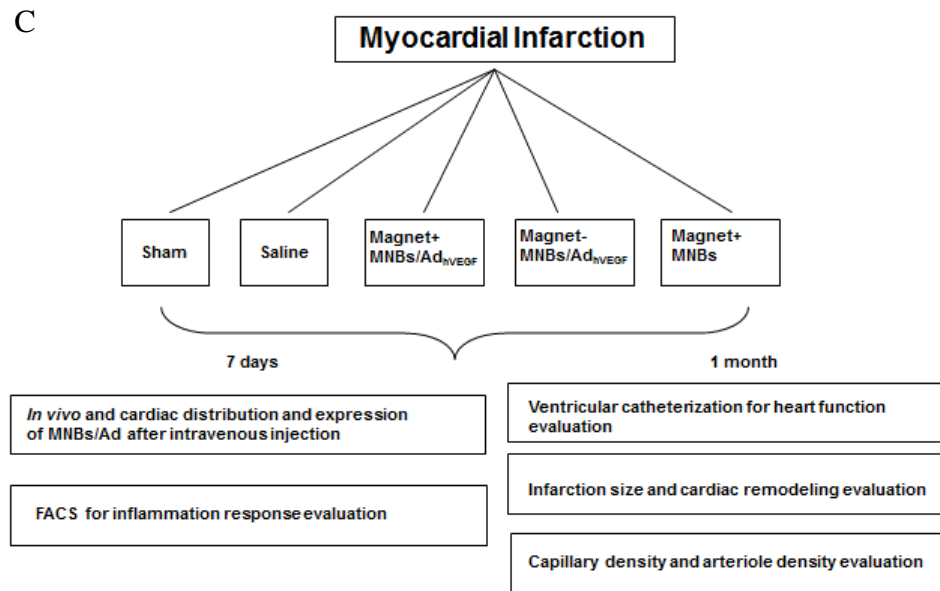


Figure 6: Experimental design. (A-B) After LAD-ligation the rats received the magnet fixed onto the area of infarcted myocardium. (C) *In vivo* experimental design. (Figure 6B quoted from ^[173])

2.11 FACS analysis for inflammatory response

Analysis of peripheral blood was performed 7 days (n = 4, for each group) after MI. To examine the effects of Ad treatment on inflammation, rat mononuclear cells were isolated from peripheral blood. Firstly, 10 ml venous blood was harvested in a heparinized blood collection tube. The blood was then transferred into a 50 ml tube. Furthermore, one new 50 ml tube with 10 ml Ficoll was prepared, and 10 ml peripheral blood was carefully overlaid onto the Ficoll. The tube was centrifuged at 2000 rpm for 30 minutes. The mononuclear cell population was then aspirated with a Pasteur pipette (approximately 1 ml) and washed in 20 ml PBS by further centrifugation at 1600 rpm for 10 minutes at 20 °C. The pellets were re-suspended in 10 ml of PBS. Then the samples of mononuclear cells were stained for flow cytometry analysis. Cells were incubated with anti-rat CD8⁺T monoclonal antibody (Santa Cruz, Dallas, USA). Subsequently, donkey anti-rat Alexa-Fluor 488 conjugated secondary antibody (Molecular probes™, Carlsbad, USA) was applied to the

*samples. The number of CD8⁺T cells in the mononuclear cell fraction of peripheral blood was examined by **fluorescence-activated cell sorting (FACS)** (Calibur, New Jersey USA).*

2.12 Quantitative Real-Time PCR and immunohistochemical staining analysis for Ad distribution

To investigate the Ad expression and distribution in vivo, mRNA levels of Ad_{hVEGF} were evaluated in different organs. Seven days after Ad injection, heart, liver, spleen, lung, and kidney from each group (n=4) were collected and snap-frozen in liquid nitrogen. Total RNA was isolated following the instructions of the TRIZOL[®] Reagent (Invitrogen, Carlsbad, USA). Firstly, the tissue sample was placed in a tube and 1 ml of TRIZOL reagent was added to the tissue sample. After 5 minutes of incubation, 0.2 ml chloroform (Sigma Aldrich, St. Louis, USA) was added to the sample. The sample was shaken 2-3 times and centrifuged at 12000 rpm, for 15 minutes. Throughout the centrifugation, the mixture was segregated into two phases: a lower red, phenol-chloroform phase and a colourless upper aqueous phase. As the RNA remains in the upper phase, this aqueous phase was transferred into a new tube without disturbing the interphase. Subsequently, 0.5 ml isopropanol (Sigma Aldrich, St. Louis, USA) was added to the aqueous phase and the sample was centrifuged at 12000 rpm, for 10 minutes. Following centrifugation, the supernatant was removed completely and the RNA pellet was washed with 75% ethanol (Sigma Aldrich, St. Louis, USA). Then the sample was centrifuged at 7500 rpm, for 5 minutes. Again, the supernatant was removed and the sample was air dried for 10 minutes. Finally, 1 µl of sample RNA was diluted with 39 µl of DEPC-treated water (Sigma Aldrich, St. Louis, USA) (1:40 dilution). 10 µl of the sample was used to determine sample concentration by OD 260 nm and 280 nm method. For quantitative Real-Time PCR, human VEGF primer (Applied Biosystems, Carlsbad, USA) was used. Amplification and detection were performed with the StepOnePlus[™] Real-Time PCR System (Applied Biosystems, Carlsbad, USA) in TaqMan Universal Master Mix (Applied Biosystems, Carlsbad, USA) according to the instructions of the manufacturer (Applied Biosystems, Carlsbad, USA) and repeated at least three times using the following program: 1 cycle of

50 °C for 2 minutes, 1 cycle of 95 °C for 10 minutes, and 40 cycles of 95 °C for 15 seconds and 60 °C for 1 minutes. *cDNA* extracts were tested in at least triplicate and negative controls were included in each assay. Cycle thresholds (C_T) for single reaction were determined with StepOne™ Software 2.0 (Applied Biosystems, Carlsbad, USA) and the target genes were normalized against GAPDH (**Equation 3:** $\Delta C_T = C_{T \text{ target}} - C_{T \text{ GAPDH}}$). Resulting ΔC_T of triplicates was averaged and $\Delta\Delta C_T$ were obtained using sham group as calibrator sample (**Equation 4:** $\Delta\Delta C_T = \Delta C_{T \text{ sample}} - \Delta C_{T \text{ calibrator sample}}$). In the current study, the $2^{-\Delta\Delta C}$ method was employed to present changes in gene expression.

2.13 Immunohistochemical staining analysis of hVEGF expression in the heart

For immunohistochemical staining detection of hVEGF expression, frozen transverse tissue sections (8 μm thickness) of hearts from MI-Magnet⁺MNBs/Ad_{hVEGF} and MI-Magnet⁻MNBs/Ad_{hVEGF} groups ($n = 4$ for each group) were selected. The slides were allowed to dry for 20 minutes at room temperature. Then a boundary between each two samples on the same slide was drawn by DAKOCytomation pen (Dako Cytomation, Glostrup, Denmark). The tissue sections were fixed by covering with 1% paraformaldehyde (Sigma Aldrich, St. Louis, USA) for 10 minutes. After fixation, the samples were washed twice with PBS. One drop of protein block solution (Dako Cytomation, Glostrup, Denmark) was added to each slide to cover the tissue section. Then the tissue sections were incubated with rabbit anti-hVEGF antibody (R&D, Minneapolis, USA) at 4 °C overnight. Subsequently, the sections were incubated with donkey anti-rabbit Alexa-Fluor 405 (Molecular probes™, Carlsbad, USA) conjugated secondary antibody. Nuclei were counterstained with TO-PRO3 (Molecular probes™, Carlsbad, USA). Finally, the slides were washed 5 times by immersing in PBS for 5 minutes at room temperature and then coverslips were used to cover the tissues and nail polish was used to seal the border. Labelled sections were observed using a Leica SP2 Confocal Microscope.

Moreover, in order to identify cell types infected by Ad_{hVEGF} in the infarcted heart, immunohistochemical staining was performed. Firstly, the $hVEGF$ expression in endothelium was evaluated. After slides were stained with $hVEGF$, the tissue sections were incubated with polyclonal goat anti-CD31 primary antibody (Santa Cruz, Dallas, USA) at 4 °C overnight. Subsequently, the sections were incubated with anti-goat Alexa-Fluor 488 secondary antibody (Molecular probesTM, Carlsbad, USA). Nuclei were counterstained with TO-PRO3. Finally, the slides were washed, covered, and sealed. *Labelled sections were observed using a Leica SP2 Confocal Microscope.*

The $hVEGF$ expression in myocardium was also detected. Firstly, the $hVEGF$ was stained following the protocol and a goat polyclonal anti-Troponin T primary antibody (Santa Cruz, Dallas, USA) was applied to the sections. Secondly, a donkey anti-goat Alexa-Fluor 568 (Molecular probesTM, Carlsbad, USA) was utilized. Counterstaining was achieved by TO-PRO3 nuclear staining. Finally, the slides were washed, covered, and sealed. The samples were analyzed using a LSM 780 confocal microscopy (Carl Zeiss, Jena, Germany).

2.14 Immunohistochemical analysis for GFP distribution and expression *in vivo*

For immunohistochemical detection of GFP expression, frozen transverse tissue sections (8 μ m thick) of hearts from MI-Magnet⁺MNBs/ Ad_{GFP} and MI-Magnet MNBs/ Ad_{GFP} ($n = 4$ for each group) were selected. The slides were allowed to dry for 20 minutes at room temperature. Then a boundary between each two sections on the same slide was drawn by DAKOCytomation pen. The tissue sections were fixed by covering with 1% paraformaldehyde for 10 minutes. After fixing, the samples were washed twice with PBS. One drop of protein block solution was added to each slide to cover the tissue section. Then the tissue sections were incubated with goat anti-GFP conjugated FITC antibody (Abcam, Cambridge, UK) at 4 °C overnight. Nuclei were counterstained with TO-PRO3. Finally, the

slides were washed, covered with the coverslips and sealed. *Labelled sections were observed using a Leica SP2 Confocal Microscope.*

2.15 Prussian blue staining for MNBs distribution *in vivo*

Frozen transverse tissue sections (8 μm thick) of hearts from MI-Magnet⁺MNBs/Ad_{GFP} and MI-Magnet⁻MNBs/Ad_{GFP} (n = 4 for each group) were selected. The slides were allowed to dry for 20 minutes at room temperature. Then a boundary between each section on the same slide was drawn by DAKOCytomation pen. The tissue sections were fixed by covering with 10% formalin (Sigma Aldrich, St. Louis, USA) for 10 minutes. Afterwards, slides were rinsed by the distilled water twice. Meanwhile, equal parts of 10% hydrochloric acid (Sigma Aldrich, St. Louis, USA) and 5% potassium ferrocyanide (Sigma Aldrich, St. Louis, USA) were mixed immediately. Slides were put into the mixed solution for 20 minutes. After staining, slides were rinsed twice with the distilled water. Then slides were stained with 1% eosin solution (Sigma Aldrich, St. Louis, USA) for 5 minutes. After staining, slides were rinsed twice with distilled water. Finally, the slides were dehydrated through 95% and 100% alcohol (Sigma Aldrich, St. Louis, USA) and then the slides were left in 100% xylene (Sigma Aldrich, St. Louis, USA) until mounting. Labelled sections were observed using a Leica SP2 Confocal Microscope.

2.16 Left Ventricular Catheterization for heart function evaluation

*4 weeks after surgery, rats underwent **pressure-volume (PV)** loop measurements according to the protocol of CardioDynamics BV (CD Leycom, Zoetermeer Netherlands). Data were collected with the Millar PV System (Ultra-Miniature PV Catheter (model SPR-1030), Millar Pressure Conductance Unit (model MPCU-200) and Millar Power Lab data-acquisition hardware; emka Technologies, Pairs, France). Calibration of pressure and volume was performed by equating the minimal and maximal conductances with minimal (0 mmHg) and maximal (100 mmHg) pressures as well as minimal and maximal blood volumes received from venous circulation. Firstly, the jugular vein was opened with fine forceps and mini-*

scissors under microscopy. Subsequently, the tube cannula was inserted into the jugular vein and 200 μ l heparin (500 g/ml, Sigma Aldrich, St. Louis, USA) was injected into body. Secondly, the carotis was opened with fine forceps and mini-scissors under microscopy and a catheter with both conductance electrodes was inserted in to the carotis gently. The catheter was pushed forward and back till it was placed behind the aortic valve and the characteristic heart pressure curve was visible. *PV loops were recorded under normal conditions (baseline) followed by stress conditions mediated by intravenous dobutamine administration (10 μ g/kg, Sigma Aldrich, St. Louis, USA). Volume signal was corrected by measurement of wall conductance (parallel volume) via hypertonic saline (5%) injection. Data were analyzed with IOX Version 1.8.3.20 software (emka Technologies, Pairs, France). As histological evaluation on hearts in different cardiac phases can lead to under- or overestimation of the analysis such as capillary density, infarct size, fibrosis etc, after PV loop measurements, rats were euthanized by 5% KCl perfusion. The overdose of KCl may cause cardiac conduction blocks and stop the heartbeat at the diastolic phase so that the histological analysis was performed in the diastolic phase of the heart.*

2.17 Determination of functional perfusion and capillary density

Hearts were isolated and aorta was cannulated using a 20 g steel cannula. After cannulation of the aorta, the hearts were perfused at constant pressure in the Langendorff mode by an aortic cannula with 7.5 mg/ml of Fluorescein Lycopersicon Esculentum (tomato) lectin (Linaris, Mannheim, Germany) suspended in 0.2-mm-filtered Krebs-Henseleit buffer (117 mM NaCl, 24 mM NaHCO₃, 11.5 mM D-[t]-glucose, 3.3 mM KCl, 1.25 mM CaCl₂, 1.2 mM MgSO₄ and 1.2 mM KH₂PO₄) equilibrated with 95% O₂ and 5% CO₂ followed by 20 ml Krebs-Henseleit buffer alone. Tomato lectin binds to the surface N-acetylglucosamine oligomers of endothelial cell lining perfused vessels, thereby delineating perfused vasculature. Direct contact of tomato lectin with endothelial cells is required for labeling. Therefore, vessels that are not perfused will not be labeled with tomato lectin. Finally hearts were embedded in O.C.T™ Compound (Tissue-Tek®, Würzburg, Germany) and snapfrozen in liquid nitrogen. To evaluate the capillary density, the infarct area was then divided into 4

horizontal levels from top to bottom. 8 μm thick cryostat sections were stained with TO-PRO3. The sections were analysed within the border zone of the heart. Capillaries were counted in 5 randomly chosen fields from the border zone (630 \times). Capillary density was expressed as capillaries per mm^2 .

2.18 Immunohistochemical staining of CD31 for determination of capillary density

*The capillary density was assessed at 4 weeks after surgery by counting the number of capillaries of the heart sections. Firstly, frozen transverse tissue sections (8 μm) of hearts from each group were dried out at room temperature for 20 minutes. Then a boundary between each two sections on the same slide was drawn by DAKOCytomation pen. Tissue sections were fixed by covering with 1% paraformaldehyde for 10 minutes. After fixing, the samples were washed twice with PBS. One drop of protein block solution was added to each slide to cover the tissue section. Then the tissue sections were incubated with polyclonal goat anti-CD31 antibody (Santa Cruz, Dallas, USA) at 4 $^{\circ}\text{C}$ overnight. Subsequently, the sections were incubated with donkey anti-goat Alexa-Fluor 568 (Molecular probesTM, Carlsbad, USA) conjugated secondary antibody. Nuclei were counterstained with DAPI (Molecular probesTM, Carlsbad, USA) or To-PRO3. Finally, the slides were washed, covered, and sealed. Labelled sections were observed using a Leica SP2 Confocal Microscope. Five sections within the border zone of each group were analyzed. Capillaries were counted in randomly chosen fields from the border zone. Results were expressed as capillaries per **high power field (HPF)**.*

2.19 Infarct size and wall thickness analysis

Heart sections of 4 horizontal infarct levels (8 μm) were stained with Fast Green (Sigma Aldrich, St. Louis, USA) and Sirius Red (Division Chroma, Hamburg, Germany). Frozen transverse tissue sections (8 μm) of hearts from each group were selected. The slides were

dried out for 20 minutes at room temperature. Then the tissue sections were fixed by covering with 10% formalin for 10 minutes. After fixing, slides were put into 0.1% Sirius Red (Sigma Aldrich, St. Louis, USA) for 3 minutes to stain fibrosis red, then transferred into 0.1% Fast Green (Sigma Aldrich, St. Louis, USA) for 10 minutes to stain cardiac tissue. After staining, slides were rinsed twice in distilled water. Then slides were stained with 1% eosin (Sigma Aldrich, St. Louis, USA) for 5 minutes and again rinsed twice in distilled water. Finally, the slides were dehydrated through 95% and 100% alcohol in sequence and then slides were left in xylene until mounting. *Labelled sections were observed using a Leica SP2 Confocal Microscope. The infarction size and wall thickness were analyzed using computerized planimetry (Axio Vision LE Rel. 4.5 software; Zeiss, Jena, Germany).*

2.20 Fibrosis analysis

To evaluate fibrosis, LV transverse tissue sections were stained with Sirius Red. Slides were analysed for positive regions of collagen deposition in the infarct border zone using computerized planimetry. *Sirius Red positive regions were examined in 5 randomly chosen fields per section (one section per level; 1000×). Fibrosis was expressed as the ratio of collagen deposition to myocardial tissue in percentage.*

2.21 Determination of arteriole density

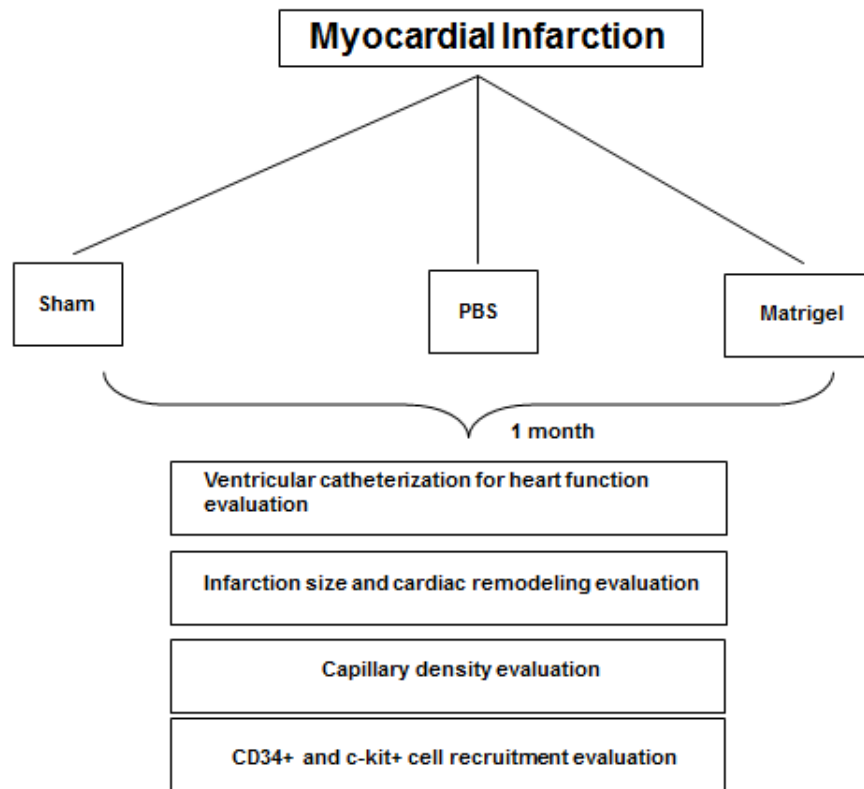
For immunohistochemical detection of arteriole density, heart sections (8 µm) from all groups were selected. Slides were dried out for 20 minutes at room temperature. Then a boundary between each two sections on the same slide was drawn by DAKOCytomation pen. The tissue sections were fixed by covering with 1% paraformaldehyde for 10 minutes. After fixing, the samples were washed twice with PBS. One drop of protein block solution was added to each slide to cover the tissue section. Then the tissue sections were incubated with polyclonal rabbit anti- α -SMA (Abcam, Cambridge, UK) primary antibody at 4 °C overnight. Subsequently, all sections were incubated with goat anti-rabbit Alexa-Fluor 568 (Molecular

probesTM, Carlsbad, USA) conjugated secondary antibody. Nuclei were counterstained with TO-PRO3. Finally, the slides were washed, covered, and sealed. Labelled sections were observed using a Zeiss LSM 780 Confocal Microscope. The sections were analysed in the border zone of the hearts. Arteriole density was assessed by counting the number of arterioles in 5 border zone randomly-chosen fields (630×). Results were expressed as arterioles per mm².

2.22 Experimental design of matrigel for cardiac repair

*For this study, Lewis rats (male, 250 ± 5 g) were purchased from Charles River Laboratories (Sulzfeld, Germany). The federal animal care committee of the Landesamt für Landwirtschaft, Lebensmittelsicherheit und Fischerei (Mecklenburg-Vorpommern, Germany) approved the study protocol (approval number M-V/TSD/7221.3-1.1-044/09). All animal procedures are in accordance with requirements of the Animal Care and Use Committee of the Medical School, University of Rostock. Details were described in **2.10**. Rats were randomly assigned to 3 groups as follows: sham operation, n = 6; MI-matrigel (MI-M), n = 11; and MI-PBS, n = 11. The animals in all groups were used for histopathological analysis and evaluation of heart function 4 weeks after MI (**Figure 7**).*

A



B

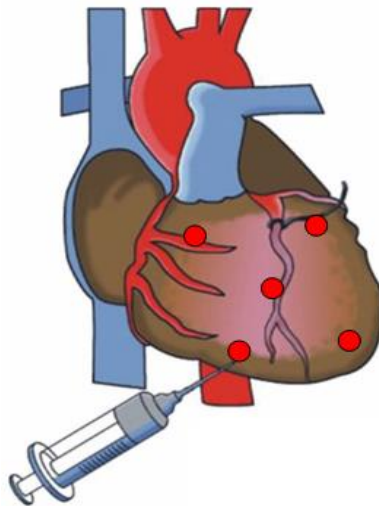


Figure 7: Experimental design. (A) *In vivo* experimental design. (B) After LAD-ligation the rats received the matrigel injection into the areas of infarcted myocardium.

2.23 MI and local matrigel administration

Rat MI model was described in 2.10. Immediately after LAD ligation, rats received 5 intramyocardial injections of either matrigel or PBS of a total volume of 250 μ l. 5 injection sites were chosen along the border of the infarcted cardiac tissue with a 31-gauge needle (BD Biosciences, New Jersey, USA). Sham operated rats underwent identical surgical procedures without permanent LAD ligation (**Figure 7B**).

2.24 Immunohistochemical staining for c-kit⁺ cells

For immunohistological detection of c-kit⁺ stem cells, frozen transverse tissue sections (8 μ m) of hearts from the MI-PBS group and the MI-M group were dried out at room temperature for 20 minutes. Then the air dried samples on the same slide were separated by drawing a boundary by DAKOCytomation pen. The tissue sections were fixed by covering with 1% paraformaldehyde for 10 minutes. After fixing, the samples were washed twice with PBS. One drop of protein block solution was added to each slide to cover the tissue section. Then the tissue sections were incubated with rabbit anti-c-kit antibody (Santa Cruz, Dallas, USA) overnight 4 °C. Subsequently, the sections of the MI-PBS group and the MI-M group were incubated with donkey anti-rabbit Alexa-Fluor 488 (Molecular probesTM, Carlsbad, USA) conjugated secondary antibody. Nuclei were counterstained with TO-PRO3. Finally, the slides were washed, covered, and sealed. Labelled sections were observed using a Leica SP2 Confocal Microscope. The number of c-kit⁺ cells was counted in 5 randomly-chosen fields (630 \times). Results were expressed as c-kit⁺ cells per HPF.

2.25 Immunohistochemical staining for CD34⁺ cells

For immunohistological detection of CD34⁺ stem cells, frozen transverse tissue sections (8 μ m) of hearts from the MI-PBS group and the MI-M group were dried at room temperature for 20 minutes. Then the air-dried samples on the same slides were separated by drawing a

boundary by DAKOCytomation pen. And the tissue sections were fixed by covering with 1% paraformaldehyde for 10 minutes. After fixing, the samples were washed twice with PBS. One drop of protein block solution was added to each slide to cover the tissue section. Then the tissue sections were incubated with goat anti-CD34 antibody (Santa Cruz, Dallas, USA) at 4 °C overnight. *Subsequently, the sections of the MI-PBS group and the MI-M group were incubated with donkey anti-goat Alexa-Fluor 488 (Molecular probes™, Carlsbad, USA) conjugated secondary antibody. Nuclei were counterstained with TO-PRO3.* Finally, the slides were washed, covered, and sealed. *Labelled sections were observed using a Leica SP2 Confocal Microscope.* The number of CD34+ cells were counted in 5 randomly zone randomly-chosen fields (630×). Results were expressed as c-kit+ cells per HPF.

2.26 Statistical analyses

Data are expressed as mean values \pm **standard error of the mean (SEM)** or values \pm **standard deviation (SD)**. One-way analysis of variance was employed for comparing differences between groups. Statistically differences were considered as significant at P values < 0.05 .

3 Results²

3.1 HUVECs vascular network formation

The effect of Ad_{hVEGF} on HUVECs tube formation was examined. The formation of capillary-like networks on matrigel was increased significantly in the Ad_{hVEGF} treated group (Figure 8). Compared to the control group, the mean tube length of the HUVECs network increased more than 50% in the presence of Ad_{hVEGF} (Figure 8). The data proved that Ad_{hVEGF} acts as an angiogenic factor to promote endothelial cell tube formation and sprouting *in vitro*.

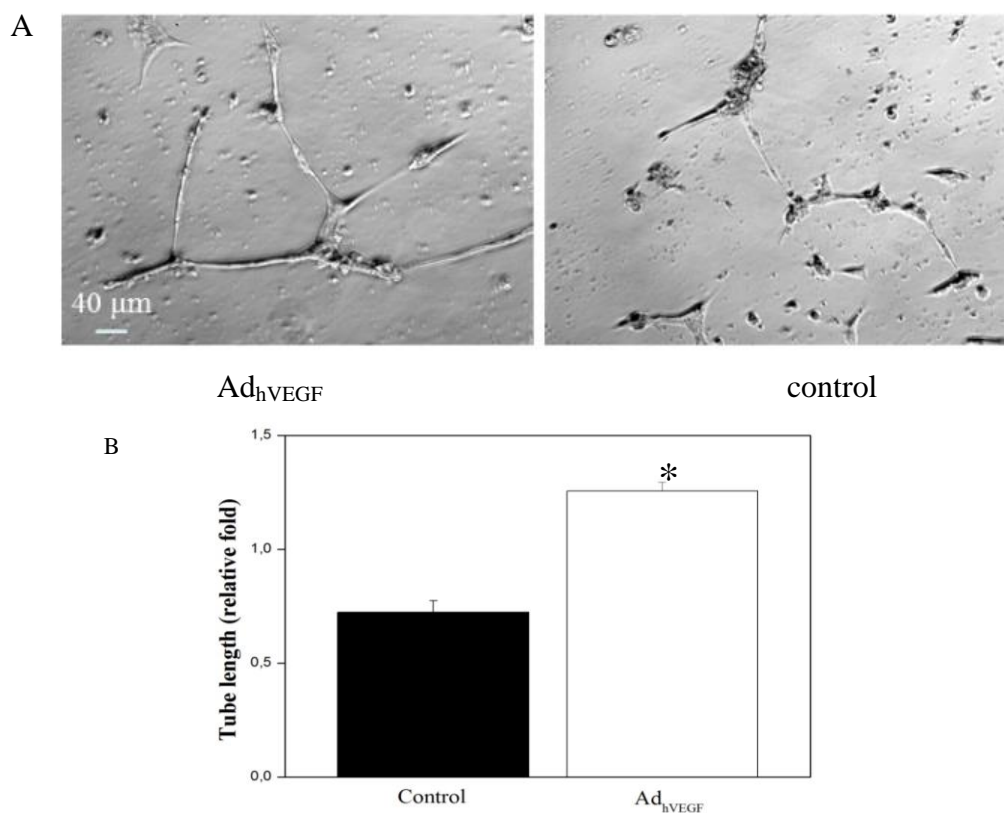


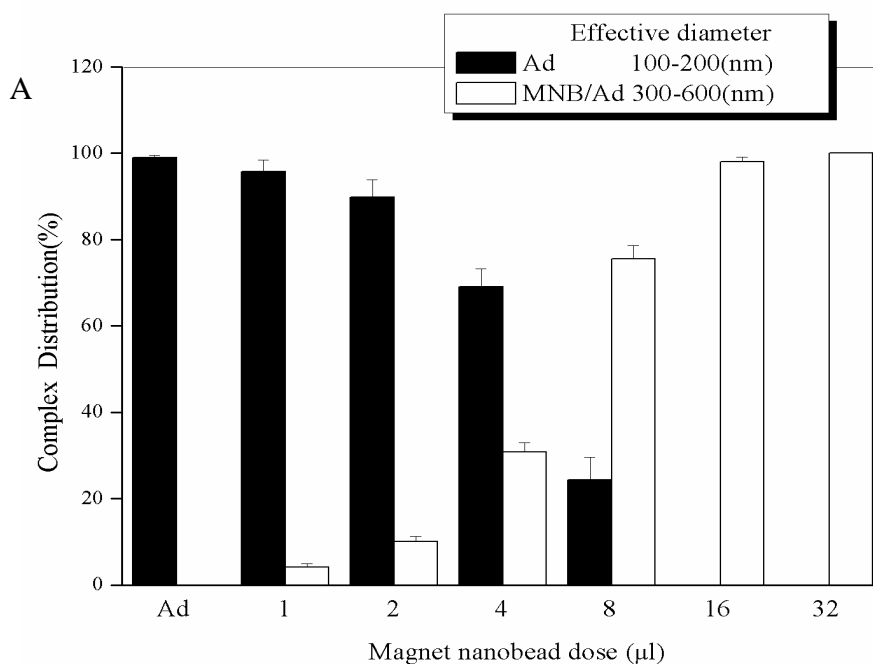
Figure 8: Tube-like network formation assay. (A) Two-dimensional tube formation was performed in the presence or absence of Ad_{hVEGF} on matrigel. (B) The formation of capillary-like networks on matrigel was enhanced significantly in the Ad_{hVEGF} treated group. Data are

² Own figures from [173] and [180] were included after obtaining permission from Public Library of Science (PLOS) ONE and Journal of Cellular and Molecular Medicine (JCMM) / John Wiley & Sons Ltd publishing houses.

expressed as mean \pm SEM. * $P < 0.05$ versus control group. (A) Scale bar = 40 μm . [Ad_hVEGF group, n = 4; control group, n = 4]

3.2 MNBs/Ad complexes characterization

After the presentation of complexes, the ZetaPLAS analyzer was used to evaluate the diameter of MNBs/Ad complexes. The actual size of Ad is 90 nm. Due to hydration, stable aqueous layers form around the Ad which increased the average diameter of Ad to 100-200 nm. The average diameter of MNBs/Ad complexes was larger than that of the naked Ad, which may be due to MNBs forming a shell around the Ad. Firstly, 8×10^7 pfu Ad were distributed into tubes, then different doses of MNBs were added to the prepare complexes with to different MNB/Ad ratios. **Figure 9** shows that by increasing doses of MNBs, free Ad group was diminished and the number of MNBs/Ad complexes was increased. At 16 μl of MNBs, approximately 100% of measured particles were MNBs/Ad complexes, whereas free Ad particles were no longer detectable. This result indicated that at an MNB dose of 16 μl , with an Ad amount 8×10^7 pfu of Ad, and, thus, a MNBs/Ad ratio of 2, Ad can completely bound to MNBs.



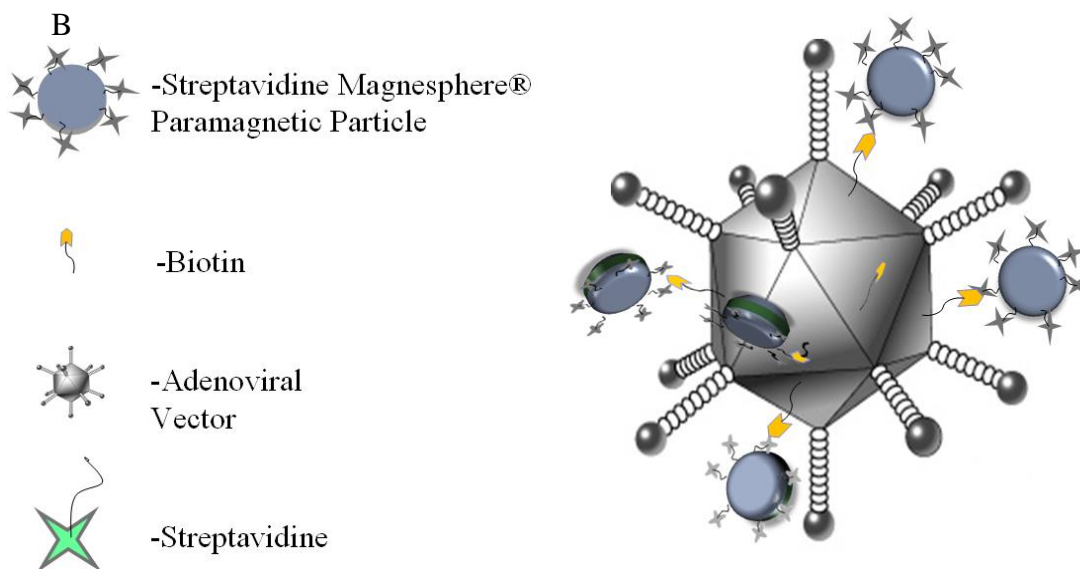
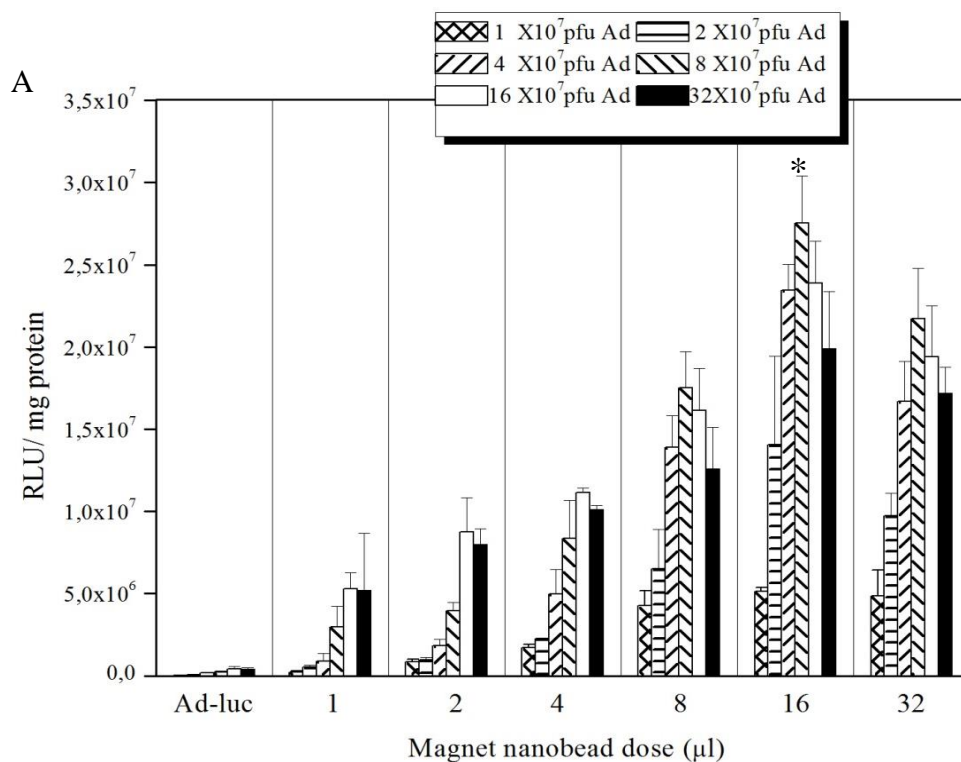


Figure 9: (A) Characterization of MNBs/Ad complexes. The amount of Ad used in the experiment was 8×10^7 pfu and MNBs doses were varied. MNBs/Ad complexes increased but the free Ad decreased with higher MNBs doses. Close to 100% of MNBs dose were combined with Ad at a dose of 16 μ l. Data are expressed as mean \pm SD. [n = 3 for each group] (B) Schematic of MNBs/Ad complexes formation. (Figure 9A quoted from [173])

3.3 HUVECs transduction efficiency and cytotoxicity of MNBs/Ad complexes *in vitro*

To investigate the impact of an external magnetic field on cell transduction, the efficiency of MNBs/Ad_{luc} complexes was assessed in HUVECs by using luciferase as reporter gene (**Figure 10A**). As HUVECs are primary endothelial cells, they provide a suitable model to evaluate the transduction capacity of MNBs/Ad_{luc} complexes on endothelium *in vivo*. The transduction efficiency was mediated by different doses of MNBs and Ad_{luc} (Ad_{luc} without MNBs were used as a control group) and the transduction efficiency was related to the binding ratio of MNBs to Ad. It was found that the coupling of MNBs to Ad_{luc} complexes improved the transduction efficiency in HUVECs considerably. At 16 μ l MNBs, 8×10^7 pfu Ad and a MNBs/Ad ratio of 2, HUVECs transduction achieved maximal efficiency. The peak transduction efficiency of HUVECs was 50 fold higher than transduction efficiency of Ad

alone. The *in vitro* cytotoxicity of MNBs/Ad_{luc} was also evaluated in HUVECs by using MTT cellular metabolic activity assay. Relative viabilities (MNBs/Ad_{luc} relative to Ad_{luc} alone) were decreased and the cytotoxicity was increased by increasing MNBs doses or Ad amounts (**Figure 10A**). However, at optimal parameters for MNBs/Ad complexes (16 μ l MNBs, 8×10^7 pfu Ad and a MNBs/Ad ratio of 2), the cellular metabolic activity was still higher than 85% (**Figure 10B**). These results suggested that transduction with optimized MNBs/Ad complexes did not induce obvious cytotoxicity and the optimized parameters of the complexes can be used for gene delivery *in vitro* or *in vivo*.



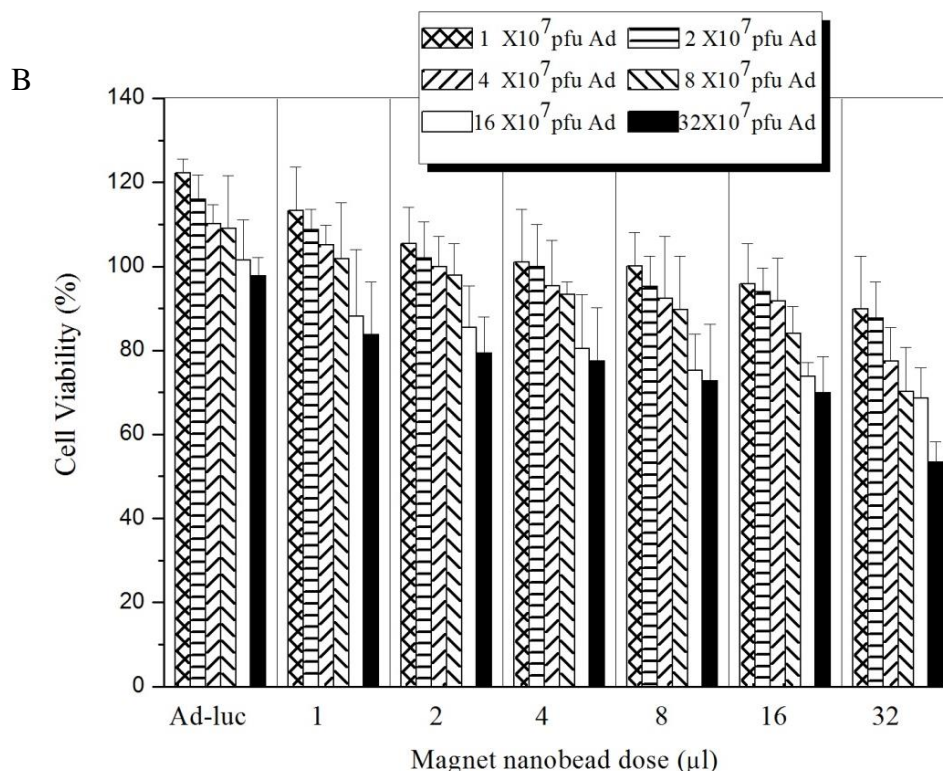


Figure 10: Transduction and cytotoxicity of MNBs/Ad_{luc} complexes in HUVECs. (A) *In vitro* luciferase expression of HUVECs transduced by MNBs/Ad_{luc} complexes for evaluation of magnetically controlled gene delivery. Relative light units were normalized to the protein content of cell lysates. At 16 µl MNBs, 8 × 10⁷ pfu Ad and a MNBs/Ad ratio of 2, transduction efficiency was enhanced significantly compared to Ad_{luc} alone treated groups. (B) *In vitro* MTT evaluation of HUVECs transduced by MNBs/Ad_{luc} complexes. The amount of Ad was expressed as pfu and MNBs doses were varied. Values are presented as a percentage of viability of MNBs/Ad_{luc} treated cells relative to that of Ad_{luc} treated cells (control). Data are expressed as mean ± SD. * *P* < 0.05 versus Ad_{luc} alone treated groups. [*n* = 6 for each group] (Figure 10 redrawn after [173])

3.4 Magnetic field guidance *in vitro*

The cells can be rendered super-paramagnetic, after they take up the MNBs, and therefore become accessible for magnetic force-guided targeting¹⁴³. **Figure 11** shows HUVECs which were fixed and stained for the lacZ gene expression. HUVECs were transduced with MNBs/Ad_{LacZ}, and cultured with gentle agitation, with three cylindrical magnets positioned under the plate prior to transduction. As a control, MNBs/Ad_{LacZ}-transduced HUVECs were cultured without application of magnetic field. After 24 hours of culture, cells were stained

with X-gal. LacZ gene expression formed a well-defined three-spot pattern (**Figure 11A**) and MNBs/Ad_{LacZ} transduced cells were retained in the confined areas above the magnets (**Figure 11B**). **Figure 12** shows a similar phenomenon. The MSCs transduction efficiency in the area under the magnet exceeded 80% and in the area far from the magnetic force was below 4%. Moreover, a clear border was visible between the areas with and without magnetic field (**Figure 12C**). GFP reporter gene expression is shown in **Figure 13**. The result has shown that nearly all Ad have been bound to MNBs. The magnetic field area displayed higher GFP expression, whereas transduction efficacy was comparatively lower in the areas without magnetic field and, thus, fewer MNBs. These phenomena indicated that MNBs can be used to position cells by the external magnetic field even in the presence of hydrodynamic forces, and that MNB-based gene expression has the potential for *in vivo* use.

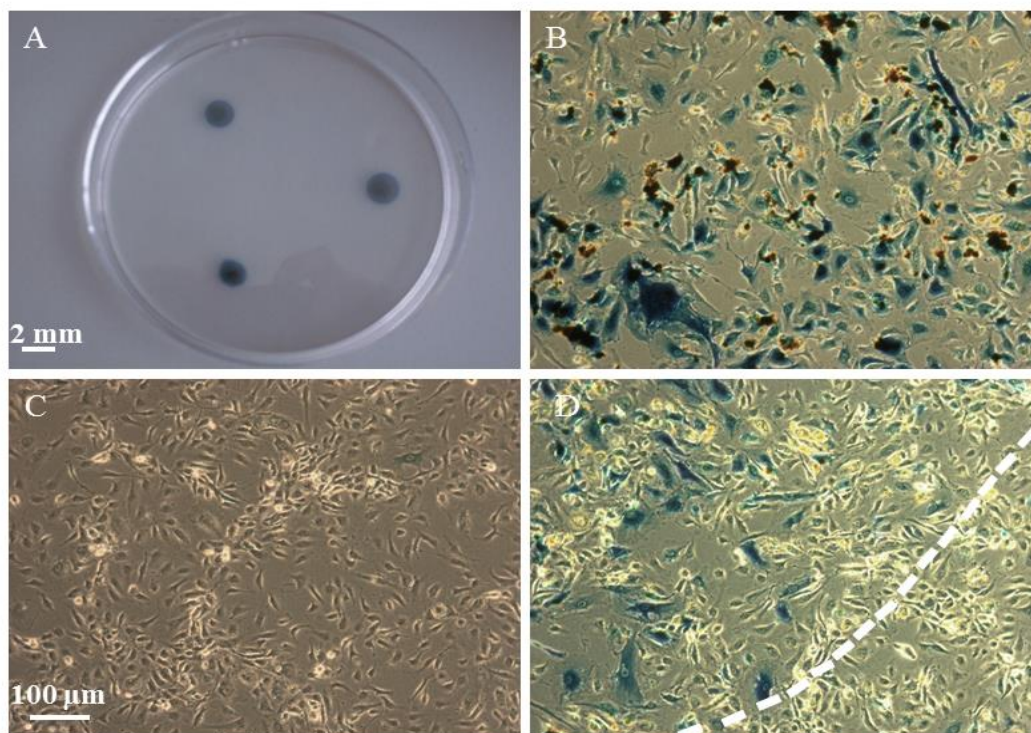


Figure 11: *In vitro*, targeted attachment of HUVECs after transduction with MNBs/Ad_{LacZ} complexes. (A) The transduced HUVECs formed a three-spot pattern determined by the locations of the magnets. (B-C) The expression of LacZ reporter gene in the adjacent area influenced by the external magnetic field and in an area far from the magnetic field. (D) The LacZ reporter gene expression was detected and a clear border was visible between the areas with and without magnetic field. (A) Scale bar = 2 mm; (B-D) Scale bar = 100 μ m. (Figure 11 quoted from [173])

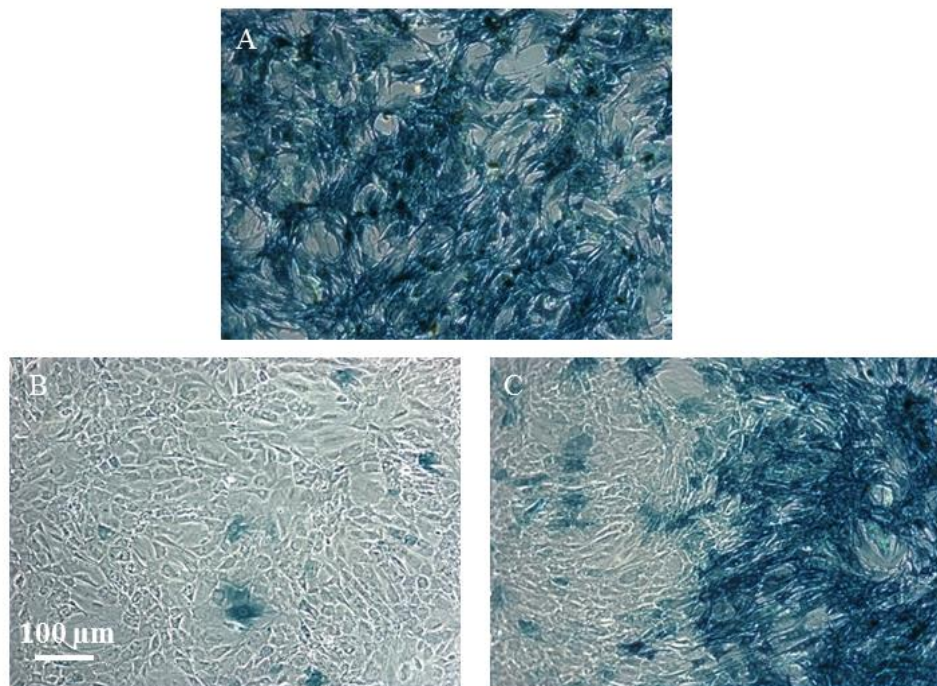


Figure 12: *In vitro*, targeted attachment of MSCs after transduction with MNBs/Ad_{LacZ} complexes. (A-B) The expression of LacZ reporter gene in the adjacent area influenced by the external magnetic field and in an area far from the magnetic field. (C) The reporter gene LacZ expression formed a clear border between the transduced and un-transduced MSCs. (A-C) Scale bar = 100 μm.

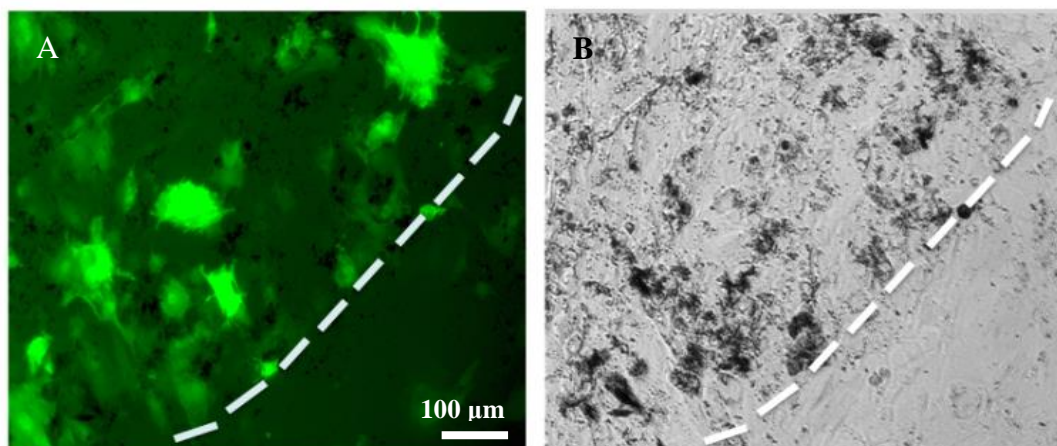


Figure 13: *In vitro* GFP expression of MSCs transduced by MNBs/Ad_{GFP} complexes and evaluation of transduction specificity. The reporter gene GFP was expressed in the confined area influenced by the external magnetic field. GFP expression formed a clear border between the areas with and without magnetic field. (A-B) Scale bar = 100 μm.

3.5 Distribution and expression of hVEGF *in vivo*

Redistribution and expression of hVEGF gene were detected and evaluated 7 days after the MNBs/Ad_{hVEGF} complexes systemic delivery. Here, a markedly higher hVEGF gene expression in myocardium was detected in the MI-M⁺MNBs/Ad_{hVEGF} group (**Figure 14A**). The hVEGF gene expression in different organs including heart, liver, spleen, lung, and kidney was determined by Real-Time PCR. Placement of a permanent magnet at the epicardium close to the heart resulted in a significant redistribution of the MNBs/Ad_{hVEGF} complexes, whereas the number of complexes in the liver was reduced compared to the MI-M⁻MNBs/Ad_{hVEGF} group (**Figure 14B**). **Figure 14C** shows a scheme of systemic delivery of MNBs/Ad_{hVEGF} complexes, guidance by an external magnetic force, targeting towards, and gene expression in the ischemic myocardium.

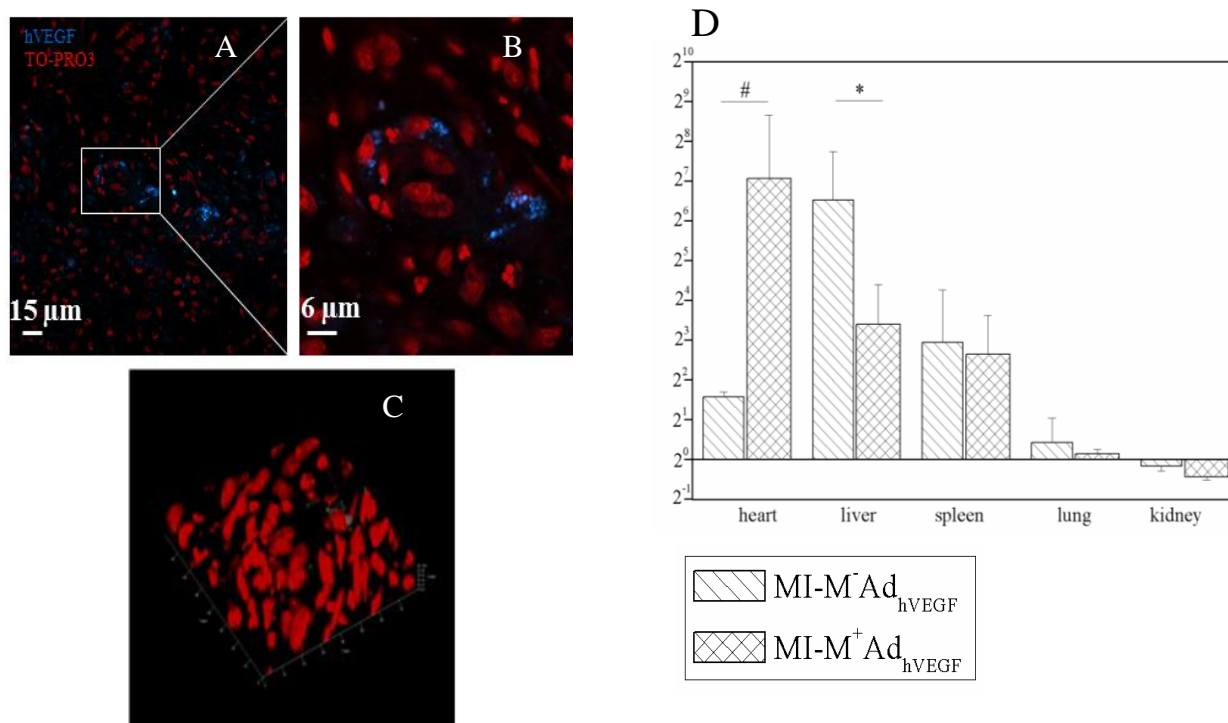


Figure 14: Real-Time PCR and immunohistochemical examination of magnetically controlled gene distribution and expression after systemic administration of MNBs/Ad_{hVEGF} complexes. (A) In MI-M⁺MNBs/Ad_{hVEGF} group, hVEGF positive transduced cells were detected in the infarcted myocardium. Sections were stained with anti-hVEGF antibody (blue) and nuclei were stained with TO-PRO3 (red). (B) Real-Time PCR analysis for hVEGF gene expression in hearts, livers, spleens, lungs and kidneys in MI-M⁺MNBs/Ad_{hVEGF}, MI-M⁻

MNBs/Ad_{hVEGF} and the MI-saline groups. The number of complexes in the heart was increased significantly compared to the MI-M⁻MNBs/Ad_{hVEGF} group * $P < 0.05$ versus hearts in MI-M⁻MNBs/Ad_{hVEGF}, # $P < 0.05$ versus livers in MI-M⁻MNBs/Ad_{hVEGF}. (A) Scale bar = 15 μm ; (B) Scale bar = 6 μm . [MI-M⁺MNBs/Ad_{hVEGF}, n = 4; MI-M⁻MNBs/Ad_{hVEGF}, n = 4; MI-Saline, n = 4] (Figure 14D quoted from [173].)

3.6 Prussian blue staining of MNBs in infarcted rat heart

In magnet positive groups, Prussian blue–positive signals were detected at the infarct site and the border region in tissue sections (**Figure 15**). Sections corresponding to the Prussian Blue–positive areas were positively tested for the presence of GFP or hVEGF protein expression in the magnet positive groups (**Figure 14A** and **Figure 16**). In contrast, little Prussian blue-positive signals were found in the magnet negative group. This result further proved that MNBs/Ad can be guided and attracted by an external magnetic field. The binding of Ad by biotin/Streptavidin with MNBs proved to be stable under *in vivo* conditions. The MNBs/Ad complexes were able to target the therapeutic gene/hVEGF towards the infarct region to promote the recovery of ischemic heart function.

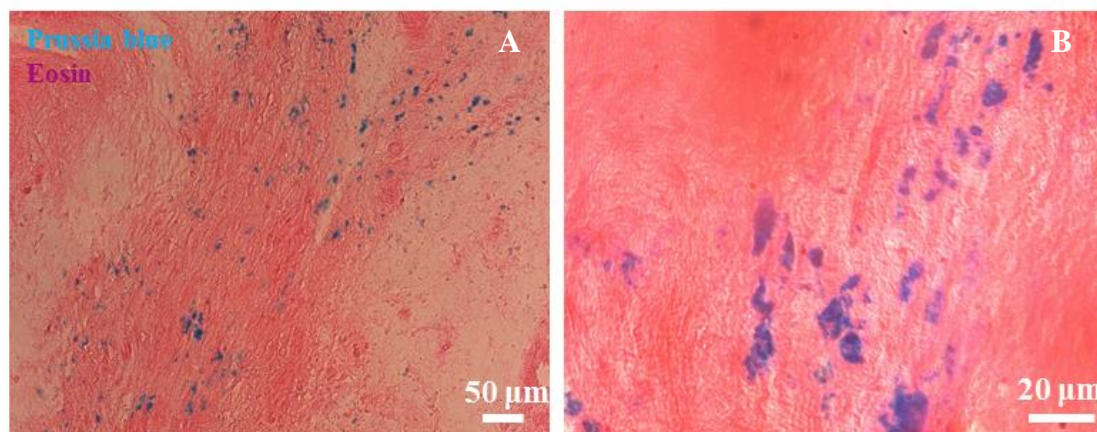


Figure 15: Analysis of MNBs in infarcted myocardium. In the MI-M⁺MNBs/Ad group, Prussian blue staining demonstrated a large number of MNBs localized in the infarcted myocardium. MNBs were stained with Prussian blue (blue) and cardiac muscle was stained with eosin (red). (A) Scale bar = 50 μm ; (B) Scale bar = 20 μm .

3.7 Expression of GFP in infarcted rat heart

Immunohistochemical staining with anti-GFP antibody proved that 24 hours as well as 7 days after systemic administration of MNBs/Ad_{GFP} complexes, strong GFP expression was present in the myocardium in the presence of the external magnetic field group. This finding demonstrated that MNBs/Ad complexes can be positioned in the infarcted myocardium by magnetic targeting.

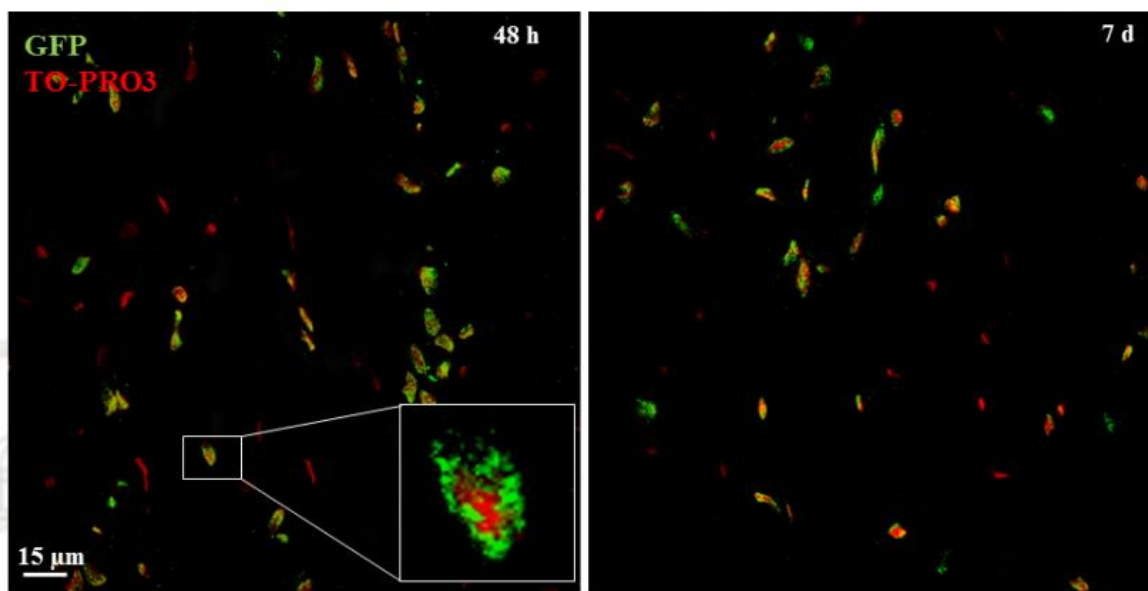


Figure 16: Immunohistochemical analysis for GFP gene expression in infarcted myocardium. In the MI-M⁺MNBs/Ad_{GFP} group, GFP positive cells were localized in the infarcted myocardium. Sections were stained with anti-GFP antibody (green) and nuclei were stained with TO-PRO3 (red). Scale bar = 15 μm. (Figure 16 redrawn after [173])

3.8 Localization of hVEGF expression in infarcted rat heart

In the MI-M⁺MNBs/Ad_{hVEGF} group, a double immunohistochemical staining with anti-hVEGF and an antibody against the endothelial marker CD31 (**Figure 17**) showed that Ad_{hVEGF} can transduce endothelium successfully. The overexpression of hVEGF may promote endothelial cell proliferation and anti-apoptosis and play an important role in replacement of cells lost in MI. Furthermore, localized expression of hVEGF was found in capillaries by immunohistochemical staining with anti-hVEGF and fluorescein tomato lectin (**Figure 18**). These results were consistent with **Figure 25** which indicated that hVEGF

expression in the border zone of the infarcted heart could increase capillary density. In addition, hVEGF expression in cardiac Troponin T-positive cells was detected in the MI-M⁺MNBs/Ad_{hVEGF} group (**Figure 19**).

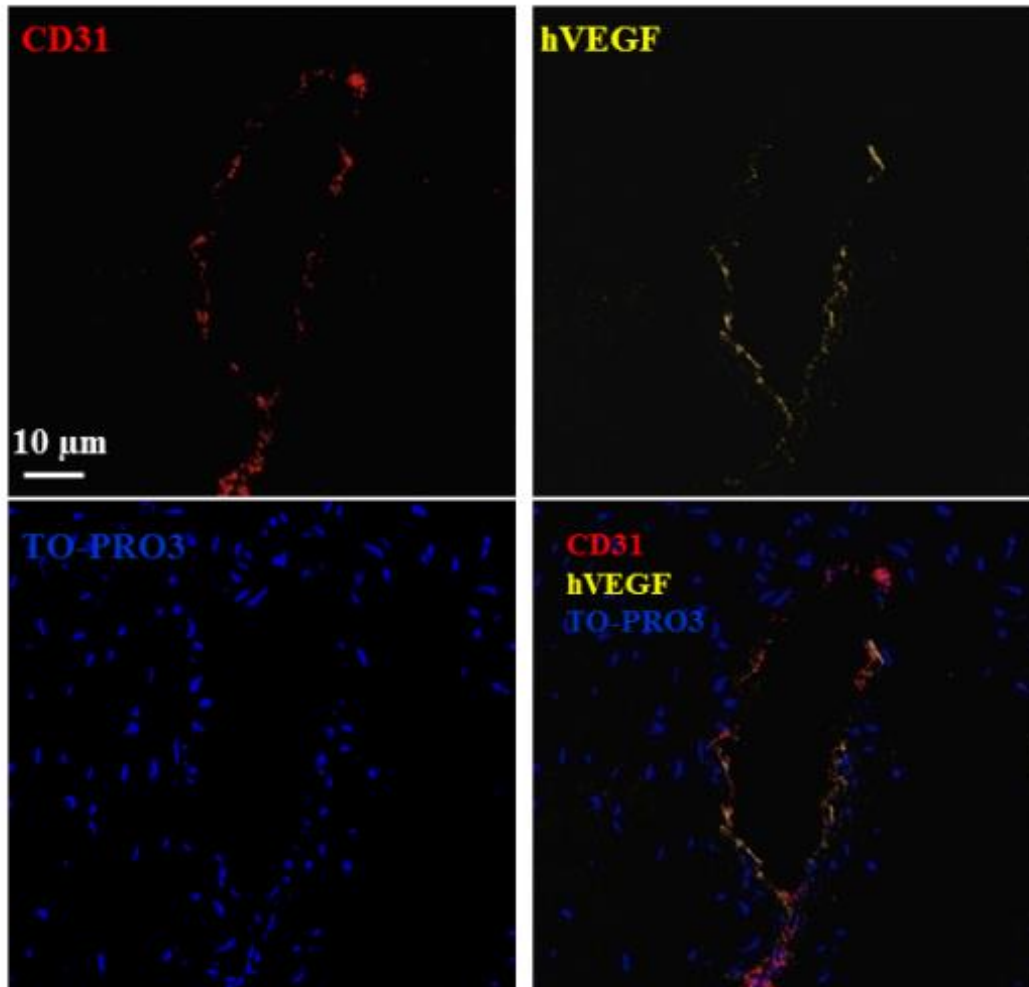


Figure 17: Localization of the expression of a systemically applied hVEGF in endothelium. Sections from the MI-M⁺MNBs/Ad_{hVEGF} group showed several transduced cells positive for hVEGF interspersed in the luminal lining of the vessel. Sections were stained with anti-hVEGF antibody (yellow), blood vessels were stained with anti-CD31 (red) and nuclei were stained with DAPI (blue). Scale bar = 10 µm. (Figure 17 quoted from [¹⁷³])

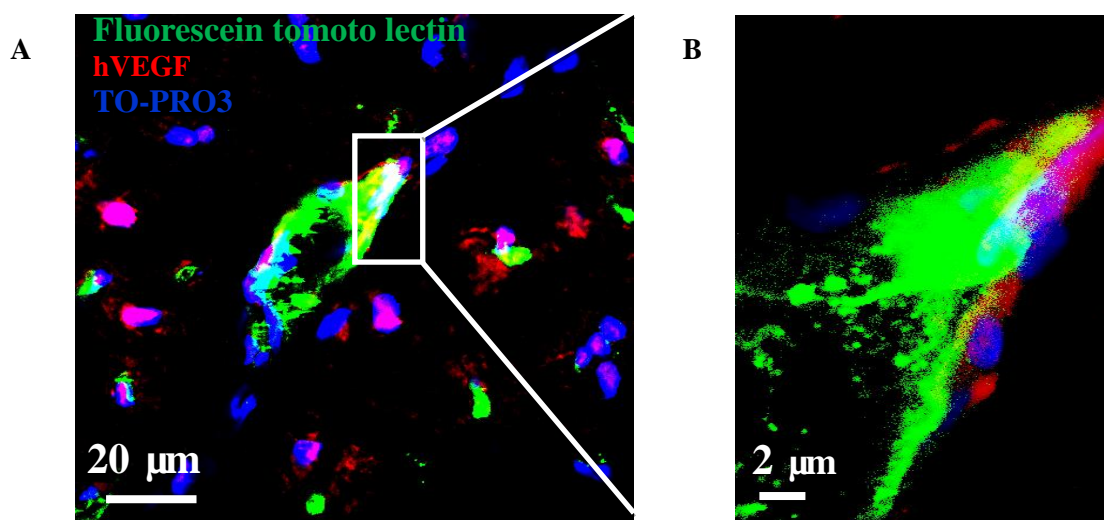


Figure 18: Localization of the expression of a systemically applied hVEGF in the capillaries. Sections from the MI-M⁺MNBs/Ad_{hVEGF} group showed Ad_{hVEGF} transduced cells positive for hVEGF in the capillaries. Sections were stained with anti-hVEGF antibody (red), capillaries were stained with fluorescein tomato lectin (green), and nuclei were stained with TO-PRO3 (blue). (A) Scale bar = 20 µm; (B) Scale bar = 2 µm.

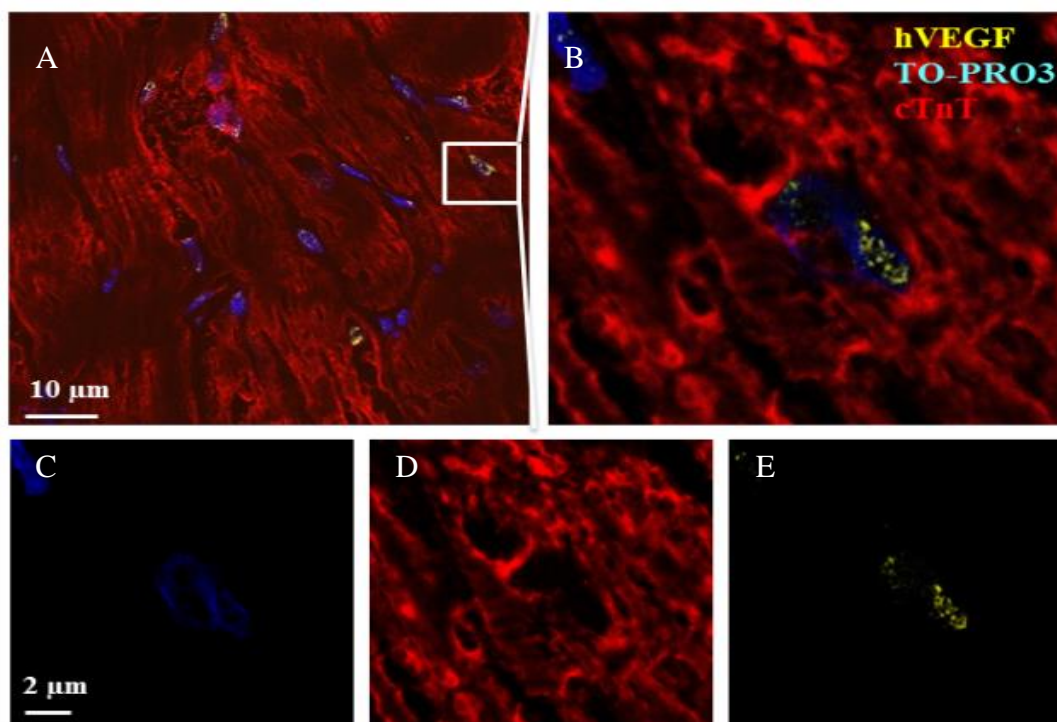


Figure 19: Occasionally hVEGF co-localized with cardiac troponin positive cells in the ischemic myocardium. Sections were stained with anti-hVEGF antibody (yellow) and anti-Troponin T antibody (red). Nuclei were stained with TO-PRO3 (blue). (A-B) Scale bar = 10 µm; (C-E) Scale bar = 2 µm. (Figure 19 quoted from [173])

3.9 Inflammatory response analysis after injection of MNBs/Ad complexes

CD8⁺T cells were mobilized to the peripheral blood after intravenous injection of MNBs/Ad complexes in the MI-M⁺MNBs/Ad_{hVEGF} group in comparison to the other groups 7 days after MI. **Figure 20** shows that the average percentage of CD8⁺T cells in peripheral blood was increased compared to the other groups, As CD8⁺T cells serve as a host defense against Ad transduction. The accumulation of MNBs/Ad complexes in to the heart by the external magnetic gradient field guiding would induce the inflammatory response and stimulate the mobilization of CD8+ T cells to the peripheral blood ¹⁸¹.

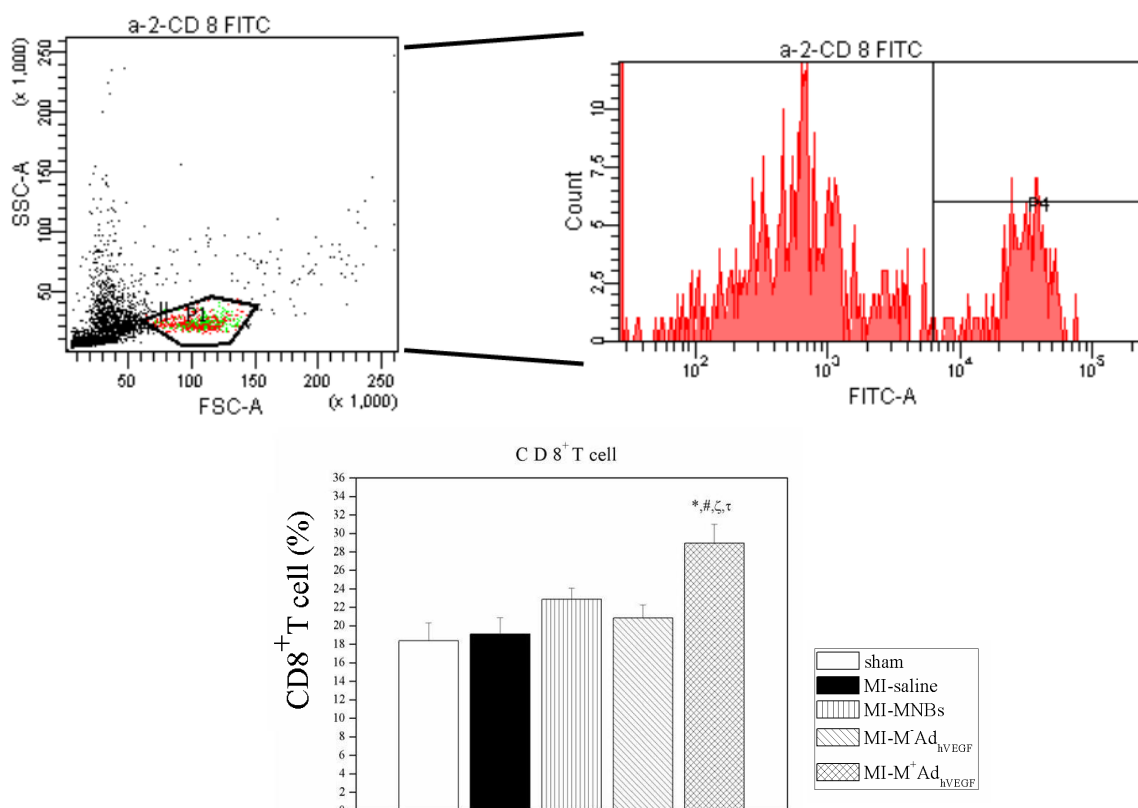
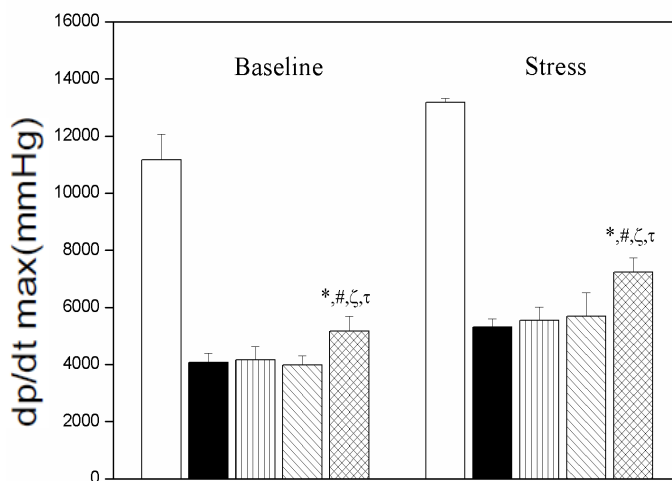


Figure 20: Inflammatory response after systemic delivery of MNBs/Ad_{hVEGF} complexes. Data are shown the results of FACS analyses of mononuclear cells from peripheral blood in the different groups. CD8⁺T cells of peripheral blood were significantly enhanced in the MI-M⁺MNBs/Ad_{hVEGF} group compared to sham and other MI treated groups. Data are mean values \pm SEM. * $P < 0.05$ MI-M⁺MNBs/Ad_{hVEGF} versus sham, # $P < 0.05$ versus MI-saline, ζ $P < 0.05$ versus MI-MNBs and τ $P < 0.05$ versus MI-M⁺MNBs/Ad_{hVEGF}. [MI-

M⁺MNBs/Ad_hVEGF, n = 4; MI-M⁻MNBs/Ad_hVEGF, n = 4; MI-MNBs, n = 4; MI-Saline, n = 4 and sham-operated, n = 4] (Figure 20 quoted from [173])

3.10 MNBs/AdhVEGF complexes injection improved cardiac function

In the MI-M⁺MNBs/Ad_hVEGF group, systolic and diastolic properties of the infarcted LV were improved both at baseline condition and under stress induction compared to the other groups. Hemodynamic measurements are summarized in Table 1. Left ventricular **peak rate of maximum pressure rise (dp/dt max)** and **peak rate of maximum pressure decline (-dp/dt max)**, two commonly used indexes of myocardial contractility were markedly decreased in all MI treated groups compared to the sham group (**Table 1**). However, in the MI-M⁺MNBs/Ad_hVEGF group, dp/dt max was significantly enhanced at baseline and under stress when compared to other MI treated groups (**Figure 21**). Furthermore, I observed an obvious enhancement in the -dp/dt max in the MI-M⁺MNBs/Ad_hVEGF group, demonstrating an increased diastolic relaxation of the myocardium in this group. Accordingly, **maximum pressure (P max)** was significantly higher both at baseline and under dobutamine stress in the MI-M⁺MNBs/Ad_hVEGF group. Heart rate was only moderately increased, in contrast to other MI treated group (**Figure 22**). hVEGF treatment produced a considerable increase of LV **ejection fraction (EF)** compared to MI-M⁻MNBs/Ad_hVEGF and other MI treated groups under stress induction (**Figure 21**). Thus, targeted hVEGF treatment significantly enhanced contractility, decreased stiffness and increased elasticity of the LV.



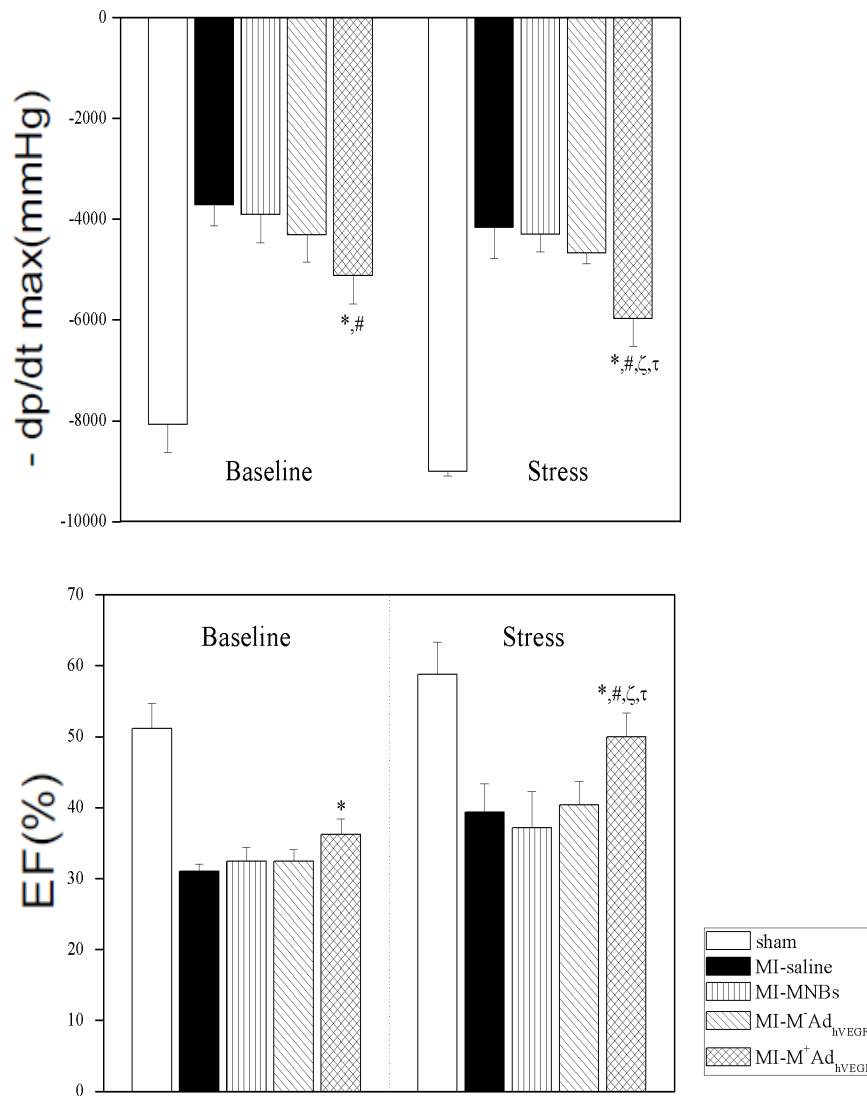


Figure 21: Intravenous MNBs/Ad_{hVEGF} injection restored cardiac function 4 weeks after MI assessed by catheterization. Left ventricular function both at baseline and under the stress condition revealed the increments of left ventricular dp/dt max and -dp/dt max under baseline and dobutamine stress compared to the MI-M⁻MNBs/Ad_{hVEGF} group. Moreover, the EF was enhanced under dobutamine stress compared to the MI-M⁻MNBs/Ad_{hVEGF} group. Data are mean values \pm SEM. * $P < 0.05$ MI-M⁺MNBs/Ad_{hVEGF} versus sham, # $P < 0.05$ versus MI-saline, ζ $P < 0.05$ versus MI-MNBs and τ $P < 0.05$ versus MI-M⁻MNBs/Ad_{hVEGF}. [MI-M⁺MNBs/Ad_{hVEGF}, n = 10; MI-M⁻MNBs/Ad_{hVEGF}, n = 10; MI-MNBs, n = 10; MI-Saline, n = 10 and sham-operated, n = 5] (Figure 21 quoted from [173])

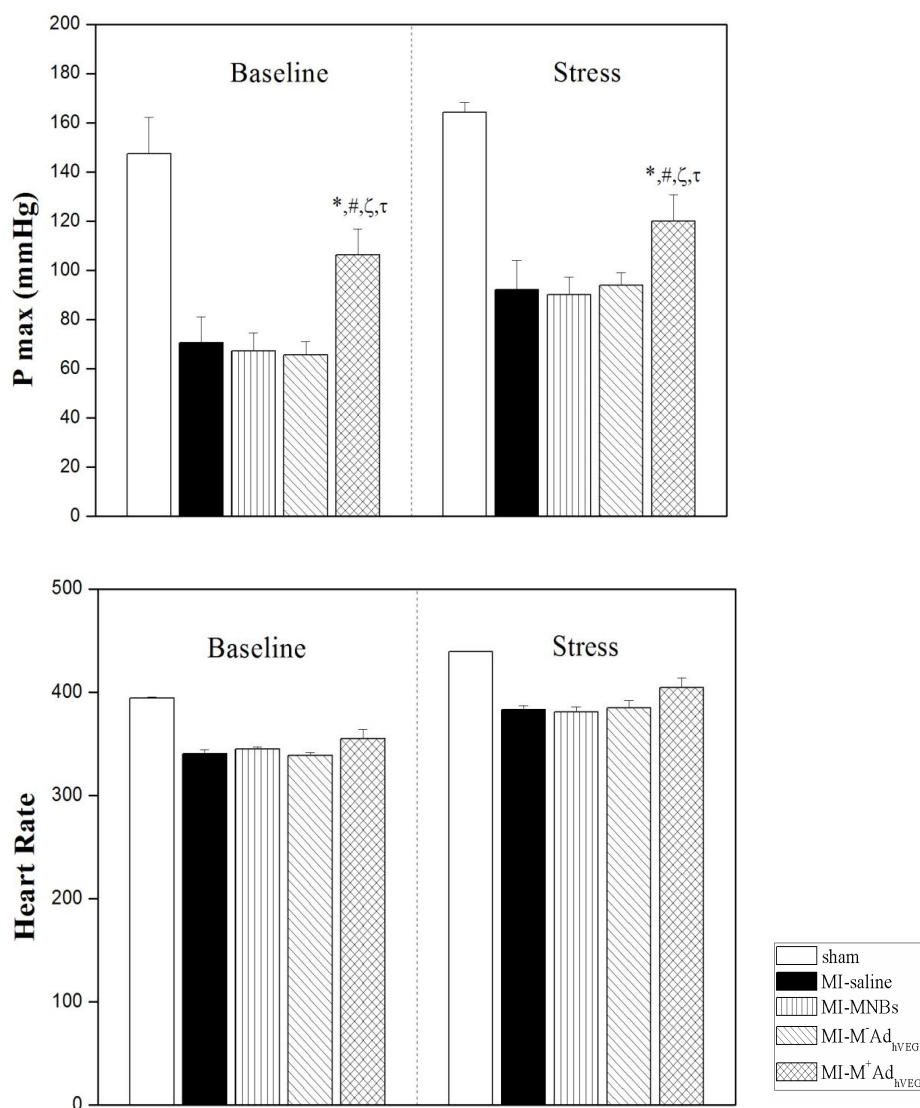


Figure 22: Intravenous MNBs/Ad_{hVEGF} injection restored cardiac function 4 weeks after MI, as assessed by catheterization. Left ventricular function at both baseline and stress conditions revealed the increments of left ventricular P max and heart rate under baseline and dobutamine stress compared with the MI-M⁺MNBs/Ad_{hVEGF} group. Data are mean values \pm SEM. * $P < 0.05$ MI-M⁺MNBs/Ad_{hVEGF} versus Sham, # $P < 0.05$ versus MI-saline, ζ $P < 0.05$ versus MI-MNBs and τ $P < 0.05$ versus MI-MNBs/Ad_{hVEGF}. [MI-M⁺MNBs/Ad_{hVEGF}, n = 10; MI-M⁺MNBs/Ad_{hVEGF}, n = 10; MI-MNBs, n = 10; MI-Saline, n = 10 and sham-operated, n = 5]

TABLE 1A Hemodynamics of the LV under baseline condition 4 weeks after MI

Parameter	Sham (n=5)	MI-Saline (n=10)	MI-MNBs (n=10)	MI-M ⁺ MNBs/Ad _h VEGF (n=10)	MI-M ⁻ MNBs /Ad _h VEGF (n=10)
Pmax (mmHg)	147.57±14.64	70.52±10.57*	67.32±7.34*	65.76±5.21*	106.30±10.53*,#,ζ,τ
dp/dt max (mmHg)	11175.95±893.72	4066.28 ±318.54*	4157.11±465.35*	3979.34 ±330.30*	5159.54 ±526.52*,#,ζ,τ
-dp/dt max (mmHg)	-8069.73±548.370	-3712.66±419.197*	-3903.72±566.31*	-4015.92± 531.272*	-5121.4±565.514*,#
EDV (μl)	189.53±7.64	273.38±22.48*	277.35±18.81*	280.58±24.36*	283.47±16.32*
ESV (μl)	93.16±5.91	188.84±10.65*	187.43±12.11*	189.28±14.98*	179.24 ±13.99*
SV (μl)	96.47±2.99	86.61±6.88	90.11±5.55	92.21±4.43	103.20±5.68
EF (%)	51.12±3.54	31.00±1.03*	32.41±2.01*	32.45±1.67*	36.40±2.17*
HR	394.56±1.31	340.65±3.72	345.22±2.25	338.81±3.11	354.990 ±9.03

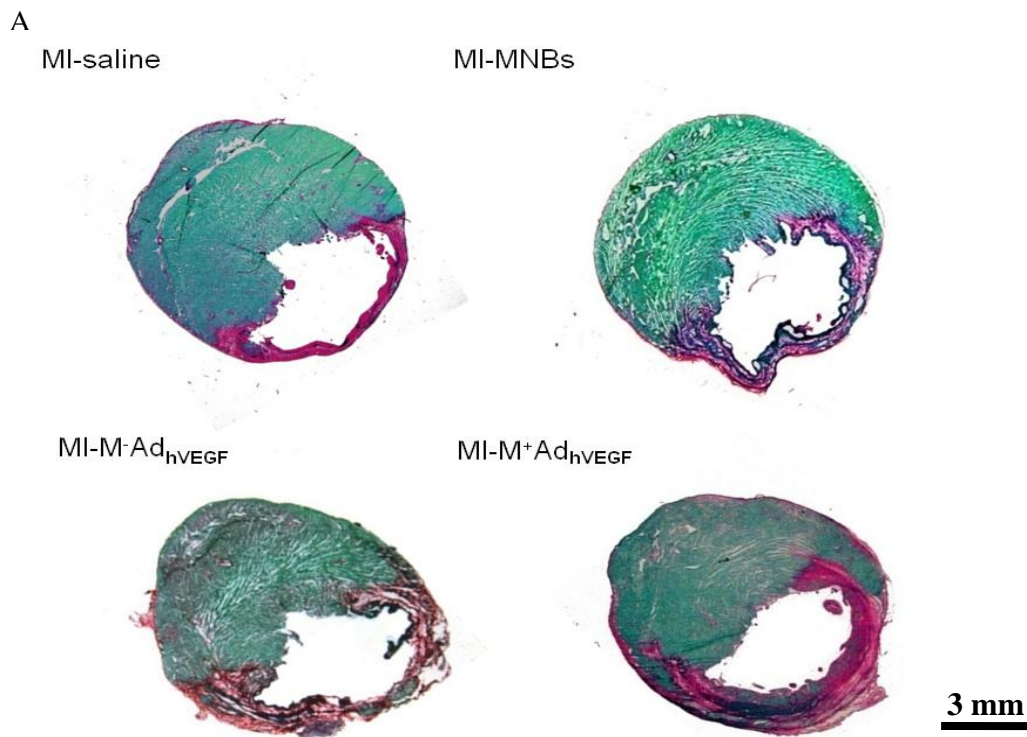
TABLE 1B Hemodynamics of the LV under stress condition 4 weeks after MI

Parameter	Sham (n=5)	MI-Saline (n=10)	MI-MNBs (n=10)	MI-M ⁺ MNBs/Ad _h VEGF (n=10)	MI-M ⁻ MNBs /Ad _h VEGF (n=10)
Pmax (mmHg)	164.39±3.86	92.29±11.86*	90.11±7.31*	93.88±5.24*	120.16±10.64*,#,ζ,τ
dp/dt max (mmHg)	13171.64±147.32	5319.63 ±270.57*	5547.43±468.45*	5685.61 ±835.52*	7229.34±501.81*,#,ζ,τ
-dp/dt max (mmHg)	-9008.18±87.54	-4438.80±151.00*	-4300.65±348.98*	-4667.98±218.60*	-5968.96±549.61*,#,ζ,τ
EDV (μl)	198.65±18.81	261.90±9.98*	275.46±10.22*	289.24±11.42*	283.25±11.30*
ESV (μl)	84.51±17.22	155.84±11.74*	162.33±9.91*	172.88±13.50*	145.33±14.26*
SV (μl)	113.66±4.26	105.41±10.65	102.13±12.21	115.42±14.04	138.25±7.3#,ζ
EF (%)	59.78±4.53	39.32±4.00*	37.12±5.11*	40.40±3.29*	49.98±3.34*,#,ζ,τ
HR	439.39±0.77	383.51±3.90	381.22±4.71	384.90±7.37	404.70 ±9.66

Table 1: (A) Hemodynamics of the LV under baseline condition 4 weeks after MI. (B) Hemodynamics of the LV under stress condition 4 weeks after MI. Values are represented as mean ± SEM, P max means maximum pressure; dp/dt indicates peak rate of maximum pressure rise (dp/dt max) and decline (-dp/dt max); EDV, end diastolic volume; ESV, endsystolic volume; SV, stroke volume; EF, ejection fraction; and HR, heart rate. Data are mean values ± SEM. * $P < 0.05$ MI-M⁺MNBs/Ad_hVEGF versus Sham, # $P < 0.05$ versus MI-saline, ζ $P < 0.05$ versus MI-MNBs and τ $P < 0.05$ versus MI-M⁻MNBs/Ad_hVEGF. [MI-M⁺MNBs/Ad_hVEGF, n = 10; MI-M⁻MNBs/Ad_hVEGF, n = 10; MI-MNBs, n = 10; MI-Saline, n = 10; and sham-operated, n = 5] (Table 1A quoted from [173])

3.11 MNBs/AdhVEGF complexes injection increased the infarct wall thickness and reduced the fibrosis

LAD ligation results in MI and causes post-infarction cardiac remodelling which plays an important role as a compensatory mechanism of heart failure. Remodelling exhibits typical histological changes including progressive ventricular chamber dilation, thinning of the left ventricular wall (Fast Green), extensive collagen deposition (Sirius Red), hypertrophy, fibrosis, and, cardiac cell apoptosis and necrosis. Fibrosis results in extensive collagen deposition (Sirius Red). Representative heart sections of 4 weeks after MI in different groups are shown in **Figure 23** and **Figure 24**. Although the infarct size did not differ significantly among different MI treated groups, LV infarct wall thickness was significantly increased in the MI-M⁺MNBs/Ad_hVEGF group compared to other MI treated groups (**Figure 23 B**). Computerized planimetry of heart cross sections indicated that more collagen deposition occurred in all MI treated groups (**Figure 24**). However, the M⁺MNBs/Ad_hVEGF group showed markedly decreased collagen deposition compared to the MI-M⁻MNBs/Ad_hVEGF group and other MI treated groups. (**Figure 24 B**).



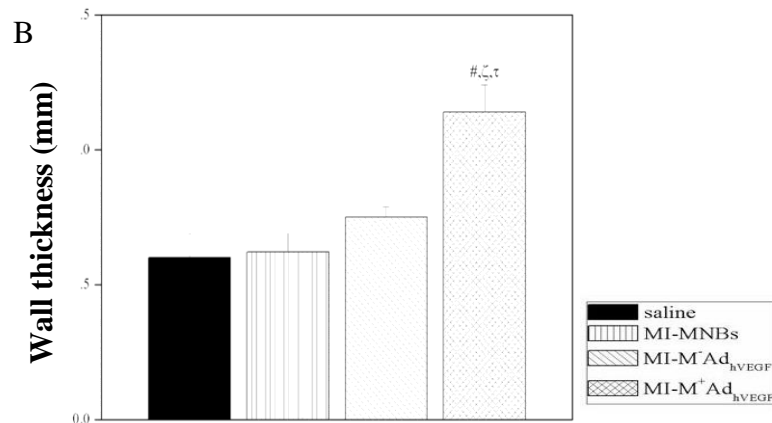
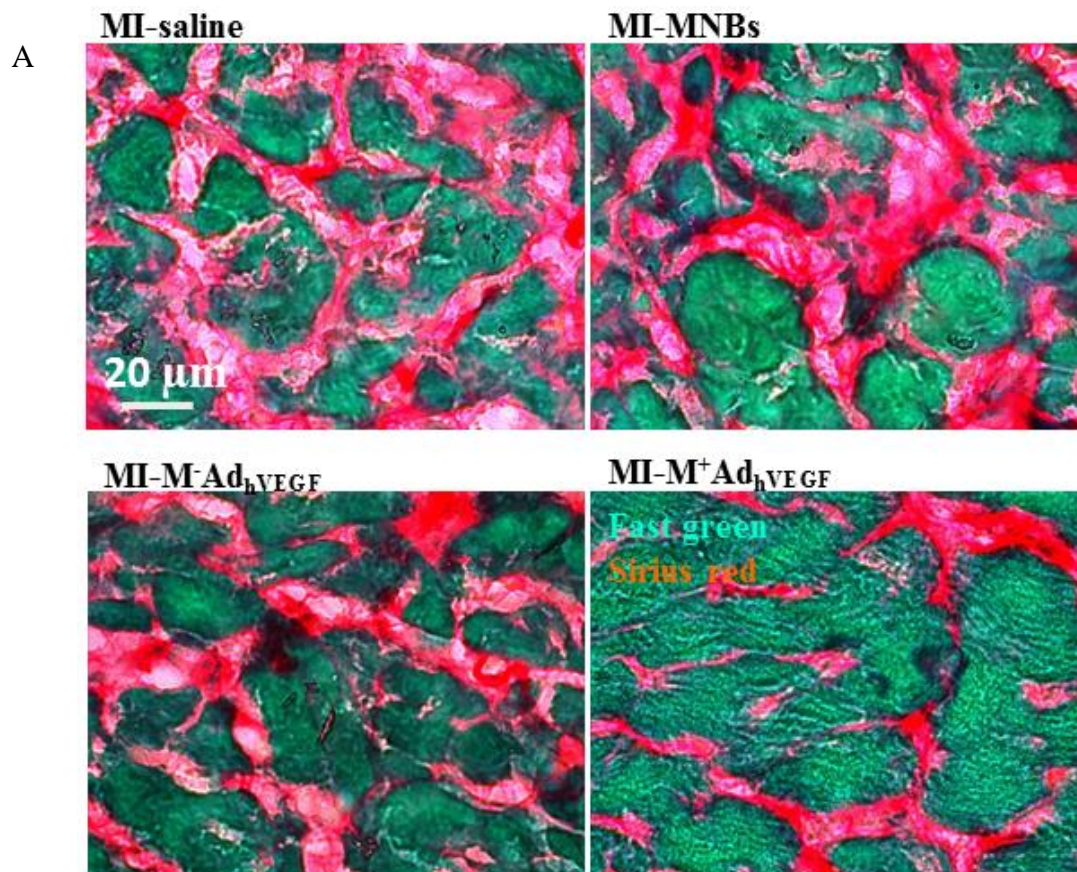


Figure 23: Effects of intravenous MNBs/Ad_{hVEGF} injection on cardiac remodelling 4 weeks after MI. (A) Representative heart cross sections stained with Sirius Red (red, fibrosis) and Fast Green (green, myocyte) from rats. (B) Infarct wall thickness was significantly increased in the MI-M⁺MNBs/Ad_{hVEGF} group compared with other MI treated groups. Data are mean values \pm SEM. * $P < 0.05$ MI-M⁺MNBs/Ad_{hVEGF} versus sham, # $P < 0.05$ versus MI-saline, ζ $P < 0.05$ versus MI-MNBs and τ $P < 0.05$ versus MI-MMNBs/Ad_{hVEGF}. (A) Scale bar = 3 mm. [MI-M⁺MNBs/Ad_{hVEGF}, n = 5; MI-MMNBs/Ad_{hVEGF}, n = 5; MI-MNBs, n = 5; MI-Saline, n = 5 and sham-operated, n = 5] (Figure 23 quoted from [173])



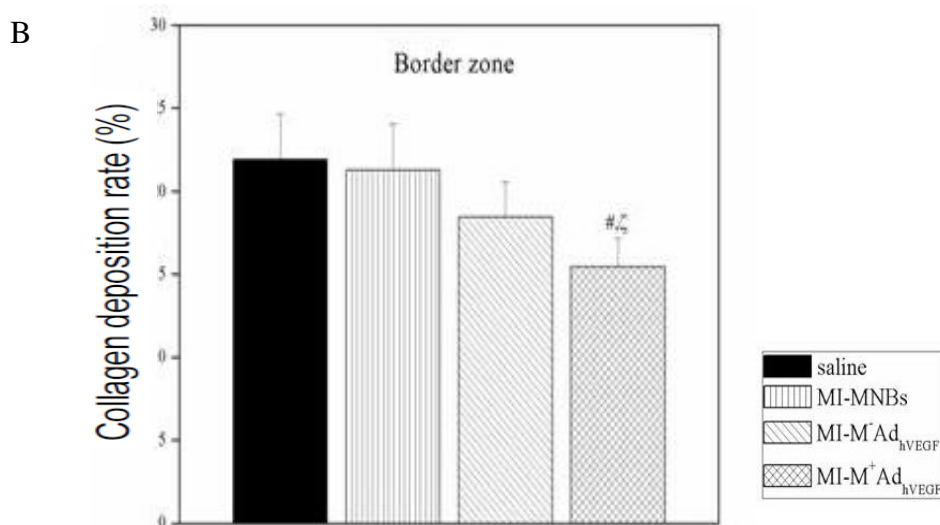


Figure 24: Fibrosis. A, Representative Sirius Red (red, fibrosis) and Fast Green (green, myocyte) immunohistochemical staining of the border zone. B, Ratio of collagen deposition declined in the MI-M⁺MNBs/Ad_{hVEGF} group compared to other MI treated groups. Data are presented as mean values \pm SEM. # $P < 0.05$ versus MI-saline, $\zeta P < 0.05$ versus MI-MNBs and $\tau P < 0.05$ versus MI-M⁻Ad_{hVEGF}. (A) Scale bar = 20 μ m. [MI-M⁺MNBs/Ad_{hVEGF}, n = 4; MI-M⁻MNBs/Ad_{hVEGF}, n = 4; MI-MNBs, n = 4; MI-Saline, n = 4 and sham-operated, n = 4] (Figure 24 quoted from [¹⁷³])

3.12 MNBs/AdhVEGF complexes injection enhanced capillary density

Capillary density was analysed by immunohistochemical staining using anti-tomato lectin and anti-CD31 antibodies (**Figure 25 A** and **Figure 26 A**) 4 weeks after MI. Capillary density in the border zone was significantly decreased in all MI treated animals. However, the MI-M⁺MNBs/Ad_{hVEGF} group showed a higher capillary density evident from both tomato lectin perfusion staining and anti-CD31 antibody staining compared to other MI treated groups (**Figure 25 B** and **Figure 26 B**).

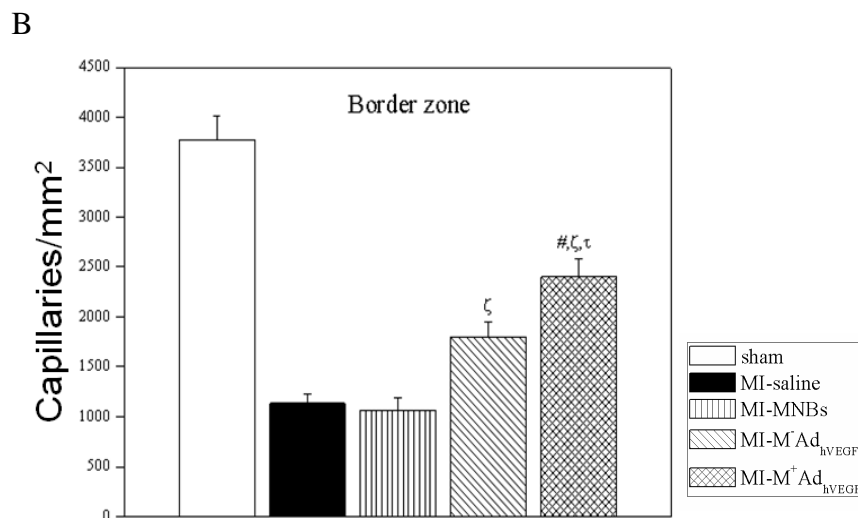
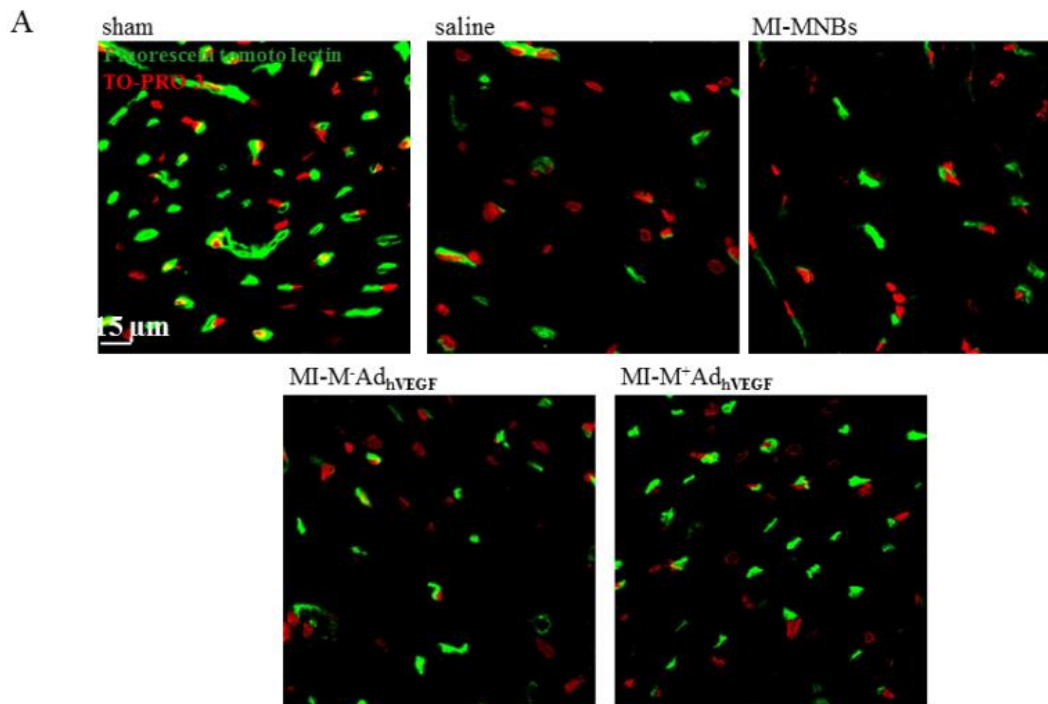


Figure 25: Intravenous MNBs/Ad_{hVEGF} administration induced angiogenesis 4 weeks after MI. (A) Representative fluorescein tomato lectin perfusion staining at the border area of infarcted myocardium. (B) Capillary density in the border zone of the LV was significantly higher in the MI-M⁺MNBs/Ad_{hVEGF} group compared to other MI treated groups. Data are mean values \pm SEM. # $P < 0.05$ versus MI-saline, $\zeta P < 0.05$ versus MI-MNBs and $\tau P < 0.05$ versus MI-M-Ad_{hVEGF}. (A) Scale bar = 15 μ m. [MI-M⁺MNBs/Ad_{hVEGF}, n = 4; MI-M⁻MNBs/Ad_{hVEGF}, n = 4; MI-MNBs, n = 4; MI-Saline, n = 4 and sham-operated, n = 4] (Figure 25 quoted from [173])

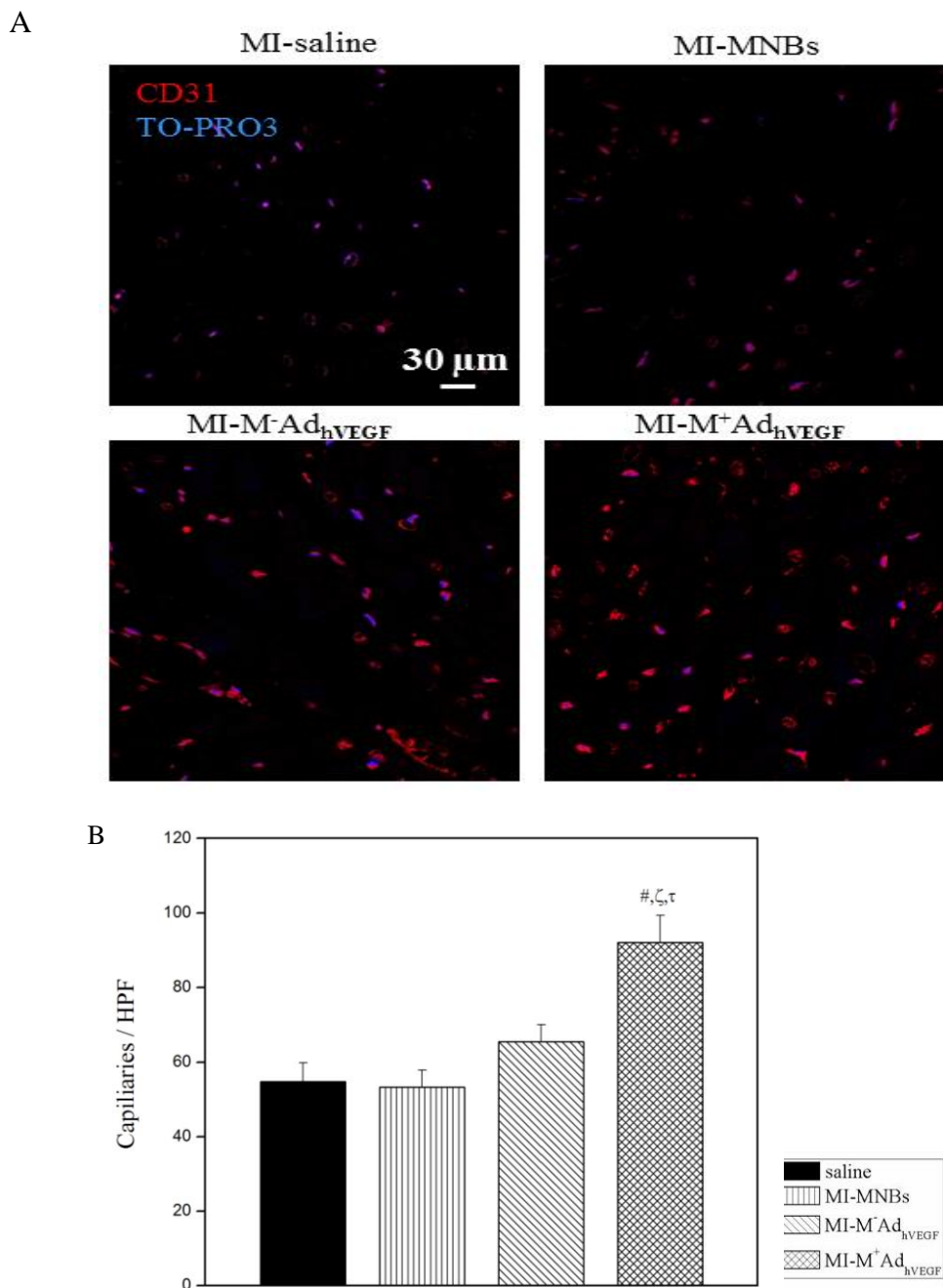
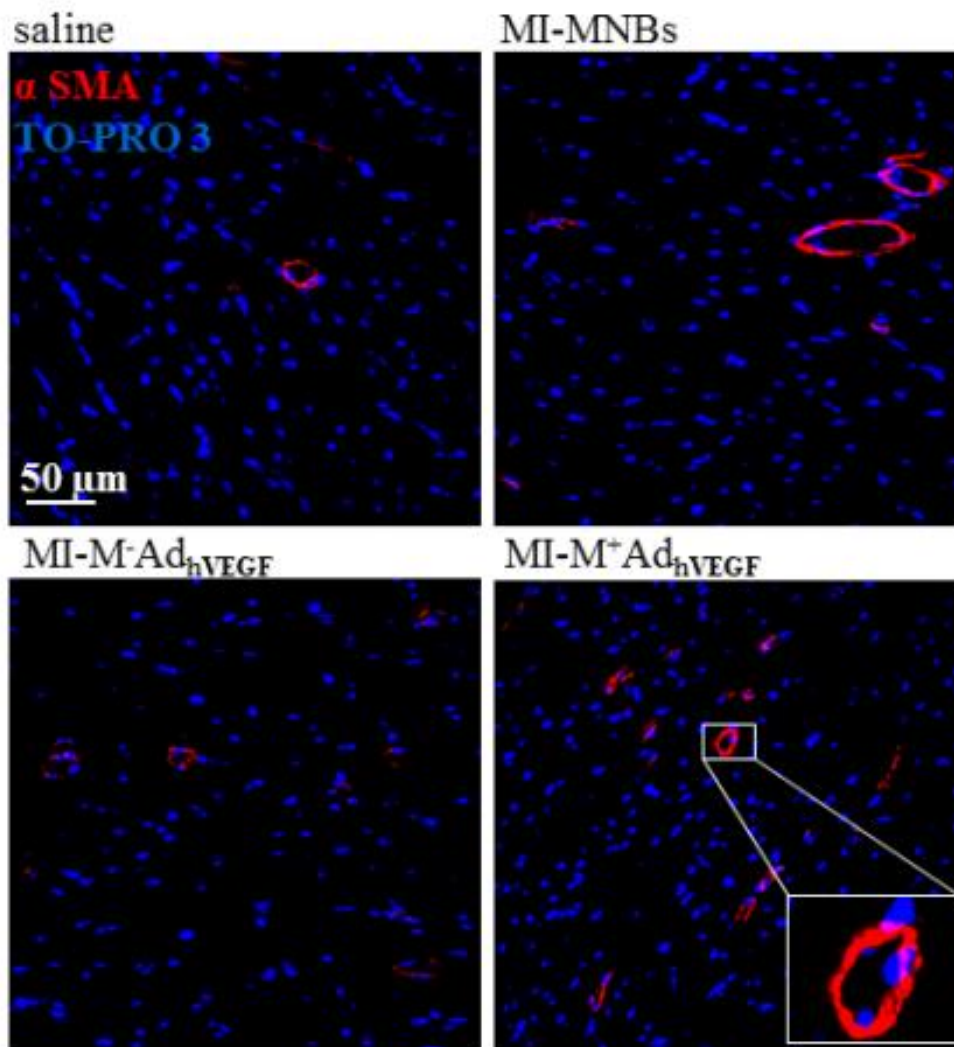


Figure 26: Intravenous MNBs/Ad_{hVEGF} delivery induced angiogenesis 4 weeks after MI. (A) Representative anti-CD31 staining at the infarct border zone. (B) Capillary density at the border zone of the LV was significantly higher in the MI-M⁺MNBs/Ad_{hVEGF} group compared to other MI treated groups. Data are mean values \pm SEM. # $P < 0.05$ versus MI-saline, $\zeta P < 0.05$ versus MI-MNBs and $\tau P < 0.05$ versus MI-M⁻Ad_{hVEGF}. (A) Scale bar = 30 μ m. [MI-M⁺MNBs/Ad_{hVEGF}, n = 4; MI-M⁻MNBs/Ad_{hVEGF}, n = 4; MI-MNBs, n = 4; MI-Saline, n = 4 and sham-operated, n = 4]

3.13 MNBs/AdhVEGF complexes injection enhanced arteriole density

MI causes arteriole loss in the ischemic cardiac tissue. Arteriole density was analysed by immunohistochemical staining (**Figure 27 A**). Indeed, in MI treated groups, hearts showed reduced densities of small (diameter < 50 μm) arterioles. Conversely, cardiac arteriole density was preserved in the border zone of the LV in the MI-M⁺MNBs/Ad_hVEGF group, in which hVEGF was overexpressed in the heart 4 weeks after MI. (**Figure 27 B**).

A



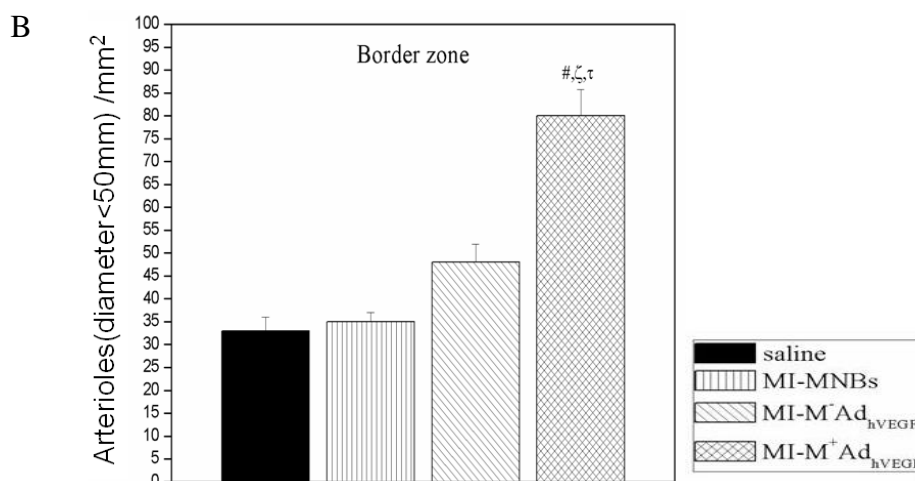


Figure 27: Intravenous MNBs/Ad_hVEGF administration induced an increase of arteriole density 4 weeks after MI. (A) Representative α SMA staining at the border area of the infarcted myocardium. (B) Arteriole density at border zone was significantly higher in the MI-M⁺MNBs/Ad_hVEGF group compared to other MI treated groups. Data are mean values \pm SEM. # $P < 0.05$ versus MI-saline, $\zeta P < 0.05$ versus MI-MNBs and $\tau P < 0.05$ versus MI-M⁻Ad_hVEGF. (A) Scale bar = 50 μ m. [MI-M⁺MNBs/Ad_hVEGF, n = 4; MI-M⁻MNBs/Ad_hVEGF, n = 4; MI-MNBs, n = 4; MI-Saline, n = 4] (Figure 27 quoted from [173])

3.14 Ad_hVEGF expression in the host connective tissue

In the experiment described below, the magnet was fixed between the third and fourth ribs. This caused inflammatory infiltration of macrophages and connective tissue was formed due to a substance foreign to the body of the rat (the magnet). Connective tissue mainly contains additional cells, such as lymphocytes, fibroblasts, and matrix proteins, e.g. collagen (**Figure 28 A**). The connective tissue was tested for hVEGF expression. However, there was little hVEGF expression in the MI-M⁺MNBs/Ad_hVEGF group and the MI-M⁻MNBs/Ad_hVEGF group (**Figure 28 B**).

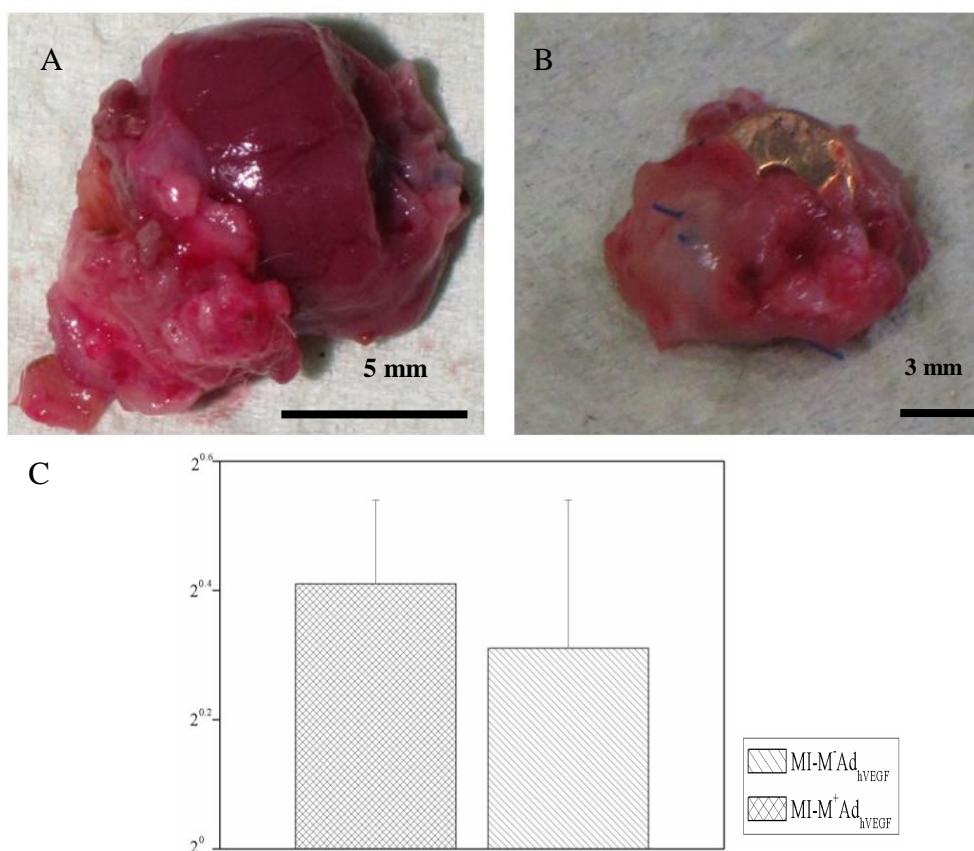


Figure 28: Magnetically controlled gene expression in connective tissue after systemic infusion of MNBs/Ad_{hVEGF}. (A) Connective tissue (B) Real-Time PCR analysis for hVEGF gene expression in host connective tissue in the MI-M⁺MNBs/Ad_{hVEGF} group and MI-M⁻MNBs/Ad_{hVEGF} group. There was no significant difference between the two groups. Data are mean values \pm SEM. (A) Scale bar = 5 mm; (B) Scale bar = 3 mm. [MI-M⁺MNBs/Ad_{hVEGF}, n = 3; MI-M⁻MNBs/Ad_{hVEGF}, n = 3]

3.15 Matrigel injection improved cardiac function

In the MI-M group, P max, dp/dt max, -dp/dt max, and EF of the infarcted LV were improved at baseline condition compared to the MI-PBS group. Hemodynamic measurements are summarized in **Table 2**

Hemodynamics of the LV 4 weeks after MI				
Parameter	Sham (n=6)	MI-PBS (n=11)	MI-M (n=11)	P *
P max (mmHg)	142.67±2.60	124.83±2.40	134.83±2.89	0.141
dp/dt max (mmHg)	10495.83±311.89	4171.17±298.99	5172.33±266.42	0.031
-dp/dt max (mmHg)	9811.83±323.28	3260.00±329.04	4175.00±200.96	0.039
EDV (μl)	211.17±8.51	288.17±19.82	266.67±16.77	0.426
ESV (μl)	70.50±4.92	183.00±21.23	155.50±14.75	0.312
SV (μl)	150.33±4.76	105.17±7.01	111.16±4.46	0.390
EF (%)	66.33±2.29	33.00±3.31	41.67±1.92	0.046
HR	399.50±5.04	360.83±6.25	392.00±7.02	0.007

Table 2: Values are represented as Mean ± SEM, * $P < 0.05$ versus MI-M, P max, maximum pressure; dp/dt max, peak rate of maximum pressure rise; -dp/dt max; peak rate of maximum pressure decline; EDV, end diastolic volume; ESV, end systolic volume; SV, stroke volume; EF, ejection fraction; and HR, heart rate. Table 2 quoted from [180])

3.16 Matrigel injection increased infarct wall thickness

LAD ligation consistently resulted in MI, exhibiting typical histological remodelling. Representative heart sections (4 weeks after MI) in different groups are shown in **Figure 29**. Although the infarct sizes were not significantly different between the MI-PBS group and the MI-M group, left wall thickness was significantly higher in MI-M group compared to the MI-PBS group. (**Figure 29 B**).

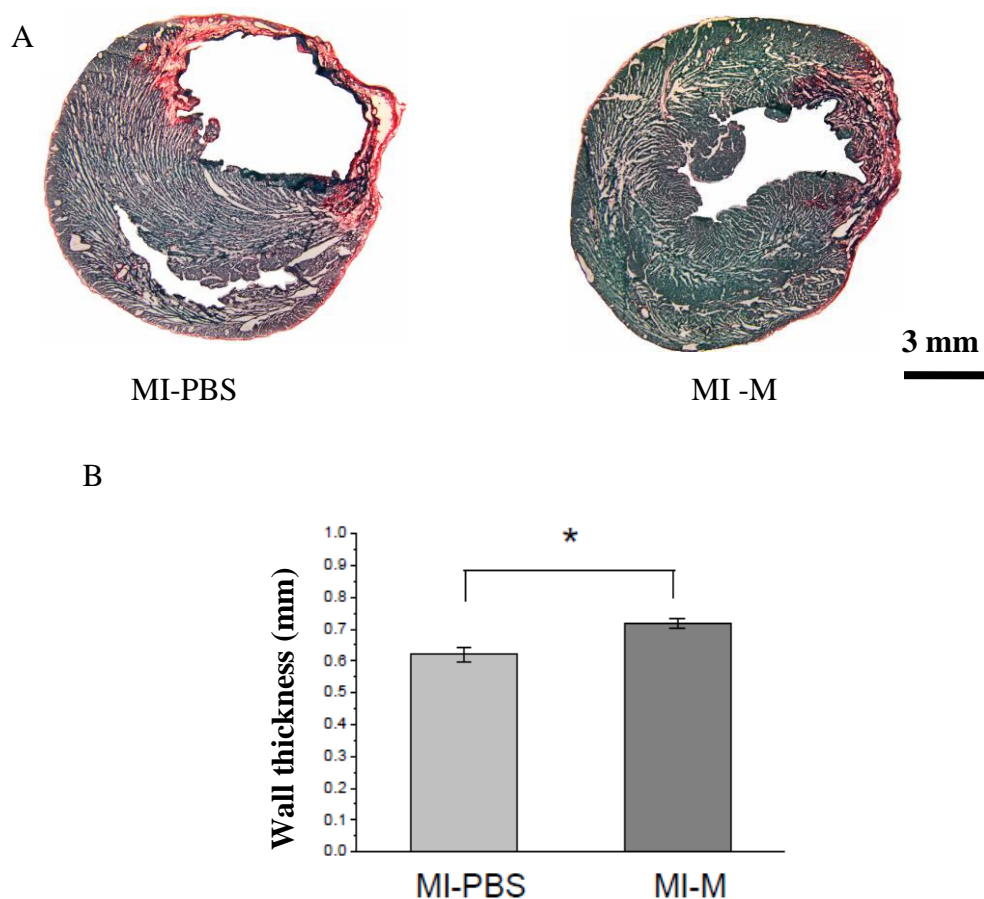


Figure 29: (A) Representative heart cross sections stained with Sirius Red (red, fibrosis) and Fast Green (green, myocyte) from rats. (B) Infarct wall thickness was significantly increased in the MI-M group compared to the MI-PBS treated group. Data are mean values \pm SEM. * $P < 0.05$ versus MI-M. (A) Scale bar = 3 mm. [MI-M, $n = 10$, MI-PBS, $n = 6$] (Figure 29A redrawn after [¹⁸⁰]; Figure 29B quoted from [¹⁸⁰])

3.17 Matrigel injection enhanced capillary density

Capillary density was evaluated by immunohistochemical staining with anti-CD31 antibody (Figure 30 A). Compared to the MI-PBS group, The MI-M group showed a higher capillary density in the border zone 4 weeks after MI. (Figure 30 B).

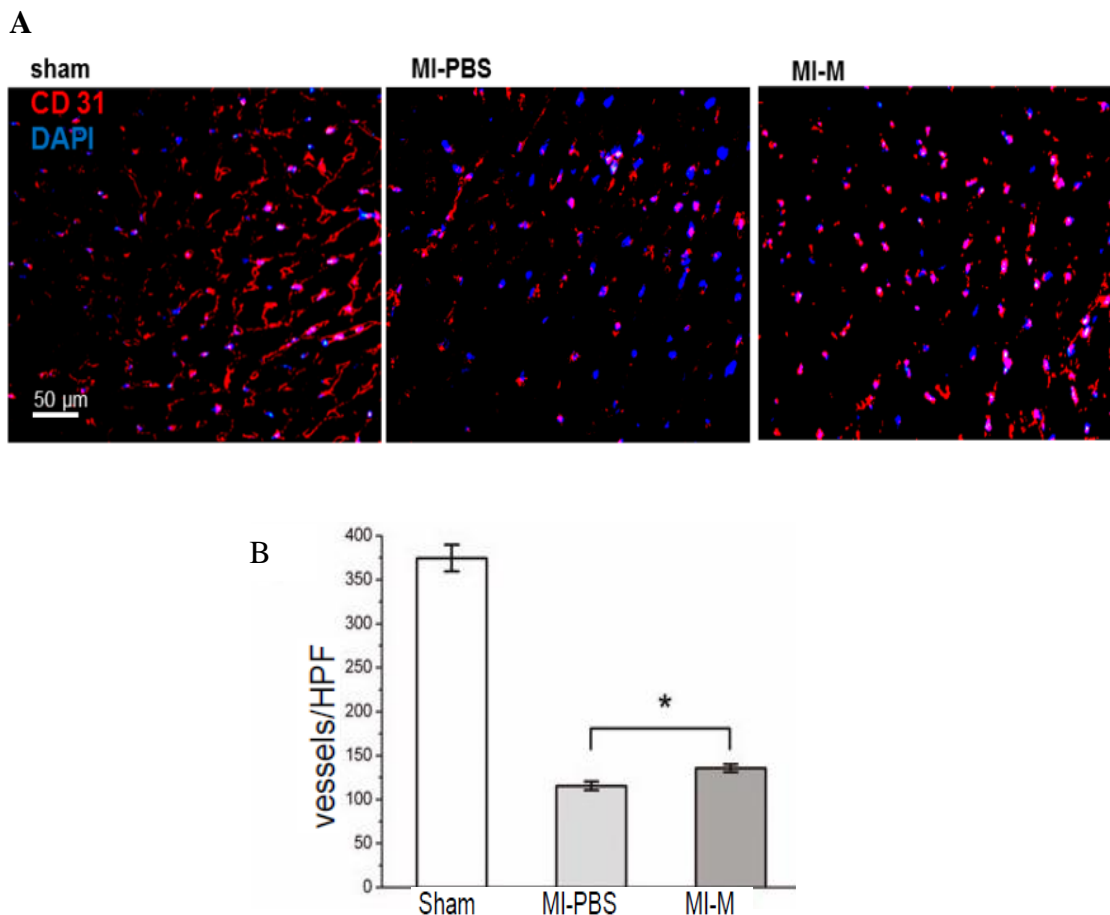


Figure 30: Local matrigel injection induced angiogenesis 4 weeks after MI. (A) Representative anti-CD31 staining at the border zone of the infarction. (B) Capillary density at the border zone of the LV was significantly higher in the MI-M⁺MNBS/Ad_hVEGF group compared to other MI treated groups. Data are mean values \pm SEM. * $P < 0.05$ MI-M versus MI-PBS. (A) Scale bar = 50 μ m. [sham, n = 6; MI-PBS, n = 6; and MI-M, n = 6] (Figure 30A redrawn after [180]; Figure 30B quoted from [180])

3.18 Matrigel injection increased CD34⁺ and c-kit⁺ cell recruitment

C-kit⁺ and CD34⁺ stem cell homing after matrigel injection was evaluated by immunohistochemical staining (Figure 31 and Figure 32). The c-kit⁺ stem cell number was significantly increased in the MI-M group compared with the MI-PBS group (Figure 31 B). Similarly, there were a markedly higher number of CD34⁺ cells in the MI-M group compared to the MI-PBS group (Figure 32 B).

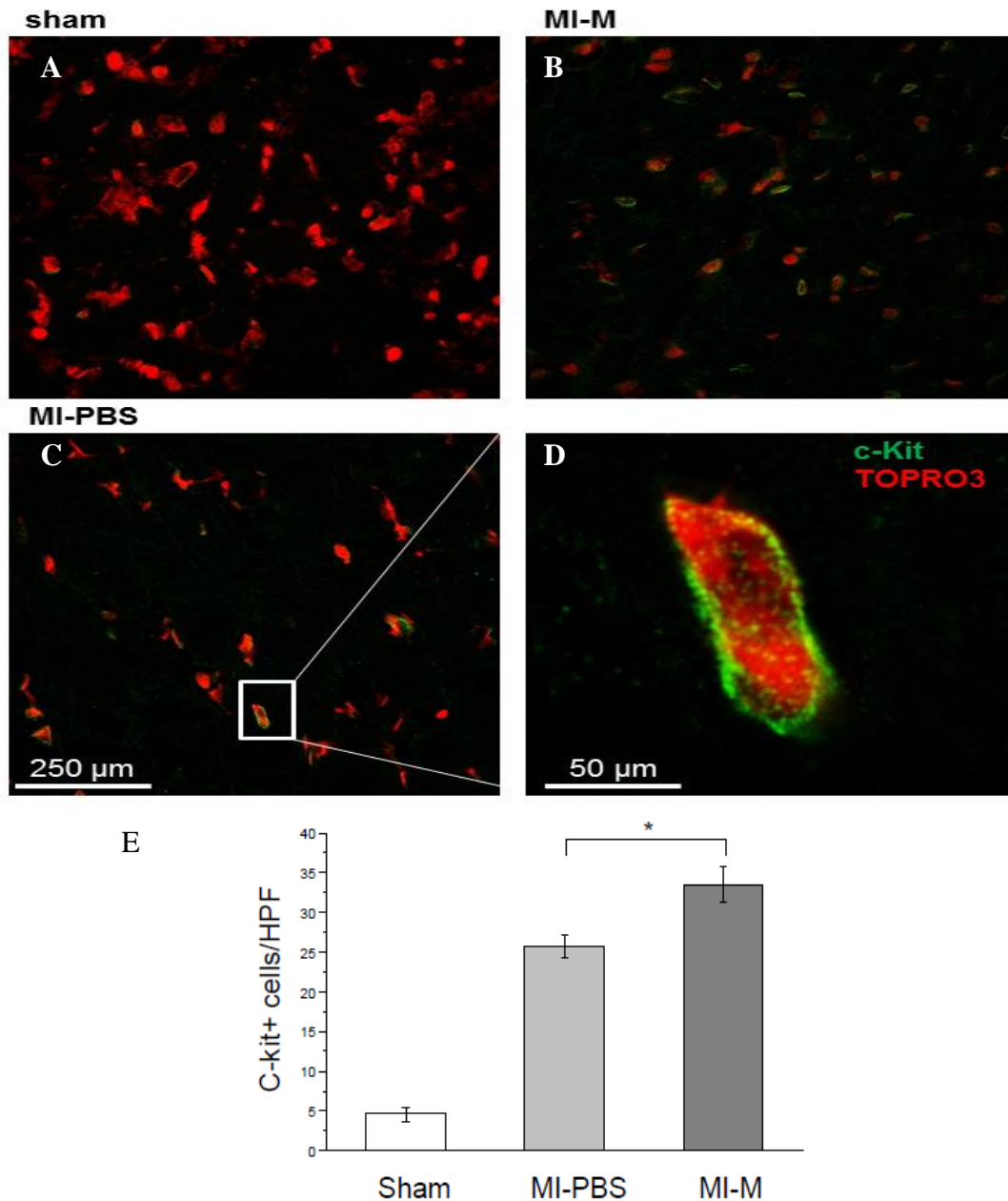


Figure 31: Local matrigel administration improved the homing of c-kit⁺ cells. (A) Representative immunohistochemical staining for c-kit⁺ cells in three groups. C-kit⁺ cells were detected at the border zone 4 weeks after MI. (B) The number of c-kit⁺ cells in the MI-M group was significantly increased than in the MI-M group, and only few c-kit⁺ cells can be detected in the sham group. Data are mean values ± SEM. * $P < 0.01$ versus MI-M. (A-C) Scale bar = 250 μm ; (D) Scale bar = 50 μm . [MI-M, $n = 5$; MI-PBS, $n = 5$, sham $n = 5$]. (Figure 31A-D redrawn after [180]; Figure 31E quoted from [180])

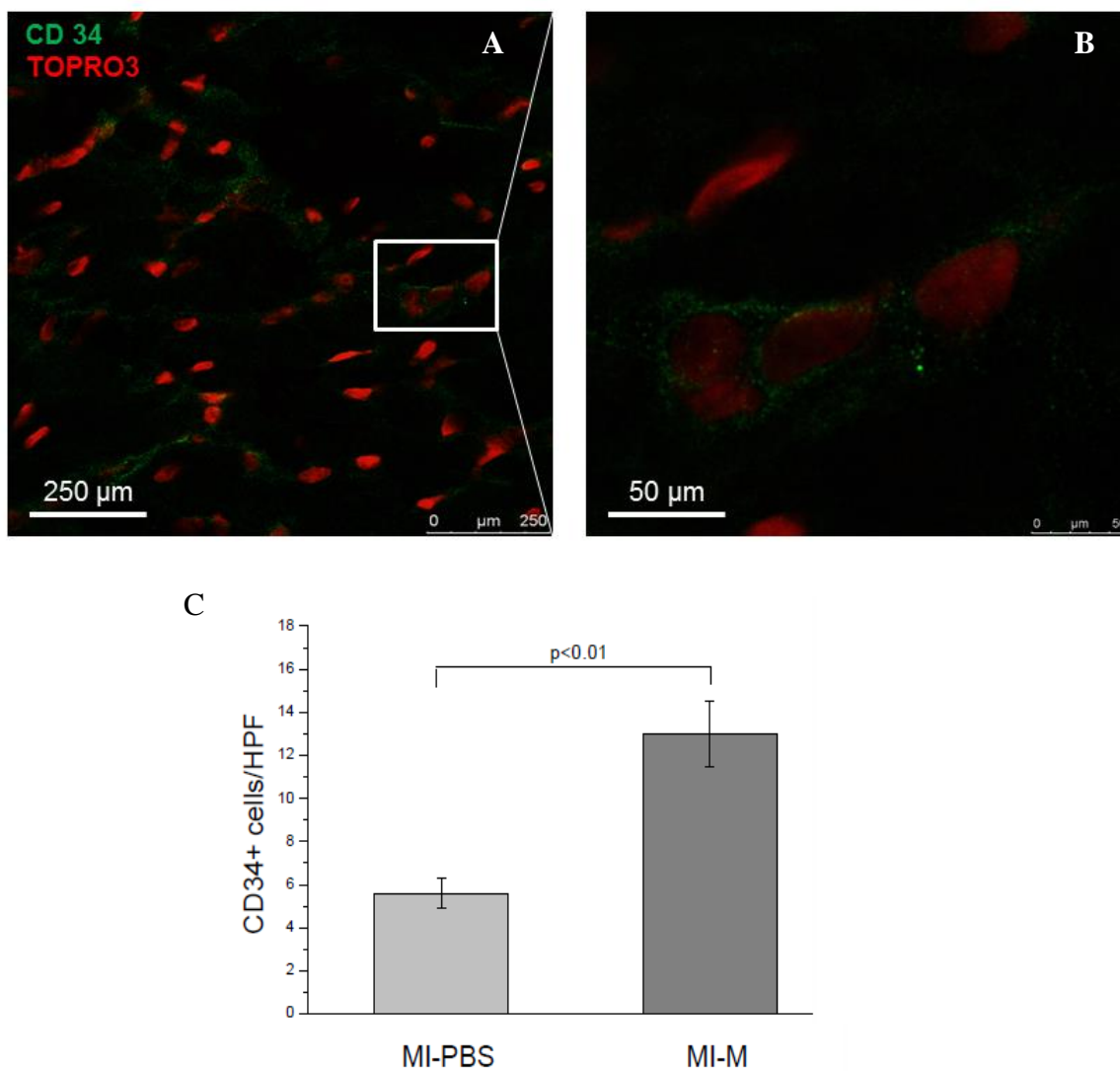


Figure 32: Local matrigel administration improved the homing of CD34+ cells. (A) CD34+ cells were detected at the border zone 4 weeks after MI. (B) The number of CD34+ stem cells in the MI-M group was significantly increased compared to the MI-PBS group. Data are mean values \pm SEM. $P < 0.01$ versus MI-M. (A) Scale bar = 250 μ m; (B) Scale bar = 50 μ m [MI-M, $n = 5$; MI-PBS, $n = 5$]. (Figure 32A-B redrawn after [180]; Figure 32C quoted from [180])

4 Discussion

4.1 MNBs/Ad_{hVEGF} complexes for cardiac repair

In the present work, a new concept of magnetofection by employing MNBs/Ad complexes was introduced. *In vitro*, the MNBs/Ad complexes' transduction efficacy and cytotoxicity in HUVECs was optimized, and the physical and chemical properties of MNBs/Ad complexes were characterized. Attachment of Ad to MNBs was complete at the optimal binding ratio. Moreover, at this binding ratio, higher transduction efficiency and comparatively lower cytotoxicity was achieved by MNBs/Ad complexes guided by external magnetic force. In addition, therapeutic genes introduced via MNBs/Ad complexes were expressed only in the defined area by magnetic guiding. *In vivo*, in a rat MI model, an epicardial magnet attracted transduction with a reporter gene, GFP or a therapeutic gene, hVEGF in the injured cardiac tissue successfully after systemic delivery of MNBs/Ad complexes (**Figure 33**). Overexpression of hVEGF promoted capillary and arteriole densities, reduced fibrosis, decreased left ventricular wall thinning, increased hemodynamic parameters in both systole and diastole, and thus improved cardiac functional recovery¹⁷³.

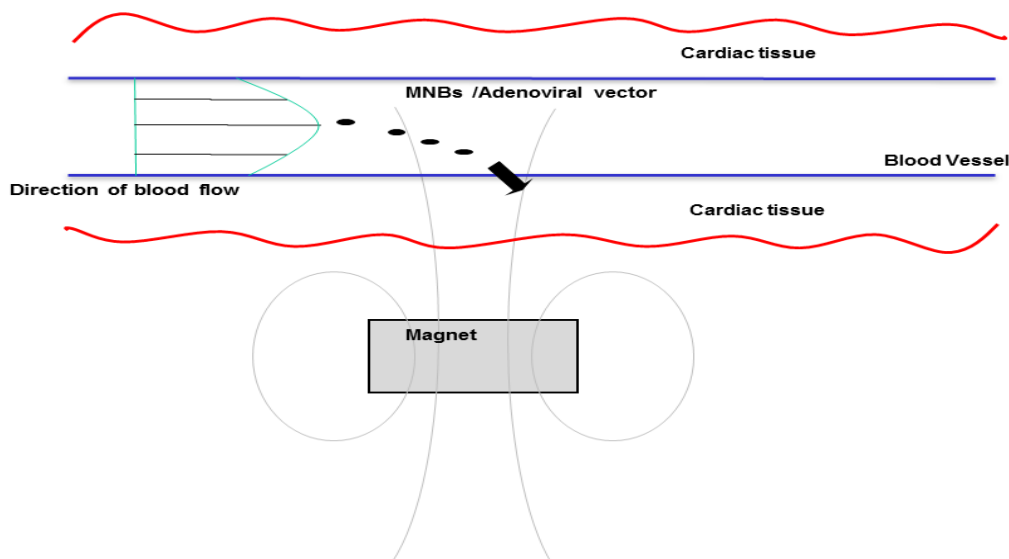


Figure 33: Schematic of MNB based Ad_{hVEGF} targeting *in vivo*. Full gray rings indicated the lines of magnetic flux due to the applied magnet. Figure 33 redrawn after [¹⁴³]

Due to MI, the ischemic myocardium can secrete a large number of cytokines including IGF-1, bFGF, and VEGF for angiogenesis and functional recovery of the heart. Angiogenesis and neovascularization are essential for supplying necessary oxygen and nutrients for wound healing. Moreover, VEGF is thought to play a key role in angiogenesis and wound healing. VEGF may regulate multiple biological functions of endothelial cells including increased production of vasoactive mediators, enhanced expression of components of the thrombolytic pathways, inhibition of thrombosis, hypotension and vasorelaxation^{131, 182}. A number of proteins belong to the VEGF family including VEGF A, B, C, D, E, and placenta growth factor. Alternative splicing of human VEGF mRNA from a single gene containing eight exons gives rise to five different isoforms consistent of 121, 145, 165, 189 and 206 amino acid residues^{132, 183, 184}. It is well known that VEGF strongly stimulates the activity of extracellular MAPK and PLC γ pathway and activation of this pathway plays an important role in the stimulation of endothelial cell proliferation as well as for neovascularisation¹²²⁻¹²⁵. VEGF can also inhibit endothelial cell apoptosis and promote the formation of new capillaries by triggering anti-apoptosis kinase pathway PI3K. In addition, VEGF may stimulate nitric oxide production which is important for anti-thrombosis and vascular protection. Yet, under ischemic conditions, the support by VEGF expression is not sufficient to form a functional capillary bed network in the ischemic zone to satisfy the demand of tissue growth concerning contractile compensation and greater request of hypertrophied myocardial cells. Thereby, the strategy consisted of the systemic delivery of Ad which encoded VEGF, so that a higher expression level of VEGF could be reached, which would be sufficient to stimulate successful neovascularization and heart functional recovery. However, *in vivo*, therapeutic gene expression in the ischemic cardiac tissue is very low after systemic administration of VEGF. Therefore, in this work tightly coupled MNBs/Ad complexes by utilizing the high affinity of the biotin-streptavidin bond were developed. The MNBs/Ad complexes were used to control selective hVEGF over-expression in the ischemic myocardium and, thus, enable improved cardiac function.

In vitro, the coupling ratio of Ad_{lac} to MNBs was optimized. At 16 μ l MNBs, 8×10^7 pfu Ad, and a MNBs/Ad ratio of 2, the MNBs/Ad complexes achieved peak transduction efficacy and

comparatively lower cytotoxicity in HUVECs. The highest transduction efficacy was 50 fold higher than that of Ad_{luc} alone. In line with these results, several other groups showed that *in vitro*, magnetofection can increase the sedimentation of the MNB-based complexes by external magnetic force, to further enhance transfection efficiency and to target the transfection. Pandori *et al.*¹⁴⁴ utilized the tight interaction between streptavidin and its ligand biotin to tether Ad to microbeads, and the conjugates improved the transduction efficacy in multiple cell lines. Moreover, concerning paramagnetic properties, the location of Ad infections was precisely controllable by a directed magnetic field. In addition, in the work of Hofmann *et al.*,¹⁴⁵ positive and negative charges were used to bind MNPs to LVs. The MNPs/LVs complexes increased viral gene transfer dramatically and the complexes could be positioned at specific areas. There are two possible mechanisms of enhanced transduction efficacy. Firstly, the MNBs/Ad complexes may sink in the medium because of guiding by magnetic force, which would allow Ad to be concentrated on the surface of the cells. The magnetic force may function as an anchor to hold Ad in proximity of the cell surface, so that Ad membrane fibre proteins may attach to cell membrane receptors for Ad more easily. Secondly, as MNBs are rapidly taken up by cells, it is a possibility that the much more MNBs/Ad complexes can be endocytosed by the cells, thus enhancing transduction efficacy¹⁴⁴. Furthermore, cellular viability and phenotype of MNBs/Ad_{luc} complex transduced HUVECs were tested. After transduction, the viability of HUVECs remained over 80% and transduced cells did not change their morphology compared with untransduced cells. This result was consistent with the work of Myokhayly' group who also demonstrated magnetofection to have but few influence on transfected cells¹⁸⁵. The average diameter of MNBs/Ad was assessed by ZetaPALS analyzer. In this experiment, two significantly different groups of particles were observed. One group consisted of free Ad (size at 100-200nm) and the other corresponded to MNBs/Ad complexes (size at 300-600nm). Results indicated that by increasing MNBs doses, the MNBs/Ad complex group became enlarged whereas the signal corresponding to free Ad was diminished. Finally, an almost constant of 100% was reached by a MNBs dose of 16 μ l. The optimal binding ratio for generating effective, non-toxic MNBs/Ad complexes was: 16 μ l MNBs, 8×10^7 pfu Ad, and a MNBs/Ad ratio of 2. This result was consistent with the MNBs/Ad transduction experiment, a fact

which may explain that the higher saturation of MNBs/Ad did not lead to a higher transduction efficacy.

Physiologically relevant models¹⁸⁶ have been used to examine the theoretical aspects of magnetic targeting *in vivo*. For most magnetic carriers, a magnetic flux density (field strength) at the target site of the order of 200-700 mTesla was proven to be necessary in order to capture particles flowing in the blood stream. Additionally, the results indicated that magnet-based therapeutic gene delivery is likely to be more effective for target sites that are close to the body surface or situated in regions of relatively slow blood flow. Generally, superparamagnetic iron oxide nanoparticles are used as magnetic components of the complex, as this type of particles exerts a strong magnetic force. The other advantage of superparamagnetic particles is their low tendency to aggregate due to magnetic dipole interactions in the absence of a magnetic field¹⁴³. Concerning the relevant *in vivo* experiment, in a rat MI model, 7 days after intravenous injection of MNBs/Ad_{hVEGF} or MNBs/Ad_{GFP} complexes, an epicardially placed magnet (1000 m Tesla), successfully accumulated the complexes, which resulted in strong reporter gene (GFP) as well as therapeutic gene (hVEGF) expression in the ischemic zone of the heart. Higher levels of hVEGF or GFP gene expression were detected by Real-Time PCR and immunohistochemical staining in the ischemic myocardium of the MI-M⁺MNBs/Ad group. These results were consistent with previous studies: Cheng and his group¹⁸⁷ successfully labelled cardiosphere-derived cells with superpara-magnetic microspheres. When magnetic force (1000 m Tesla) was applied, cells were visibly attracted towards the magnet and accumulated around the ischemic zone compared to the group without magnet application. Results confirmed that magnetic targeting enhanced cell retention (at 24 hours) and engraftment (at 3 weeks) 3 fold compared to the non-targeted group. Moreover, echocardiography analysis proved that a significant heart function improvement as well as a decrease in left ventricular remodelling occurred in the magnetic targeting group. Moreover, Li *et al.*¹⁸⁸ coupled magnetic MNBs to DNA and PEI. In a murine model, a magnet placed epicardially effectively attracted MNBs/DNA/PEI complexes to the heart, resulting in strong reporter and therapeutic gene expression in the myocardium. Additionally, Hofmann *et al.*¹⁴⁵ used charge to attach MNPs to LVs, and application of and

external magnetic field significantly guided LVs transduction to the vascular system. Experimentally, the MNBs/Ad_{lacZ} and MNBs/Ad_{GFP} complexes could be directed to specific locations defined by external magnets both *in vitro* and *in vivo*. Hence, MNBs/Ad complexes may acquire an important role for confined therapeutic gene expression targeted towards tissues or organs. In combination with viral agents, the complexes may avoid spreading of viral particles in surrounding tissues and, therefore, limit uncontrolled infection of untargeted organs. Moreover, the complexes can limit the virus load necessary for effective transduction¹⁴⁴. 7 days after MI surgery, the magnet was surrounded by connective tissue. However, hVEGF expression was very few in the connective tissue by Real-Time PCR evaluation. This result also confirmed external magnetic field can restrict gene expression to the targeted region.

In addition, in present experiments, the results proved that MNBs/Ad_{GFP} were successfully targeted towards the ischemic heart area and the transduced genes were expressed locally at different time points. It also proved that magnetic gene trapping from the blood circulation was fast and effective. Normally, one cycle of systemic blood circulation which transports oxygen-rich blood away from the heart, to the rest of the body, and returns oxygen-depleted blood back to the heart is completed in less than 3 minutes. So, theoretically, MNBs may be attracted by external magnetic force in a short time (less than half hour). Sato's group¹⁸⁹ performed a common rat carotic artery injury model and administrated endothelial progenitor cells/super-paramagnetic nanoparticle complexes in the common carotic artery under magnetic guiding for 10 minutes. They found a marked increase in cell retention at the site of injury at 24 hours after implantation *in vivo*. In the MNPs/LV transduction experiments performed by Hofmann and his group¹⁴⁵, the complexes were also injected into the carotid artery via catheter and a NdFeB magnet was placed at the right abdominal wall close to the liver for 30 minutes. Again, the complexes were found to be redistributed significantly to the liver 6 days after injection, as compared to the non-targeted group. For future use in the clinic, it is highly probable that the technique of MNB-based gene therapy will work with application of the magnet for a short time during heart surgery.

In animal experiments and clinical trials, delivery of VEGF gene or protein showed a great potential for improving cardiac function after MI^{139, 190-194}. In this study, hVEGF gene has been proven to enhance vascular network formation by HUVECs *in vitro* and stimulate endothelial cell proliferation, promoted angiogenesis, and improved right ventricular performance *in vivo*. So far, the cell types mainly overexpressing VEGF *in vivo* were not clear. In order to gain knowledge on the mechanism of VEGF-enhanced ischemic heart regeneration, the VEGF expression of endothelium as well as myocardium was analyzed and the results demonstrated that hVEGF systemic administration of Ad_{hVEGF} improved right ventricular performance. hVEGF expression in myocardium was detected by Real-Time PCR and immunohistochemical staining after 7 days MI in the MI-M⁺MNBs/Ad_{hVEGF} transduced rat group, showed hVEGF gene expression in the endothelium. This result indicated that Ad_{hVEGF} could successfully transduce endothelial cells *in vivo*. It is well known that VEGF strongly stimulates endothelial cell proliferation and induces endothelial nitric oxide synthase. The important functions of these two mediators include neovascularization, inhibition of platelet accumulation and leukocyte adhesion^{121, 195}. In addition, a significant increase in capillary and arteriole densities occurred in the border zone of ischemic heart. This is consistent with previous reports that hVEGF induced neovascularization and angiogenesis around the infarct zone^{194, 196, 197}. Moreover, I found Ad_{hVEGF} can penetrate the vessel wall and transduce cardiomyocytes to a low extent. The group of Guerrero *et al.*¹⁹⁶ showed that VEGF gene therapy promoted cardiomyogenesis after MI. Furthermore, the groups of Laguens and Vera proved that an increased number of mitotic cardiomyocytes were detected in sheep and pig MI models after overexpression of VEGF gene^{194, 197}. The increase of capillary and arteriole density, and cardiomyogenesis may act jointly to cause the LV functional improvement in hVEGF-treated animals.

VEGF gene delivery for therapeutic angiogenesis is of great importance in clinical trials. Post-infarction, a mature scar is formed which contains collagen I and collagen III as well as some newly formed microvessels. However, the neovascularization is insufficient to support the contractility of the ischemic myocardium. The aim of therapeutic angiogenesis is to induce the formation of a collateral blood supply, which allows for a sufficient support of the

ischemic tissue with oxygen and nutrients, and thus to allow for repair of the myocardial damage. Especially VEGF has a high potential to induce angiogenesis. To date, over one thousand patients with ischemic heart disease who are taking part in clinical trials assessing the functions of recombinant angiogenic growth factors or therapeutic genes encoding for growth factors, including VEGF^{135, 136}. In all these clinical trials evaluating angiogenesis therapy for ischemic heart disease, intramyocardial^{140, 198} and intracoronary¹⁴¹ deliveries are the two main ways of delivery for gene transfer. However, intravenous delivery is only used as an auxiliary method combined to intracoronary delivery¹⁹⁹. As intracoronary injection has certain advantages such as cardiac specific delivery, this technique has been widely used in most research projects as well as in clinical trials of gene and cellular therapies. Concerning intracoronary delivery of vascular growth factor genes, Laitinen *et al.*²⁰⁰ were the first to test intracoronary injection of Ad_{VEGF} in patients treated with PCI. They found that myocardial perfusion significantly increased within the Ad_{VEGF} treated group. This result also indicates that intracoronary infusion may enhance transduction efficacy, and increasing the efficacy of Ad might be of importance for the clinical outcome¹³⁵. Furthermore, the intracoronary injection of recombinant VEGF protein was initially tested in a small phase I clinical trial in patients suffering from severe CAD for whom conventional surgical procedures were not suitable. The outcome has proven that intracoronary infusion of recombinant VEGF-A protein is safe and well tolerated and may be a promising treatment to improve myocardial perfusion and exercise capacity of patients^{201, 202}. However, some research groups²⁰³⁻²⁰⁵ showed that the uptake of genes by the myocardium following intracoronary infusion was not very high, in contrast to that in non-cardiac filter organs including liver and spleen. A double blind placebo-controlled Phase II trial was designed to evaluate safety and efficacy of combined intracoronary and intravenous infusions of VEGF protein for angiogenesis after MI¹⁹⁹. A total of 178 patients were randomised to receive a 20-minute intracoronary infusion of placebo or VEGF followed by intravenous deliveries on days 3, 6 and 9, with evaluation after 2 and 3 months. The study has proven that the treatment strategy was safe and well tolerated, but it was not possible to detect any improvement in the VEGF protein compared to the placebo group. Overall, the disappointing results from clinical trials of angiogenic cytokine treatment may be due to an insufficient concentration of the

growth factors within the myocardium. Clinical trials have proven that only 3%-5% of the angiogenic cytokines which have been delivered by intracoronary infusion were taken up into the cardiac tissue^{135, 189}. In addition, intracoronary injection carries the risk to affect the endothelial lining and vessel wall with the effect of potential complications²⁰⁶.

Direct intra-myocardial injection is another main method for therapeutic gene delivery. In broad terms, the advantages of this approach include the ability to target delivery of therapeutic agents to one or more specific regions within the myocardium. By intracoronary injection, a large amount of therapeutic agents will not be taken up from the vascular compartment of the heart during their first pass, and therefore they will be delivered to other tissues²⁰⁷. Nevertheless, intra-myocardial injection has the potential to achieve higher local concentrations at target zones, such as areas of infarction and peri-infarction, with a simultaneous reduction of the required dose. Several research groups^{198, 208, 209} have proven that intramyocardial infusion was successfully performed in animal models. Maca *et al.*²⁰⁸ found that after direct injection of Ad containing VEGF into ischemic myocardium of pig hearts, both myocardial perfusion and function were significantly improved. Furthermore, the safety and efficacy of adenoviral transduction with the VEGF gene was tested in several clinical trials^{140, 198, 209}. In a study undertaken by the group of Rosengart¹⁴⁰, Ad_{VEGF} was injected intramyocardially into an ischemic area as an add-on to conventional CABG (n = 15) or as stand-alone therapy via a minithoracotomy. No evidence of systemic or cardiac-related adverse effects was found and no adenovirus was detected in peripheral blood samples. A trend towards improved myocardial perfusion and reduced angina pectoris was observed by angiography. Although of potential clinical importance, this approach for intramyocardial delivery has several limitations. Firstly, considerable risk and expense is associated with the invasive nature of this procedure. Secondly, even if mechanical function is improved, some studies have raised the question whether deleterious secondary effects of heterogeneous integration may occur, such as a risk of arrhythmia^{210, 211}.

Intravenous injection may provide a non-invasive alternative that would be tolerated well by patients with MI. However, most of the genes delivered intravenously are expressed in the

liver and only a very small portion, normally $< 0.5\%$ of the dose, is taken up by the myocardium^{189, 212}. Thus, the expression rate of the angiogenic gene in the heart may be insufficient to support angiogenesis. In the context of intravenous gene therapy, increasing cardiac specificity including the use of cardiac specific promoters and viral vectors that provide relative cardiac tropism is one of the possibilities to solve this problem. As an alternative approach, in our group, a novel technique of magnetic force-enhanced gene delivery in cardiovascular system was developed which has a great potential for rapid and efficient transduction.

Ad can efficiently infect and express their genes in a wide range of cell types and tissues containing dividing and non-dividing cells, and do not insert into host chromosomes. Still, one of the main disadvantages consists in the fact that Ad may cause a strong immune response. The inflammatory response is characterized by an increase of inflammatory cytokines and stimulation of inflammatory cell types such as macrophages, neutrophils, and CD8⁺ T cells. In the presented work, I used a recent type of Ad which were deficient in the E2, E3, and E4 regions, resulting in reduced immunogenicity²¹³. I still found an enhancement of CD8⁺ T cells mobilized to peripheral blood in the MI-Magnet⁺MNBs/Ad_{hVEGF} group 7 days after intravenous injection. It is well known that CD8⁺ T cells are believed to be directed against the viral infections and CD8⁺ T cells may secrete a series of apoptosis and necrosis-inducing cytokines including interferon- γ , TNF- α and interleukin-2^{214, 215}.

Another obvious drawback was the limited duration of Ad medicated transgene expression, because the adenoviral genome does not insert into host cell chromosomes during the infection. The experiment of transgene expression persistence showed that the effect of Ad mediated gene delivery lasted 4 weeks with a decline towards the end of that time period. Therefore, long-term expression and low immunogenicity may be better achieved by other gene carriers. AAV have several advantages including low cytotoxicity and immunogenicity, and long term expression. Normally, growth of collateral capillaries and arteries requires long term transgene expression²¹⁶. Especially AAV 8 and 9 are superior to other serotypes in

transducing myocardium and endothelium^{217, 218}. Therefore, AAV are ideal candidates for non-invasive gene transfer to the heart, and MNBs/AAV have the potential to efficiently induce therapeutic gene expression in the heart for cardiac regeneration.

In summary, the data presented above showed that MNB-assisted gene transduction may achieve not only high efficacy and comparatively low cytotoxicity, but also targeted gene expression. Importantly, *in vivo*, therapeutic gene expression in the injured myocardium by external magnetic field guiding, can promote neovascularization, reduce infarct wall thickness and improve cardiac function. So far, current experiments may serve as a proof-of-concept in a small animal model only. In the next step, additional data on MNB-based therapeutic transduction for MI, such as the required strength and duration of magnetic force in a large animal model, is important to advance the process of clinical translation. In summary, MNB-assisted Ad transfer, positioning and therapeutic gene expression is a promising technique for combined gene or cell therapies. It enables systemic administration of therapeutic genes and magnet-based, site-directed targeting.

4.2 Matrigel for cardiac repair

In the present study, local administration of matrigel into the ischemic heart significantly improved heart function, including systolic and diastolic blood pressure and EF 4 weeks after rat MI. Injection of matrigel did not reduce infarct size but markedly enhanced left ventricular wall thickness. Moreover, intracardiac injection of matrigel increased capillary density. Finally, significantly higher c-kit⁺ and CD34⁺ stem cell recruitment to the ischemic heart occurred after matrigel treatment¹⁸⁰.

In the experiments, the c-kit⁺ cell number was much higher in the MI-M group than in the MI-PBS group. It is well known that the SCF and c-kit tyrosine kinase receptor ligand plays an important role in promoting the homing of c-kit⁺ stem cells (also positive for CD34). SCF expression is upregulated in the ischemic cardiac tissue after MI. Overexpression of SCF

increases the c-kit⁺ cell mobilization towards the injured myocardium following the SCF gradient⁷¹⁻⁷⁴. Moreover, after the c-kit receptor is stimulated by SCF, c-kit⁺ cells can co-express GATA4, Nkx2.5, and myocyte-specific enhancer factor 2C which may promote the c-kit⁺ cells' potential to differentiate into cardiomyocytes²¹⁹. In addition, Wnt/ β -catenin signalling may occur in cardiac progenitor c-kit⁺ cells to stimulation of cardiomyocytes self-renewal through proliferation, maintaining the cardiomyocyte turnover in the heart after cell loss²²⁰. Several experiments confirmed that c-kit⁺ cell therapy may enhance the contractile function, promote angiogenesis and restore cardiac function^{211, 221-223}. These results were consistent with the findings in current experiments. Thereby, matrigel which contains various growth factors such as bFGF, PDGF, and TGF- β may support the homing c-kit⁺ stem cells with nutrients, thus promoting cell proliferation, inhibiting apoptosis, further improving neovascularization and cardiac function. Therefore, it is possible that the observation of an increased number of c-kit⁺ cells in cardiac tissue can be attributed to the support of matrigel.

A large number of hydrophilic natural or synthetic biopolymers can be applied for tissue engineering or drug delivery due to their flexibility, which is very similar to natural tissue²²⁴⁻²²⁶. Currently, biopolymers can be used in ischemic heart therapy²²⁷. The use of biopolymers alone can increase thickness and stabilizing of ischemic myocardium. When used as scaffolds, biopolymers may be used to deliver a diversity of stem cells or therapeutic molecules such as growth factors to improve cardiac function^{174, 228}. Fibrin as a natural cross-linked 3-dimensional biopolymer has been widely used for cardiac therapy^{227, 229-231}. In a rat MI model, several groups have proven that intramyocardial administration of fibrin biopolymer one week after MI may improve cardiac properties, decrease infarct size, and increase neovascularization^{227, 229, 230}. In a porcine MI model, Mukherjee *et al.*²³¹ successfully injected biopolymers locally, including both fibrin and alginate, a bioinert material, to prevent LV remodeling after MI. Additionally, chitosan as a linear polysaccharide has been explored for MI therapy with a view to its biocompatibility and biodegradability²³². Lu *et al.*²²⁸ showed that in a rat MI model, local delivery of chitosan biopolymer can enhance diastolic and systolic indexes, preserve the geometric dimensions LV, and decrease infarct wall thickness^{174, 233}.

Matrigel as a commercial biopolymer is derived from base membranes. Since matrigel is a 3-dimensional scaffolding matrix, it may also prevent ischemic heart remodelling by supporting the structure of left ventricular wall. The conventionally used rigid or solid matrices disrupt the continuity of the cardiac architecture, and create excess shear stress in the ischemic myocardium²³⁴. However, matrigel remains liquid until the intracardiac injection, and its 3-dimensional matrix may adapt to the geometry and structure of the left ventricular space. Kofidis' group¹⁷⁶ proved that matrigel was sufficient to improve left ventricular wall thickness 2 weeks after MI and to prevent deterioration of cardiac function. This result was consistent with current findings, which indicated that local matrigel administration may increase left ventricular wall thickness. The structural enhancement of the injured area of the LV may be the mechanism of functional cardiac tissue improvement.

Additionally, intramyocardial injection of matrigel significantly increased capillary density and promoted angiogenesis. FGF is a pro-angiogenic growth factor which may promote the formation of new vasculature¹⁷⁴. Several groups reported that local injection of FGF increased capillary density and attenuated the LV remodelling^{235, 236}. PDGF delivery recruited smooth muscle cells to support immature neovascularization. Hao *et al.*¹⁶⁹ showed that the dual release of the growth factors of VEGF and PDGF in the ischemic myocardium significantly increased the number of α -SMA containing blood vessels around the injection site 4 weeks after MI. Matrigel contains pro-angiogenic factors including both bFGF and PDGF may, thus, improve the functional recovery by promoting angiogenesis.

Matrigel plays an important role in MI therapy, but it also has some disadvantages. Matrigel is derived from the basement membrane and secreted by mouse sarcoma. Also, its components are not well defined till now and it has the potential to promote tumor cell invasion¹⁷⁶. Although, in the present work, I did not find tumor formation in the myocardium, the next step should focus on the biological mechanisms of matrigel, especially clinically relevant parameters. At present, matrigel shows some merits better than other types of biopolymers.

In summary, matrigel as a biopolymer was able to adopt the behavior of the ischemic cardiac environment, which may support the host tissue. Additionally, local injection of matrigel after MI recruited c-kit⁺ and CD34⁺ stem cells, promoted angiogenesis, reduced left ventricular wall thinning, and improved heart function. In further experiments, this type of 3-dimensional matrix may be used as a vehicle for the delivery of therapeutic stem cells to the injured heart. The appropriate matrix environment may improve cell retention and engraftment in the damaged myocardium suffering from ischemia. Matrigel alone or matrigel based cell therapy offers therefore a great potential in MI therapy.

4.3 Biotechnological techniques for myocardial angiogenesis and functional recovery

Gene therapy offers new possibilities concerning the restrictions of current treatment for cardiac ischemia. Continuous therapeutic gene expression at targeted sites may be used to regain the myocardial functions that are impaired during MI progression. VEGF is one of the best candidates for induction of therapeutically effective angiogenesis in the ischemic heart. A variety of animal MI models have proven that VEGF gene therapy may increase neovascularization²³⁷, promote vessel formation²³⁸, significantly induce angiogenesis, and improve cardiac functional properties^{237, 239}. Meanwhile, VEGF gene therapy for myocardial ischemia significantly improved cardiac function in a clinical trial²⁴⁰. Magnetofection as a novel gene delivery technique can minimize the vector dose but maintain efficiency while confining the risk to the target area^{142, 144, 241}. With application of a permanent magnet, magnetic complexes may migrate along the high magnetic gradient fields *in vitro* and *in vivo*^{189, 242}. In current experiments, a new technique of magnetofection was utilized, MNB based VEGF gene delivery. This therapy successfully increased angiogenesis and enhanced cardiac function after MI.

Biopolymers such as matrigel, fibrin, and collagen have been developed and widely studied as translatable materials for MI therapy^{164, 176, 229, 243}. Especially matrigel, as a natural biopolymer, is able to adopt the geometry of the host tissues. Furthermore, matrigel may

serve as vehicle for delivery of biologically therapeutic molecules^{183, 195}. In present experiments, the new technique of local matrigel delivery offered a less invasive and more effective approach for MI therapy. Intramyocardial administration of matrigel promoted neovessel formation, increased capillary density, and preserved LV remodeling.

Future work will serve to further analyze and evaluate the various new techniques for cardiac disease treatment and focus on clinically relevant parameters, such as the selection of suitable animal models and appropriate modes of delivery. Knowledge gained from such work may lead to a clear illustration of the effects of new biotechnological approaches for the treatment of patients with ischemic heart disease.

5 Conclusions

The objective of the present work was the development of novel biomedical techniques for cardiac regeneration employing targeted gene transfer and biomaterial-based tissue engineering. Using a rat model of MI, the therapeutic effect of stable magnetic field-guided MNBs/Ad_{hVEGF} complexes was evaluated on the one hand and intracardiac matrigel injection on the other hand. Based on my experimental results, the following conclusions can be drawn:

Targeted delivery of human VEGF gene via complexes of magnetic nanoparticle-Adenoviral vectors enhances cardiac regeneration

In this study, stable MNBs/Ad complexes were developed and systematically administered encoding hVEGF under external magnetic guidance for cardiac regeneration.

This research demonstrated that (1) High affinity and effective binding properties of biotin and streptavidin can form extremely stable magnetofection complexes. (2) The MNBs/Ad complexes could be directly targeted towards specific locations defined by an external magnet. (3) *In vivo*, magnetic force effectively targeted VEGF gene expression to the ischemic zone of the heart. VEGF expression promoted angiogenesis and improved heart function.

It follows, therefore, that systemic administration of MNBs/Ad complexes guided by external application of magnetic force may be a useful, non-invasive, gene-based therapeutical approach to enhance post-infarction myocardial repair.

Intracardiac injection of matrigel induces stem cell recruitment and improves cardiac functions in a rat MI model

In this study, intracardiac delivery of matrigel recruited CD34⁺ and c-kit⁺ stem cells, promoted angiogenesis and improved cardiac function after ischemia.

Findings indicated that: (1) Matrigel contained ECM components which may prevent negative remodelling of the myocardium by providing three-dimensional support to the infarcted area. (2) Matrigel contained various growth factors and a natural micro-environment for the homing of c-kit⁺ and CD34⁺ cells which may provide additional nutrients to the ischemic myocardium, promote cell proliferation and mediate angiogenesis.

Hence matrigel as a three dimensional matrix is able to support host tissue, influence stem cell recruitment as well as survival and cell proliferation. In present study, matrigel therefore shows promising results to treat MI and human derived “matrigel analogs” may have a great potential for cardiac regeneration.

Perspectives on the future of MI therapy

Future large animal studies and finally clinical trials with magnetic guiding based angiogenic gene therapy or matrigel mediated cardiac protection will help determine whether these novel techniques could provide new treatment modalities in patients with ischemic heart disease.

References

1. Muller JE. Diagnosis of myocardial infarction: Historical notes from the soviet union and the united states. *Am J Cardiol.* 1977;40:269-271
2. Reimer KA, Lowe JE, Rasmussen MM, Jennings RB. The wavefront phenomenon of ischemic cell death. 1. Myocardial infarct size vs duration of coronary occlusion in dogs. *Circulation.* 1977;56:786-794
3. Ferreira R. The reduction of infarct size--forty years of research. *Rev Port Cardiol.*29:1037-1053
4. Bolooki H, Vargas A. Myocardial revascularization after acute myocardial-infarction. *Archives of Surgery.* 1976;111:1216-1224
5. Aryan HE, Nakaji P, Lu DC, Alksne JF. Multimodality treatment of trigeminal neuralgia: Impact of radiosurgery and high resolution magnetic resonance imaging. *J Clin Neurosci.* 2006;13:239-244
6. Goldstein DJ, Seldomridge JA, Chen JM, Catanese KA, DeRosa CM, Weinberg AD, Smith CR, Rose EA, Levin HR, Oz MC. Use of aprotinin in lvad recipients reduces blood loss, blood use, and perioperative mortality. *Ann Thorac Surg.* 1995;59:1063-1067; discussion 1068
7. Efstratiadis T, Munsch C, Crossman D, Taylor K. Aprotinin used in emergency coronary operation after streptokinase treatment. *Ann Thorac Surg.* 1991;52:1320-1321
8. Bolli R. Mechanism of myocardial "stunning". *Circulation.* 1990;82:723-738
9. Applebaum R, House R, Rademaker A, Garibaldi A, Davis Z, Guillory J, Chen A, Hoeksema T. Coronary artery bypass grafting within thirty days of acute myocardial infarction. Early and late results in 406 patients. *J Thorac Cardiovasc Surg.* 1991;102:745-752
10. Di Donato M, Sabatier M, Dor V, Gensini GF, Toso A, Maioli M, Stanley AW, Athanasuleas C, Buckberg G. Effects of the dor procedure on left ventricular dimension and shape and geometric correlates of mitral regurgitation one year after surgery. *J Thorac Cardiovasc Surg.* 2001;121:91-96
11. Conci E, Pachinger O, Metyler B. Mouse models for myocardial ischemia/reperfusion. *J Cardiologie.* 2006;13:239-244
12. Abbate A, Bussani R, Amin MS, Vetovec GW, Baldi A. Acute myocardial infarction and heart failure: Role of apoptosis. *Int J Biochem Cell Biol.* 2006;38:1834-1840

-
13. Frangogiannis NG. The mechanistic basis of infarct healing. *Antioxid Redox Signal*. 2006;8:1907-1939
 14. Bujak M, Ren G, Kweon HJ, Dobaczewski M, Reddy A, Taffet G, Wang XF, Frangogiannis NG. Essential role of smad3 in infarct healing and in the pathogenesis of cardiac remodeling. *Circulation*. 2007;116:2127-2138
 15. Ren G, Michael LH, Entman ML, Frangogiannis NG. Morphological characteristics of the microvasculature in healing myocardial infarcts. *J Histochem Cytochem*. 2002;50:71-79
 16. Dobaczewski M, Bujak M, Zymek P, Ren G, Entman ML, Frangogiannis NG. Extracellular matrix remodeling in canine and mouse myocardial infarcts. *Cell Tissue Res*. 2006;324:475-488
 17. Bujak M, Frangogiannis NG. The role of il-1 in the pathogenesis of heart disease. *Arch Immunol Ther Exp (Warsz)*. 2009;57:165-176
 18. Fujita T. Evolution of the lectin-complement pathway and its role in innate immunity. *Nat Rev Immunol*. 2002;2:346-353
 19. Nijmeijer R, Lagrand WK, Visser CA, Meijer CJ, Niessen HW, Hack CE. Crp, a major culprit in complement-mediated tissue damage in acute myocardial infarction? *Int Immunopharmacol*. 2001;1:403-414
 20. Rossen RD, Michael LH, Kagiya A, Savage HE, Hanson G, Reisberg MA, Moake JN, Kim SH, Self D, Weakley S. Mechanism of complement activation after coronary artery occlusion: Evidence that myocardial ischemia in dogs causes release of constituents of myocardial subcellular origin that complex with human c1q in vivo. *Circ Res*. 1988;62:572-584
 21. Hill JH, Ward PA. The phlogistic role of c3 leukotactic fragments in myocardial infarcts of rats. *J Exp Med*. 1971;133:885-900
 22. Rossen RD, Michael LH, Hawkins HK, Youker K, Dreyer WJ, Baughn RE, Entman ML. Cardiolipin-protein complexes and initiation of complement activation after coronary artery occlusion. *Circ Res*. 1994;75:546-555
 23. Yasojima K, Schwab C, McGeer EG, McGeer PL. Human heart generates complement proteins that are upregulated and activated after myocardial infarction. *Circ Res*. 1998;83:860-869
 24. Frangogiannis NG. The immune system and cardiac repair. *Pharmacol Res*. 2008;58:88-111

-
25. Bonvini RF, Hendiri T, Camenzind E. Inflammatory response post-myocardial infarction and reperfusion: A new therapeutic target? *European Heart Journal Supplements*. 2005;7:I27-I36
 26. Chakraborti T, Mandal A, Mandal M, Das S, Chakraborti S. Complement activation in heart diseases. Role of oxidants. *Cell Signal*. 2000;12:607-617
 27. Devasagayam TP, Tilak JC, Bloor KK, Sane KS, Ghaskadbi SS, Lele RD. Free radicals and antioxidants in human health: Current status and future prospects. *J Assoc Physicians India*. 2004;52:794-804
 28. Shingu M, Nonaka S, Nishimukai H, Nobunaga M, Kitamura H, Tomo-Oka K. Activation of complement in normal serum by hydrogen peroxide and hydrogen peroxide-related oxygen radicals produced by activated neutrophils. *Clin Exp Immunol*. 1992;90:72-78
 29. Shingu M, Nobunaga M. Chemotactic activity generated in human serum from the fifth component of complement by hydrogen peroxide. *Am J Pathol*. 1984;117:201-206
 30. Patel KD, Zimmerman GA, Prescott SM, McEver RP, McIntyre TM. Oxygen radicals induce human endothelial cells to express gmp-140 and bind neutrophils. *J Cell Biol*. 1991;112:749-759
 31. Lakshminarayanan V, Beno DW, Costa RH, Roebuck KA. Differential regulation of interleukin-8 and intercellular adhesion molecule-1 by h₂o₂ and tumor necrosis factor-alpha in endothelial and epithelial cells. *J Biol Chem*. 1997;272:32910-32918
 32. Lakshminarayanan V, Drab-Weiss EA, Roebuck KA. H₂o₂ and tumor necrosis factor-alpha induce differential binding of the redox-responsive transcription factors ap-1 and nf-kappab to the interleukin-8 promoter in endothelial and epithelial cells. *J Biol Chem*. 1998;273:32670-32678
 33. Sellak H, Franzini E, Hakim J, Pasquier C. Reactive oxygen species rapidly increase endothelial icam-1 ability to bind neutrophils without detectable upregulation. *Blood*. 1994;83:2669-2677
 34. Kloner RA, Jennings RB. Consequences of brief ischemia: Stunning, preconditioning, and their clinical implications: Part 2. *Circulation*. 2001;104:3158-3167
 35. Kloner RA, Jennings RB. Consequences of brief ischemia: Stunning, preconditioning, and their clinical implications: Part 1. *Circulation*. 2001;104:2981-2989
 36. Bolli R, Marban E. Molecular and cellular mechanisms of myocardial stunning. *Physiol Rev*. 1999;79:609-634

-
37. Herskowitz A, Choi S, Ansari AA, Wesselingh S. Cytokine mrna expression in postischemic/reperfused myocardium. *Am J Pathol.* 1995;146:419-428
 38. Nian M, Lee P, Khaper N, Liu P. Inflammatory cytokines and postmyocardial infarction remodeling. *Circulation research.* 2004;94:1543-1553
 39. Frangogiannis NG, Youker KA, Rossen RD, Gwechenberger M, Lindsey MH, Mendoza LH, Michael LH, Ballantyne CM, Smith CW, Entman ML. Cytokines and the microcirculation in ischemia and reperfusion. *Journal of molecular and cellular cardiology.* 1998;30:2567-2576
 40. Finkel MS, Oddis CV, Jacob TD, Watkins SC, Hattler BG, Simmons RL. Negative inotropic effects of cytokines on the heart mediated by nitric oxide. *Science.* 1992;257:387-389
 41. Aoyama T, Takimoto Y, Pennica D, Inoue R, Shinoda E, Hattori R, Yui Y, Sasayama S. Augmented expression of cardiotrophin-1 and its receptor component, gp130, in both left and right ventricles after myocardial infarction in the rat. *J Mol Cell Cardiol.* 2000;32:1821-1830
 42. Engel D, Peshock R, Armstrong RC, Sivasubramanian N, Mann DL. Cardiac myocyte apoptosis provokes adverse cardiac remodeling in transgenic mice with targeted tnf overexpression. *Am J Physiol Heart Circ Physiol.* 2004;287:H1303-1311
 43. Yokoyama T, Vaca L, Rossen RD, Durante W, Hazarika P, Mann DL. Cellular basis for the negative inotropic effects of tumor necrosis factor-alpha in the adult mammalian heart. *J Clin Invest.* 1993;92:2303-2312
 44. Siwik DA, Chang DL, Colucci WS. Interleukin-1beta and tumor necrosis factor-alpha decrease collagen synthesis and increase matrix metalloproteinase activity in cardiac fibroblasts in vitro. *Circ Res.* 2000;86:1259-1265
 45. Maekawa N, Wada H, Kanda T, Niwa T, Yamada Y, Saito K, Fujiwara H, Sekikawa K, Seishima M. Improved myocardial ischemia/reperfusion injury in mice lacking tumor necrosis factor-alpha. *J Am Coll Cardiol.* 2002;39:1229-1235
 46. Monden Y, Kubota T, Inoue T, Tsutsumi T, Kawano S, Ide T, Tsutsui H, Sunagawa K. Tumor necrosis factor-alpha is toxic via receptor 1 and protective via receptor 2 in a murine model of myocardial infarction. *Am J Physiol Heart Circ Physiol.* 2007;293:H743-753
 47. Sims JE, March CJ, Cosman D, Widmer MB, MacDonald HR, McMahan CJ, Grubin CE, Wignall JM, Jackson JL, Call SM, et al. Cdna expression cloning of the il-1 receptor, a member of the immunoglobulin superfamily. *Science.* 1988;241:585-589

-
48. Matsushima K, Oppenheim JJ. Interleukin 8 and mcaf: Novel inflammatory cytokines inducible by il 1 and tnf. *Cytokine*. 1989;1:2-13
 49. Marui N, Offermann MK, Swerlick R, Kunsch C, Rosen CA, Ahmad M, Alexander RW, Medford RM. Vascular cell adhesion molecule-1 (vcam-1) gene transcription and expression are regulated through an antioxidant-sensitive mechanism in human vascular endothelial cells. *J Clin Invest*. 1993;92:1866-1874
 50. Suzuki K, Murtuza B, Smolenski RT, Sammut IA, Suzuki N, Kaneda Y, Yacoub MH. Overexpression of interleukin-1 receptor antagonist provides cardioprotection against ischemia-reperfusion injury associated with reduction in apoptosis. *Circulation*. 2001;104:I308-I303
 51. Hwang MW, Matsumori A, Furukawa Y, Ono K, Okada M, Iwasaki A, Hara M, Miyamoto T, Touma M, Sasayama S. Neutralization of interleukin-1beta in the acute phase of myocardial infarction promotes the progression of left ventricular remodeling. *J Am Coll Cardiol*. 2001;38:1546-1553
 52. Wollert KC, Drexler H. The role of interleukin-6 in the failing heart. *Heart Fail Rev*. 2001;6:95-103
 53. Hafezi-Moghadam A, Thomas KL, Prorock AJ, Huo Y, Ley K. L-selectin shedding regulates leukocyte recruitment. *J Exp Med*. 2001;193:863-872
 54. Ma XL, Weyrich AS, Lefer DJ, Buerke M, Albertine KH, Kishimoto TK, Lefer AM. Monoclonal antibody to l-selectin attenuates neutrophil accumulation and protects ischemic reperfused cat myocardium. *Circulation*. 1993;88:649-658
 55. Weyrich AS, Ma XY, Lefer DJ, Albertine KH, Lefer AM. In vivo neutralization of p-selectin protects feline heart and endothelium in myocardial ischemia and reperfusion injury. *J Clin Invest*. 1993;91:2620-2629
 56. Briaud SA, Ding ZM, Michael LH, Entman ML, Daniel S, Ballantyne CM. Leukocyte trafficking and myocardial reperfusion injury in icam-1/p-selectin-knockout mice. *American journal of physiology. Heart and circulatory physiology*. 2001;280:H60-67
 57. Di Filippo C, Rossi F, D'Amico M. Targeting polymorphonuclear leukocytes in acute myocardial infarction. *ScientificWorldJournal*. 2007;7:121-134
 58. Fan H, Sun B, Gu Q, Lafond-Walker A, Cao S, Becker LC. Oxygen radicals trigger activation of nf-kappab and ap-1 and upregulation of icam-1 in reperfused canine heart. *Am J Physiol Heart Circ Physiol*. 2002;282:H1778-1786

-
59. Gasic AC, McGuire G, Krater S, Farhood AI, Goldstein MA, Smith CW, Entman ML, Taylor AA. Hydrogen peroxide pretreatment of perfused canine vessels induces icam-1 and cd18-dependent neutrophil adherence. *Circulation*. 1991;84:2154-2166
 60. Simon SI, Burns AR, Taylor AD, Gopalan PK, Lynam EB, Sklar LA, Smith CW. L-selectin (cd62l) cross-linking signals neutrophil adhesive functions via the mac-1 (cd11b/cd18) beta 2-integrin. *J Immunol*. 1995;155:1502-1514
 61. Weiss SJ. Tissue destruction by neutrophils. *N Engl J Med*. 1989;320:365-376
 62. Janoff A. Elastase in tissue injury. *Annu Rev Med*. 1985;36:207-216
 63. Jordan JE, Zhao ZQ, Vinten-Johansen J. The role of neutrophils in myocardial ischemia-reperfusion injury. *Cardiovasc Res*. 1999;43:860-878
 64. Mainardi CL, Hasty DL, Seyer JM, Kang AH. Specific cleavage of human type iii collagen by human polymorphonuclear leukocyte elastase. *J Biol Chem*. 1980;255:12006-12010
 65. Simpson DM, Ross R. The neutrophilic leukocyte in wound repair a study with antineutrophil serum. *J Clin Invest*. 1972;51:2009-2023
 66. Birdsall HH, Green DM, Trial J, Youker KA, Burns AR, MacKay CR, LaRosa GJ, Hawkins HK, Smith CW, Michael LH, Entman ML, Rossen RD. Complement c5a, tgf-beta 1, and mcp-1, in sequence, induce migration of monocytes into ischemic canine myocardium within the first one to five hours after reperfusion. *Circulation*. 1997;95:684-692
 67. Weihrauch D, Arras M, Zimmermann R, Schaper J. Importance of monocytes/macrophages and fibroblasts for healing of micronecroses in porcine myocardium. *Mol Cell Biochem*. 1995;147:13-19
 68. Frangogiannis NG, Smith CW, Entman ML. The inflammatory response in myocardial infarction. *Cardiovasc Res*. 2002;53:31-47
 69. Frangogiannis NG, Burns AR, Michael LH, Entman ML. Histochemical and morphological characteristics of canine cardiac mast cells. *Histochem J*. 1999;31:221-229
 70. Frangogiannis NG, Lindsey ML, Michael LH, Youker KA, Bressler RB, Mendoza LH, Spengler RN, Smith CW, Entman ML. Resident cardiac mast cells degranulate and release preformed tnf-alpha, initiating the cytokine cascade in experimental canine myocardial ischemia/reperfusion. *Circulation*. 1998;98:699-710
 71. Ma N, Stamm C, Kaminski A, Li W, Kleine HD, Muller-Hilke B, Zhang L, Ladilov Y, Egger D, Steinhoff G. Human cord blood cells induce angiogenesis following myocardial infarction in nod/scid-mice. *Cardiovasc Res*. 2005;66:45-54

-
72. Elmadbouh I, Haider H, Jiang S, Idris NM, Lu G, Ashraf M. Ex vivo delivered stromal cell-derived factor-1alpha promotes stem cell homing and induces angiomyogenesis in the infarcted myocardium. *J Mol Cell Cardiol.* 2007;42:792-803
 73. Wang W, Li W, Ong LL, Lutzow K, Lendlein A, Furlani D, Gabel R, Kong D, Wang J, Li RK, Steinhoff G, Ma N. Localized and sustained sdf-1 gene release mediated by fibronectin films: A potential method for recruiting stem cells. *Int J Artif Organs.* 2009;32:141-149
 74. Wang W, Li W, Ong LL, Furlani D, Kaminski A, Liebold A, Lutzow K, Lendlein A, Wang J, Li RK, Steinhoff G, Ma N. Localized sdf-1alpha gene release mediated by collagen substrate induces cd117+ stem cell homing. *J Cell Mol Med.* 2010;14:392-402
 75. Hatamochi A, Fujiwara K, Ueki H. Effects of histamine on collagen synthesis by cultured fibroblasts derived from guinea pig skin. *Arch Dermatol Res.* 1985;277:60-64
 76. He S, Peng Q, Walls AF. Potent induction of a neutrophil and eosinophil-rich infiltrate in vivo by human mast cell tryptase: Selective enhancement of eosinophil recruitment by histamine. *J Immunol.* 1997;159:6216-6225
 77. Ruoss SJ, Hartmann T, Caughey GH. Mast cell tryptase is a mitogen for cultured fibroblasts. *J Clin Invest.* 1991;88:493-499
 78. Gruber BL, Kew RR, Jelaska A, Marchese MJ, Garlick J, Ren S, Schwartz LB, Korn JH. Human mast cells activate fibroblasts: Tryptase is a fibrogenic factor stimulating collagen messenger ribonucleic acid synthesis and fibroblast chemotaxis. *J Immunol.* 1997;158:2310-2317
 79. Souders CA, Bowers SL, Baudino TA. Cardiac fibroblast: The renaissance cell. *Circ Res.* 2009;105:1164-1176
 80. Tomasek JJ, Gabbiani G, Hinz B, Chaponnier C, Brown RA. Myofibroblasts and mechano-regulation of connective tissue remodelling. *Nat Rev Mol Cell Biol.* 2002;3:349-363
 81. Gabbiani G. The myofibroblast in wound healing and fibrocontractive diseases. *J Pathol.* 2003;200:500-503
 82. Hinz B, Phan SH, Thannickal VJ, Galli A, Bochaton-Piallat ML, Gabbiani G. The myofibroblast: One function, multiple origins. *Am J Pathol.* 2007;170:1807-1816
 83. Gwechenberger M, Moertl D, Pacher R, Huelsmann M. Oncostatin-m in myocardial ischemia/reperfusion injury may regulate tissue repair. *Croat Med J.* 2004;45:149-157

-
84. Liao Z, Brar BK, Cai Q, Stephanou A, O'Leary RM, Pennica D, Yellon DM, Latchman DS. Cardiostrophin-1 (ct-1) can protect the adult heart from injury when added both prior to ischaemia and at reperfusion. *Cardiovasc Res.* 2002;53:902-910
 85. Gritman K, Van Winkle DM, Lorentz CU, Pennica D, Habecker BA. The lack of cardiostrophin-1 alters expression of interleukin-6 and leukemia inhibitory factor mrna but does not impair cardiac injury response. *Cytokine.* 2006;36:9-16
 86. Freed DH, Cunnington RH, Dangerfield AL, Sutton JS, Dixon IM. Emerging evidence for the role of cardiostrophin-1 in cardiac repair in the infarcted heart. *Cardiovasc Res.* 2005;65:782-792
 87. Rollins BJ. Chemokines. *Blood.* 1997;90:909-928
 88. Zou Y, Takano H, Mizukami M, Akazawa H, Qin Y, Toko H, Sakamoto M, Minamino T, Nagai T, Komuro I. Leukemia inhibitory factor enhances survival of cardiomyocytes and induces regeneration of myocardium after myocardial infarction. *Circulation.* 2003;108:748-753
 89. Gallucci RM, Simeonova PP, Matheson JM, Kommineni C, Guriel JL, Sugawara T, Luster MI. Impaired cutaneous wound healing in interleukin-6-deficient and immunosuppressed mice. *FASEB J.* 2000;14:2525-2531
 90. Fukuda S, Kaga S, Sasaki H, Zhan L, Zhu L, Otani H, Kalfin R, Das DK, Maulik N. Angiogenic signal triggered by ischemic stress induces myocardial repair in rat during chronic infarction. *J Mol Cell Cardiol.* 2004;36:547-559
 91. Mack CA, Magovern CJ, Budenbender KT, Patel SR, Schwarz EA, Zanzonico P, Ferris B, Sanborn T, Isom P, Isom OW, Crystal RG, Rosengart TK. Salvage angiogenesis induced by adenovirus-mediated gene transfer of vascular endothelial growth factor protects against ischemic vascular occlusion. *J Vasc Surg.* 1998;27:699-709
 92. Pearlman JD, Hibberd MG, Chuang ML, Harada K, Lopez JJ, Gladstone SR, Friedman M, Sellke FW, Simons M. Magnetic resonance mapping demonstrates benefits of vegf-induced myocardial angiogenesis. *Nat Med.* 1995;1:1085-1089
 93. Carmeliet P. Mechanisms of angiogenesis and arteriogenesis. *Nat Med.* 2000;6:389-395
 94. Ferrari R, Ceconi C, Campo G, Cangiano E, Cavazza C, Secchiero P, Tavazzi L. Mechanisms of remodelling: A question of life (stem cell production) and death (myocyte apoptosis). *Circ J.* 2009;73:1973-1982
 95. Pfeffer MA, Braunwald E. Ventricular remodeling after myocardial infarction. Experimental observations and clinical implications. *Circulation.* 1990;81:1161-1172

-
96. Rouleau JL, de Champlain J, Klein M, Bichet D, Moye L, Packer M, Dagenais GR, Sussex B, Arnold JM, Sestier F, et al. Activation of neurohumoral systems in postinfarction left ventricular dysfunction. *J Am Coll Cardiol.* 1993;22:390-398
 97. Sutton MG, Sharpe N. Left ventricular remodeling after myocardial infarction: Pathophysiology and therapy. *Circulation.* 2000;101:2981-2988
 98. Cleutjens JP, Kandala JC, Guarda E, Guntaka RV, Weber KT. Regulation of collagen degradation in the rat myocardium after infarction. *J Mol Cell Cardiol.* 1995;27:1281-1292
 99. Lew WY, Chen ZY, Guth B, Covell JW. Mechanisms of augmented segment shortening in nonischemic areas during acute ischemia of the canine left ventricle. *Circ Res.* 1985;56:351-358
 100. Yamazaki T, Komuro I, Kudoh S, Zou Y, Shiojima I, Mizuno T, Takano H, Hiroi Y, Ueki K, Tobe K, et al. Angiotensin ii partly mediates mechanical stress-induced cardiac hypertrophy. *Circ Res.* 1995;77:258-265
 101. Bogoyevitch MA, Glennon PE, Andersson MB, Clerk A, Lazou A, Marshall CJ, Parker PJ, Sugden PH. Endothelin-1 and fibroblast growth factors stimulate the mitogen-activated protein kinase signaling cascade in cardiac myocytes. The potential role of the cascade in the integration of two signaling pathways leading to myocyte hypertrophy. *J Biol Chem.* 1994;269:1110-1119
 102. Sadoshima J, Izumo S. Molecular characterization of angiotensin ii--induced hypertrophy of cardiac myocytes and hyperplasia of cardiac fibroblasts. Critical role of the at1 receptor subtype. *Circ Res.* 1993;73:413-423
 103. Ball SG. The sympathetic nervous system and converting enzyme inhibition. *J Cardiovasc Pharmacol.* 1989;13 Suppl 3:S17-21
 104. Johnston CI, Risvanis J. Preclinical pharmacology of angiotensin ii receptor antagonists: Update and outstanding issues. *Am J Hypertens.* 1997;10:306S-310S
 105. Chung O, Stoll M, Unger T. Physiologic and pharmacologic implications of at1 versus at2 receptors. *Blood Press Suppl.* 1996;2:47-52
 106. Chung O, Kuhl H, Stoll M, Unger T. Physiological and pharmacological implications of at1 versus at2 receptors. *Kidney Int Suppl.* 1998;67:S95-99
 107. Nio Y, Matsubara H, Murasawa S, Kanasaki M, Inada M. Regulation of gene transcription of angiotensin ii receptor subtypes in myocardial infarction. *J Clin Invest.* 1995;95:46-54

-
108. Fortuno MA, Ravassa S, Fortuno A, Zalba G, Diez J. Cardiomyocyte apoptotic cell death in arterial hypertension: Mechanisms and potential management. *Hypertension*. 2001;38:1406-1412
 109. Katz AM. The cardiomyopathy of overload: An unnatural growth response in the hypertrophied heart. *Ann Intern Med*. 1994;121:363-371
 110. Narula J, Kolodgie FD, Virmani R. Apoptosis and cardiomyopathy. *Curr Opin Cardiol*. 2000;15:183-188
 111. Bing OH. Hypothesis: Apoptosis may be a mechanism for the transition to heart failure with chronic pressure overload. *J Mol Cell Cardiol*. 1994;26:943-948
 112. Diez J, Fortuno MA, Ravassa S. Apoptosis in hypertensive heart disease. *Curr Opin Cardiol*. 1998;13:317-325
 113. Folkman J. Angiogenesis in cancer, vascular, rheumatoid and other disease. *Nat Med*. 1995;1:27-31
 114. Bauters C, Asahara T, Zheng LP, Takeshita S, Bunting S, Ferrara N, Symes JF, Isner JM. Physiological assessment of augmented vascularity induced by vegf in ischemic rabbit hindlimb. *Am J Physiol*. 1994;267:H1263-1271
 115. Takeshita S, Tsurumi Y, Couffinahl T, Asahara T, Bauters C, Symes J, Ferrara N, Isner JM. Gene transfer of naked DNA encoding for three isoforms of vascular endothelial growth factor stimulates collateral development in vivo. *Lab Invest*. 1996;75:487-501
 116. Wheeler-Jones C, Abu-Ghazaleh R, Cospedal R, Houliston RA, Martin J, Zachary I. Vascular endothelial growth factor stimulates prostacyclin production and activation of cytosolic phospholipase a2 in endothelial cells via p42/p44 mitogen-activated protein kinase. *FEBS Lett*. 1997;420:28-32
 117. Kroll J, Waltenberger J. A novel function of vegf receptor-2 (kdr): Rapid release of nitric oxide in response to vegf-a stimulation in endothelial cells. *Biochem Biophys Res Commun*. 1999;265:636-639
 118. Shen BQ, Lee DY, Zioncheck TF. Vascular endothelial growth factor governs endothelial nitric-oxide synthase expression via a kdr/flk-1 receptor and a protein kinase c signaling pathway. *J Biol Chem*. 1999;274:33057-33063
 119. Cunningham SA, Waxham MN, Arrate PM, Brock TA. Interaction of the flt-1 tyrosine kinase receptor with the p85 subunit of phosphatidylinositol 3-kinase. Mapping of a novel site involved in binding. *J Biol Chem*. 1995;270:20254-20257

-
120. Waltenberger J, Claesson-Welsh L, Siegbahn A, Shibuya M, Heldin CH. Different signal transduction properties of kdr and flt1, two receptors for vascular endothelial growth factor. *J Biol Chem.* 1994;269:26988-26995
 121. Abedi H, Zachary I. Vascular endothelial growth factor stimulates tyrosine phosphorylation and recruitment to new focal adhesions of focal adhesion kinase and paxillin in endothelial cells. *J Biol Chem.* 1997;272:15442-15451
 122. Xia P, Aiello LP, Ishii H, Jiang ZY, Park DJ, Robinson GS, Takagi H, Newsome WP, Jirousek MR, King GL. Characterization of vascular endothelial growth factor's effect on the activation of protein kinase c, its isoforms, and endothelial cell growth. *J Clin Invest.* 1996;98:2018-2026
 123. Wellner M, Maasch C, Kupprion C, Lindschau C, Luft FC, Haller H. The proliferative effect of vascular endothelial growth factor requires protein kinase c-alpha and protein kinase c-zeta. *Arterioscler Thromb Vasc Biol.* 1999;19:178-185
 124. Higaki T, Sawada S, Kono Y, Imamura H, Tada Y, Yamasaki S, Toratani A, Sato T, Komatsu S, Akamatsu N, Tamagaki T, Tsuda Y, Tsuji H, Nakagawa M. A role of protein kinase c in the regulation of cytosolic phospholipase a(2) in bradykinin-induced pgi(2) synthesis by human vascular endothelial cells. *Microvasc Res.* 1999;58:144-155
 125. Takahashi T, Ueno H, Shibuya M. Vegf activates protein kinase c-dependent, but ras-independent raf-mek-map kinase pathway for DNA synthesis in primary endothelial cells. *Oncogene.* 1999;18:2221-2230
 126. Ku DD, Zaleski JK, Liu S, Brock TA. Vascular endothelial growth factor induces edrf-dependent relaxation in coronary arteries. *Am J Physiol.* 1993;265:H586-592
 127. Laitinen M, Zachary I, Breier G, Pakkanen T, Hakkinen T, Luoma J, Abedi H, Risau W, Soma M, Laakso M, Martin JF, Yla-Herttuala S. Vegf gene transfer reduces intimal thickening via increased production of nitric oxide in carotid arteries. *Hum Gene Ther.* 1997;8:1737-1744
 128. van der Zee R, Murohara T, Luo Z, Zollmann F, Passeri J, Lekutat C, Isner JM. Vascular endothelial growth factor/vascular permeability factor augments nitric oxide release from quiescent rabbit and human vascular endothelium. *Circulation.* 1997;95:1030-1037
 129. Tsurumi Y, Murohara T, Krasinski K, Chen D, Witzenbichler B, Kearney M, Couffinhal T, Isner JM. Reciprocal relation between vegf and no in the regulation of endothelial integrity. *Nat Med.* 1997;3:879-886

-
130. Murohara T, Horowitz JR, Silver M, Tsurumi Y, Chen D, Sullivan A, Isner JM. Vascular endothelial growth factor/vascular permeability factor enhances vascular permeability via nitric oxide and prostacyclin. *Circulation*. 1998;97:99-107
 131. Zachary I, Mathur A, Yla-Herttuala S, Martin J. Vascular protection: A novel nonangiogenic cardiovascular role for vascular endothelial growth factor. *Arterioscler Thromb Vasc Biol*. 2000;20:1512-1520
 132. Zachary I, Glikli G. Signaling transduction mechanisms mediating biological actions of the vascular endothelial growth factor family. *Cardiovasc Res*. 2001;49:568-581
 133. Ahn A, Frishman WH, Gutwein A, Passeri J, Nelson M. Therapeutic angiogenesis: A new treatment approach for ischemic heart disease--part i. *Cardiol Rev*. 2008;16:163-171
 134. Ahn A, Frishman WH, Gutwein A, Passeri J, Nelson M. Therapeutic angiogenesis: A new treatment approach for ischemic heart disease--part ii. *Cardiol Rev*. 2008;16:219-229
 135. Kastrup J. Gene therapy and angiogenesis in patients with coronary artery disease. *Expert Rev Cardiovasc Ther*. 8:1127-1138
 136. Zachary I, Morgan RD. Therapeutic angiogenesis for cardiovascular disease: Biological context, challenges, prospects. *Heart*. 97:181-189
 137. Hammond HK, McKirnan MD. Angiogenic gene therapy for heart disease: A review of animal studies and clinical trials. *Cardiovasc Res*. 2001;49:561-567
 138. Rissanen TT, Yla-Herttuala S. Current status of cardiovascular gene therapy. *Mol Ther*. 2007;15:1233-1247
 139. Orlic D, Kajstura J, Chimenti S, Limana F, Jakoniuk I, Quaini F, Nadal-Ginard B, Bodine DM, Leri A, Anversa P. Mobilized bone marrow cells repair the infarcted heart, improving function and survival. *Proc Natl Acad Sci U S A*. 2001;98:10344-10349
 140. Rosengart TK, Lee LY, Patel SR, Sanborn TA, Parikh M, Bergman GW, Hachamovitch R, Szulc M, Kligfield PD, Okin PM, Hahn RT, Devereux RB, Post MR, Hackett NR, Foster T, Grasso TM, Lesser ML, Isom OW, Crystal RG. Angiogenesis gene therapy: Phase i assessment of direct intramyocardial administration of an adenovirus vector expressing vegf121 cDNA to individuals with clinically significant severe coronary artery disease. *Circulation*. 1999;100:468-474
 141. Hedman M, Hartikainen J, Syvanne M, Stjernvall J, Hedman A, Kivela A, Vanninen E, Mussalo H, Kauppila E, Simula S, Narvanen O, Rantala A, Peuhkurinen K, Nieminen MS, Laakso M, Yla-Herttuala S. Safety and feasibility of catheter-based

-
- local intracoronary vascular endothelial growth factor gene transfer in the prevention of postangioplasty and in-stent restenosis and in the treatment of chronic myocardial ischemia: Phase ii results of the kuopio angiogenesis trial (kat). *Circulation*. 2003;107:2677-2683
142. Mah C, Fraites TJ, Jr., Zolotukhin I, Song S, Flotte TR, Dobson J, Batich C, Byrne BJ. Improved method of recombinant aav2 delivery for systemic targeted gene therapy. *Molecular therapy : the journal of the American Society of Gene Therapy*. 2002;6:106-112
143. Dobson J. Gene therapy progress and prospects: Magnetic nanoparticle-based gene delivery. *Gene Ther*. 2006;13:283-287
144. Pandori M, Hobson D, Sano T. Adenovirus-microbead conjugates possess enhanced infectivity: A new strategy for localized gene delivery. *Virology*. 2002;299:204-212
145. Hofmann A, Wenzel D, Becher UM, Freitag DF, Klein AM, Eberbeck D, Schulte M, Zimmermann K, Bergemann C, Gleich B, Roell W, Weyh T, Trahms L, Nickenig G, Fleischmann BK, Pfeifer A. Combined targeting of lentiviral vectors and positioning of transduced cells by magnetic nanoparticles. *Proc Natl Acad Sci U S A*. 2009;106:44-49
146. Verma IM, Somia N. Gene therapy -- promises, problems and prospects. *Nature*. 1997;389:239-242
147. Delyagina E, Li W, Ma N, Steinhoff G. Magnetic targeting strategies in gene delivery. *Nanomedicine (Lond)*.6:1593-1604
148. Fazel S, Tang GH, Angoulvant D, Cimini M, Weisel RD, Li RK, Yau TM. Current status of cellular therapy for ischemic heart disease. *Ann Thorac Surg*. 2005;79:S2238-2247
149. Assmus B, Honold J, Schachinger V, Britten MB, Fischer-Rasokat U, Lehmann R, Teupe C, Pistorius K, Martin H, Abolmaali ND, Tonn T, Dimmeler S, Zeiher AM. Transcoronary transplantation of progenitor cells after myocardial infarction. *N Engl J Med*. 2006;355:1222-1232
150. Lunde K, Solheim S, Aakhus S, Arnesen H, Abdelnoor M, Egeland T, Endresen K, Ilebakk A, Mangschau A, Fjeld JG, Smith HJ, Taraldsrud E, Groggaard HK, Bjornerheim R, Brekke M, Muller C, Hopp E, Ragnarsson A, Brinchmann JE, Forfang K. Intracoronary injection of mononuclear bone marrow cells in acute myocardial infarction. *N Engl J Med*. 2006;355:1199-1209
151. Wollert KC, Meyer GP, Lotz J, Ringes-Lichtenberg S, Lippolt P, Breidenbach C, Fichtner S, Korte T, Hornig B, Messinger D, Arseniev L, Hertenstein B, Ganser A,

-
- Drexler H. Intracoronary autologous bone-marrow cell transfer after myocardial infarction: The boost randomised controlled clinical trial. *Lancet*. 2004;364:141-148
152. Orlic D, Kajstura J, Chimenti S, Jakoniuk I, Anderson SM, Li B, Pickel J, McKay R, Nadal-Ginard B, Bodine DM, Leri A, Anversa P. Bone marrow cells regenerate infarcted myocardium. *Nature*. 2001;410:701-705
153. Balsam LB, Wagers AJ, Christensen JL, Kofidis T, Weissman IL, Robbins RC. Haematopoietic stem cells adopt mature haematopoietic fates in ischaemic myocardium. *Nature*. 2004;428:668-673
154. Murry CE, Soonpaa MH, Reinecke H, Nakajima H, Nakajima HO, Rubart M, Pasumarthi KB, Virag JI, Bartelmez SH, Poppa V, Bradford G, Dowell JD, Williams DA, Field LJ. Haematopoietic stem cells do not transdifferentiate into cardiac myocytes in myocardial infarcts. *Nature*. 2004;428:664-668
155. Wagers AJ, Sherwood RI, Christensen JL, Weissman IL. Little evidence for developmental plasticity of adult hematopoietic stem cells. *Science*. 2002;297:2256-2259
156. Rosenzweig A. Cardiac cell therapy--mixed results from mixed cells. *N Engl J Med*. 2006;355:1274-1277
157. Chabot B, Stephenson DA, Chapman VM, Besmer P, Bernstein A. The proto-oncogene c-kit encoding a transmembrane tyrosine kinase receptor maps to the mouse w locus. *Nature*. 1988;335:88-89
158. Beltrami AP, Barlucchi L, Torella D, Baker M, Limana F, Chimenti S, Kasahara H, Rota M, Musso E, Urbanek K, Leri A, Kajstura J, Nadal-Ginard B, Anversa P. Adult cardiac stem cells are multipotent and support myocardial regeneration. *Cell*. 2003;114:763-776
159. Kabrun N, Buhring HJ, Choi K, Ullrich A, Risau W, Keller G. Flk-1 expression defines a population of early embryonic hematopoietic precursors. *Development*. 1997;124:2039-2048
160. Nishikawa SI, Nishikawa S, Hirashima M, Matsuyoshi N, Kodama H. Progressive lineage analysis by cell sorting and culture identifies flk1+ve-cadherin+ cells at a diverging point of endothelial and hemopoietic lineages. *Development*. 1998;125:1747-1757
161. Lanza R, Moore MA, Wakayama T, Perry AC, Shieh JH, Hendriks J, Leri A, Chimenti S, Monsen A, Nurzynska D, West MD, Kajstura J, Anversa P. Regeneration of the infarcted heart with stem cells derived by nuclear transplantation. *Circ Res*. 2004;94:820-827

-
162. Fazel S, Cimini M, Chen L, Li S, Angoulvant D, Fedak P, Verma S, Weisel RD, Keating A, Li RK. Cardioprotective c-kit⁺ cells are from the bone marrow and regulate the myocardial balance of angiogenic cytokines. *J Clin Invest.* 2006;116:1865-1877
 163. Buckberg GD. Basic science review: The helix and the heart. *J Thorac Cardiovasc Surg.* 2002;124:863-883
 164. Kofidis T, de Bruin JL, Hoyt G, Lebl DR, Tanaka M, Yamane T, Chang CP, Robbins RC. Injectable bioartificial myocardial tissue for large-scale intramural cell transfer and functional recovery of injured heart muscle. *The Journal of thoracic and cardiovascular surgery.* 2004;128:571-578
 165. Kleinman HK, McGarvey ML, Liotta LA, Robey PG, Tryggvason K, Martin GR. Isolation and characterization of type iv procollagen, laminin, and heparan sulfate proteoglycan from the ehs sarcoma. *Biochemistry.* 1982;21:6188-6193
 166. Norrby K. In vivo models of angiogenesis. *J Cell Mol Med.* 2006;10:588-612
 167. Ruvinov E, Leor J, Cohen S. The promotion of myocardial repair by the sequential delivery of igf-1 and hgf from an injectable alginate biomaterial in a model of acute myocardial infarction. *Biomaterials.* 2011;32:565-578
 168. Hsieh PC, Davis ME, Gannon J, MacGillivray C, Lee RT. Controlled delivery of pdgf-bb for myocardial protection using injectable self-assembling peptide nanofibers. *The Journal of clinical investigation.* 2006;116:237-248
 169. Hao X, Silva EA, Mansson-Broberg A, Grinnemo KH, Siddiqui AJ, Dellgren G, Wardell E, Brodin LA, Mooney DJ, Sylven C. Angiogenic effects of sequential release of vegf-a165 and pdgf-bb with alginate hydrogels after myocardial infarction. *Cardiovascular research.* 2007;75:178-185
 170. Passaniti A, Taylor RM, Pili R, Guo Y, Long PV, Haney JA, Pauly RR, Grant DS, Martin GR. A simple, quantitative method for assessing angiogenesis and antiangiogenic agents using reconstituted basement membrane, heparin, and fibroblast growth factor. *Lab Invest.* 1992;67:519-528
 171. Isaji M, Miyata H, Ajisawa Y, Takehana Y, Yoshimura N. Tranilast inhibits the proliferation, chemotaxis and tube formation of human microvascular endothelial cells in vitro and angiogenesis in vivo. *Br J Pharmacol.* 1997;122:1061-1066
 172. Kisucka J, Butterfield CE, Duda DG, Eichenberger SC, Saffaripour S, Ware J, Ruggeri ZM, Jain RK, Folkman J, Wagner DD. Platelets and platelet adhesion support angiogenesis while preventing excessive hemorrhage. *Proc Natl Acad Sci U S A.* 2006;103:855-860

-
173. Zhang Y, Li W, Ou L, Wang W, Delyagina E, Lux C, Sorg H, Riehemann K, Steinhoff G, Ma N. Targeted delivery of human vegf gene via complexes of magnetic nanoparticle-adenoviral vectors enhanced cardiac regeneration. *PloS one*. 2012;7:e39490
 174. Tous E, Purcell B, Ifkovits JL, Burdick JA. Injectable acellular hydrogels for cardiac repair. *Journal of cardiovascular translational research*. 2011;4:528-542
 175. Min JY, Yang Y, Converso KL, Liu L, Huang Q, Morgan JP, Xiao YF. Transplantation of embryonic stem cells improves cardiac function in postinfarcted rats. *J Appl Physiol*. 2002;92:288-296
 176. Kofidis T, Lebl DR, Martinez EC, Hoyt G, Tanaka M, Robbins RC. Novel injectable bioartificial tissue facilitates targeted, less invasive, large-scale tissue restoration on the beating heart after myocardial injury. *Circulation*. 2005;112:I173-177
 177. Zimmermann WH, Schneiderbanger K, Schubert P, Didie M, Munzel F, Heubach JF, Kostin S, Neuhuber WL, Eschenhagen T. Tissue engineering of a differentiated cardiac muscle construct. *Circ Res*. 2002;90:223-230
 178. Zimmermann WH, Didie M, Wasmeier GH, Nixdorff U, Hess A, Melnychenko I, Boy O, Neuhuber WL, Weyand M, Eschenhagen T. Cardiac grafting of engineered heart tissue in syngenic rats. *Circulation*. 2002;106:I151-157
 179. Zhang P, Zhang H, Wang H, Wei Y, Hu S. Artificial matrix helps neonatal cardiomyocytes restore injured myocardium in rats. *Artif Organs*. 2006;30:86-93
 180. Ou L, Li W, Zhang Y, Wang W, Liu J, Sorg H, Furlani D, Gabel R, Mark P, Klopsch C, Wang L, Lutzow K, Lendlein A, Wagner K, Klee D, Liebold A, Li RK, Kong D, Steinhoff G, Ma N. Intracardiac injection of matrigel induces stem cell recruitment and improves cardiac functions in a rat myocardial infarction model. *Journal of cellular and molecular medicine*. 2011;15:1310-1318
 181. Curato C, Slavic S, Dong J, Skorska A, Altarche-Xifro W, Miteva K, Kaschina E, Thiel A, Imboden H, Wang JA, Steckelings U, Steinhoff G, Unger T, Li J. Identification of noncytotoxic and il-10-producing cd8(+) at2r(+) t cell population in response to ischemic heart injury. *Journal of Immunology*. 2010;185:6286-6293
 182. Servos S, Zachary I, Martin JF. Vegf modulates no production: The basis of a cytoprotective effect? *Cardiovasc Res*. 1999;41:509-510
 183. Neufeld G, Cohen T, Gitay-Goren H, Poltorak Z, Tessler S, Sharon R, Gengrinovitch S, Levi BZ. Similarities and differences between the vascular endothelial growth factor (vegf) splice variants. *Cancer Metastasis Rev*. 1996;15:153-158

-
184. Poltorak Z, Cohen T, Sivan R, Kandelis Y, Spira G, Vlodayvsky I, Keshet E, Neufeld G. Vegf145, a secreted vascular endothelial growth factor isoform that binds to extracellular matrix. *J Biol Chem.* 1997;272:7151-7158
 185. Mykhaylyk O, Steingotter A, Perea H, Aigner J, Botnar R, Plank C. Nucleic acid delivery to magnetically-labeled cells in a 2d array and at the luminal surface of cell culture tube and their detection by mri. *J Biomed Nanotechnol.* 2009;5:692-706
 186. Watts RWE. The metabolic basis of inherited disease, 6th edition - scriver,cr, beaudet,al, sly,ws, valle,d. *Nature.* 1989;342:868-869
 187. Cheng K, Li TS, Malliaras K, Davis DR, Zhang Y, Marban E. Magnetic targeting enhances engraftment and functional benefit of iron-labeled cardiosphere-derived cells in myocardial infarction. *Circulation research.* 2010;106:1570-1581
 188. Li W, Ma N, Ong LL, Kaminski A, Skrabal C, Ugurlucan M, Lorenz P, Gatzen HH, Lutzow K, Lendlein A, Putzer BM, Li RK, Steinhoff G. Enhanced thoracic gene delivery by magnetic nanobead-mediated vector. *The journal of gene medicine.* 2008;10:897-909
 189. Sato K, Laham RJ, Pearlman JD, Novicki D, Sellke FW, Simons M, Post MJ. Efficacy of intracoronary versus intravenous fgf-2 in a pig model of chronic myocardial ischemia. *The Annals of thoracic surgery.* 2000;70:2113-2118
 190. Ferrarini M, Arsic N, Recchia FA, Zentilin L, Zacchigna S, Xu X, Linke A, Giacca M, Hintze TH. Adeno-associated virus-mediated transduction of vegf165 improves cardiac tissue viability and functional recovery after permanent coronary occlusion in conscious dogs. *Circulation research.* 2006;98:954-961
 191. Jacquier A, Higgins CB, Martin AJ, Do L, Saloner D, Saeed M. Injection of adeno-associated viral vector encoding vascular endothelial growth factor gene in infarcted swine myocardium: Mr measurements of left ventricular function and strain. *Radiology.* 2007;245:196-205
 192. Saeed M, Saloner D, Martin A, Do L, Weber O, Ursell PC, Jacquier A, Lee R, Higgins CB. Adeno-associated viral vector-encoding vascular endothelial growth factor gene: Effect on cardiovascular mr perfusion and infarct resorption measurements in swine. *Radiology.* 2007;243:451-460
 193. Zhou L, Ma W, Yang Z, Zhang F, Lu L, Ding Z, Ding B, Ha T, Gao X, Li C. Vegf165 and angiopoietin-1 decreased myocardium infarct size through phosphatidylinositol-3 kinase and bcl-2 pathways. *Gene therapy.* 2005;12:196-202
 194. Vera Janavel G, Crottogini A, Cabeza Meckert P, Cuniberti L, Mele A, Papouchado M, Fernandez N, Bercovich A, Criscuolo M, Melo C, Laguens R. Plasmid-mediated

-
- vegf gene transfer induces cardiomyogenesis and reduces myocardial infarct size in sheep. *Gene therapy*. 2006;13:1133-1142
195. Gao F, He T, Wang H, Yu S, Yi D, Liu W, Cai Z. A promising strategy for the treatment of ischemic heart disease: Mesenchymal stem cell-mediated vascular endothelial growth factor gene transfer in rats. *The Canadian journal of cardiology*. 2007;23:891-898
196. Guerrero M, Athota K, Moy J, Mehta LS, Laguens R, Crottogini A, Borrelli M, Corry P, Schoenherr D, Gentry R, Boura J, Grines CL, Raff GL, Shanley CJ, O'Neill WW. Vascular endothelial growth factor-165 gene therapy promotes cardiomyogenesis in reperfused myocardial infarction. *Journal of interventional cardiology*. 2008;21:242-251
197. Laguens R, Cabeza Meckert P, Vera Janavel G, Del Valle H, Lascano E, Negroni J, Werba P, Cuniberti L, Martinez V, Melo C, Papouchado M, Ojeda R, Criscuolo M, Crottogini A. Entrance in mitosis of adult cardiomyocytes in ischemic pig hearts after plasmid-mediated rhvegf165 gene transfer. *Gene therapy*. 2002;9:1676-1681
198. Stewart DJ, Hilton JD, Arnold JM, Gregoire J, Rivard A, Archer SL, Charbonneau F, Cohen E, Curtis M, Buller CE, Mendelsohn FO, Dib N, Page P, Ducas J, Plante S, Sullivan J, Macko J, Rasmussen C, Kessler PD, Rasmussen HS. Angiogenic gene therapy in patients with nonrevascularizable ischemic heart disease: A phase 2 randomized, controlled trial of advegf(121) (advegf121) versus maximum medical treatment. *Gene Ther*. 2006;13:1503-1511
199. Henry TD, Annex BH, McKendall GR, Azrin MA, Lopez JJ, Giordano FJ, Shah PK, Willerson JT, Benza RL, Berman DS, Gibson CM, Bajamonde A, Rundle AC, Fine J, McCluskey ER. The viva trial: Vascular endothelial growth factor in ischemia for vascular angiogenesis. *Circulation*. 2003;107:1359-1365
200. Laitinen M, Hartikainen J, Hiltunen MO, Eranen J, Kiviniemi M, Narvanen O, Makinen K, Manninen H, Syvanne M, Martin JF, Laakso M, Yla-Herttuala S. Catheter-mediated vascular endothelial growth factor gene transfer to human coronary arteries after angioplasty. *Hum Gene Ther*. 2000;11:263-270
201. Henry TD, Rocha-Singh K, Isner JM, Kereiakes DJ, Giordano FJ, Simons M, Losordo DW, Hendel RC, Bonow RO, Eppler SM, Zioncheck TF, Holmgren EB, McCluskey ER. Intracoronary administration of recombinant human vascular endothelial growth factor to patients with coronary artery disease. *Am Heart J*. 2001;142:872-880

-
202. Hendel RC, Henry TD, Rocha-Singh K, Isner JM, Kereiakes DJ, Giordano FJ, Simons M, Bonow RO. Effect of intracoronary recombinant human vascular endothelial growth factor on myocardial perfusion: Evidence for a dose-dependent effect. *Circulation*. 2000;101:118-121
 203. Hofmann M, Wollert KC, Meyer GP, Menke A, Arseniev L, Hertenstein B, Ganser A, Knapp WH, Drexler H. Monitoring of bone marrow cell homing into the infarcted human myocardium. *Circulation*. 2005;111:2198-2202
 204. Lazarous DF, Shou M, Stiber JA, Hodge E, Thirumurti V, Goncalves L, Unger EF. Adenoviral-mediated gene transfer induces sustained pericardial vegf expression in dogs: Effect on myocardial angiogenesis. *Cardiovasc Res*. 1999;44:294-302
 205. Hou D, Youssef EA, Brinton TJ, Zhang P, Rogers P, Price ET, Yeung AC, Johnstone BH, Yock PG, March KL. Radiolabeled cell distribution after intramyocardial, intracoronary, and interstitial retrograde coronary venous delivery: Implications for current clinical trials. *Circulation*. 2005;112:1150-156
 206. Mariani JA, Kaye DM. Delivery of gene and cellular therapies for heart disease. *J Cardiovasc Transl Res*. 3:417-426
 207. Kornowski R, Fuchs S, Leon MB, Epstein SE. Delivery strategies to achieve therapeutic myocardial angiogenesis. *Circulation*. 2000;101:454-458
 208. Mack CA, Patel SR, Schwarz EA, Zanzonico P, Hahn RT, Ilercil A, Devereux RB, Goldsmith SJ, Christian TF, Sanborn TA, Kovetski I, Hackett N, Isom OW, Crystal RG, Rosengart TK. Biologic bypass with the use of adenovirus-mediated gene transfer of the complementary deoxyribonucleic acid for vascular endothelial growth factor 121 improves myocardial perfusion and function in the ischemic porcine heart. *J Thorac Cardiovasc Surg*. 1998;115:168-176; discussion 176-167
 209. Fuchs S, Dib N, Cohen BM, Okubagzi P, Diethrich EB, Campbell A, Macko J, Kessler PD, Rasmussen HS, Epstein SE, Kornowski R. A randomized, double-blind, placebo-controlled, multicenter, pilot study of the safety and feasibility of catheter-based intramyocardial injection of advegf121 in patients with refractory advanced coronary artery disease. *Catheter Cardiovasc Interv*. 2006;68:372-378
 210. Thompson CA, Nasser BA, Makower J, Houser S, McGarry M, Lamson T, Pomerantseva I, Chang JY, Gold HK, Vacanti JP, Oesterle SN. Percutaneous transvenous cellular cardiomyoplasty. A novel nonsurgical approach for myocardial cell transplantation. *J Am Coll Cardiol*. 2003;41:1964-1971
 211. Losordo DW, Schatz RA, White CJ, Udelson JE, Veereshwarayya V, Durgin M, Poh KK, Weinstein R, Kearney M, Chaudhry M, Burg A, Eaton L, Heyd L, Thorne T,

-
- Shturman L, Hoffmeister P, Story K, Zak V, Dowling D, Traverse JH, Olson RE, Flanagan J, Sodano D, Murayama T, Kawamoto A, Kusano KF, Wollins J, Welt F, Shah P, Soukas P, Asahara T, Henry TD. Intramyocardial transplantation of autologous cd34+ stem cells for intractable angina: A phase i/ia double-blind, randomized controlled trial. *Circulation*. 2007;115:3165-3172
212. Lazarous DF, Shou M, Stiber JA, Dadhania DM, Thirumurti V, Hodge E, Unger EF. Pharmacodynamics of basic fibroblast growth factor: Route of administration determines myocardial and systemic distribution. *Cardiovasc Res*. 1997;36:78-85
213. Vemula SV, Mittal SK. Production of adenovirus vectors and their use as a delivery system for influenza vaccines. *Expert opinion on biological therapy*. 2010;10:1469-1487
214. Yang TC, Millar J, Groves T, Zhou W, Grinshtein N, Parsons R, Eveleigh C, Xing Z, Wan Y, Bramson J. On the role of cd4+ t cells in the cd8+ t-cell response elicited by recombinant adenovirus vaccines. *Mol Ther*. 2007;15:997-1006
215. Stone D, David A, Bolognani F, Lowenstein PR, Castro MG. Viral vectors for gene delivery and gene therapy within the endocrine system. *The Journal of endocrinology*. 2000;164:103-118
216. Markkanen JE, Rissanen TT, Kivela A, Yla-Herttuala S. Growth factor-induced therapeutic angiogenesis and arteriogenesis in the heart--gene therapy. *Cardiovascular research*. 2005;65:656-664
217. Katare R, Caporali A, Zentilin L, Avolio E, Sala-Newby G, Oikawa A, Cesselli D, Beltrami AP, Giacca M, Emanuelli C, Madeddu P. Intravenous gene therapy with pim-1 via a cardiotropic viral vector halts the progression of diabetic cardiomyopathy through promotion of prosurvival signaling. *Circ Res*.108:1238-1251
218. Meloni M, Descamps B, Caporali A, Zentilin L, Floris I, Giacca M, Emanuelli C. Nerve growth factor gene therapy using adeno-associated viral vectors prevents cardiomyopathy in type 1 diabetic mice. *Diabetes*.61:229-240
219. Yaniz-Galende E, Chen J, Chemaly ER, Liang L, Hulot JS, McCollum L, Arias T, Fuster V, Zsebo K, Hajjar RJ. Stem cell factor gene transfer promotes cardiac repair after myocardial infarction via in situ recruitment and expansion of c-kit+ cells. *Circ Res*.
220. Kajstura J, Gurusamy N, Ogorek B, Goichberg P, Clavo-Rondon C, Hosoda T, D'Amario D, Bardelli S, Beltrami AP, Cesselli D, Bussani R, del Monte F, Quaini F, Rota M, Beltrami CA, Buchholz BA, Leri A, Anversa P. Myocyte turnover in the aging human heart. *Circ Res*.107:1374-1386

-
221. Stamm C, Westphal B, Kleine HD, Petzsch M, Kittner C, Klinge H, Schumichen C, Nienaber CA, Freund M, Steinhoff G. Autologous bone-marrow stem-cell transplantation for myocardial regeneration. *Lancet*. 2003;361:45-46
 222. Ratajczak MZ, Kucia M, Reza R, Majka M, Janowska-Wieczorek A, Ratajczak J. Stem cell plasticity revisited: Cxcr4-positive cells expressing mrna for early muscle, liver and neural cells 'hide out' in the bone marrow. *Leukemia*. 2004;18:29-40
 223. Fukuda K, Yuasa S. Stem cells as a source of regenerative cardiomyocytes. *Circ Res*. 2006;98:1002-1013
 224. Lee KY, Mooney DJ. Hydrogels for tissue engineering. *Chemical reviews*. 2001;101:1869-1879
 225. Nguyen MK, Lee DS. Injectable biodegradable hydrogels. *Macromolecular bioscience*. 2010;10:563-579
 226. Yu L, Ding J. Injectable hydrogels as unique biomedical materials. *Chemical Society reviews*. 2008;37:1473-1481
 227. Huang NF, Yu J, Sievers R, Li S, Lee RJ. Injectable biopolymers enhance angiogenesis after myocardial infarction. *Tissue engineering*. 2005;11:1860-1866
 228. Shapira K, Dikovsky D, Habib M, Gepstein L, Seliktar D. Hydrogels for cardiac tissue regeneration. *Bio-medical materials and engineering*. 2008;18:309-314
 229. Christman KL, Fok HH, Sievers RE, Fang Q, Lee RJ. Fibrin glue alone and skeletal myoblasts in a fibrin scaffold preserve cardiac function after myocardial infarction. *Tissue engineering*. 2004;10:403-409
 230. Christman KL, Vardanian AJ, Fang Q, Sievers RE, Fok HH, Lee RJ. Injectable fibrin scaffold improves cell transplant survival, reduces infarct expansion, and induces neovasculature formation in ischemic myocardium. *Journal of the American College of Cardiology*. 2004;44:654-660
 231. Mukherjee R, Zavadzka JA, Saunders SM, McLean JE, Jeffords LB, Beck C, Stroud RE, Leone AM, Koval CN, Rivers WT, Basu S, Sheehy A, Michal G, Spinale FG. Targeted myocardial microinjections of a biocomposite material reduces infarct expansion in pigs. *The Annals of thoracic surgery*. 2008;86:1268-1276
 232. Kim IY, Seo SJ, Moon HS, Yoo MK, Park IY, Kim BC, Cho CS. Chitosan and its derivatives for tissue engineering applications. *Biotechnology advances*. 2008;26:1-21
 233. Lu WN, Lu SH, Wang HB, Li DX, Duan CM, Liu ZQ, Hao T, He WJ, Xu B, Fu Q, Song YC, Xie XH, Wang CY. Functional improvement of infarcted heart by co-injection of embryonic stem cells with temperature-responsive chitosan hydrogel. *Tissue engineering. Part A*. 2009;15:1437-1447

-
234. Muller-Ehmsen J, Kedes LH, Schwinger RH, Kloner RA. Cellular cardiomyoplasty--a novel approach to treat heart disease. *Congestive heart failure*. 2002;8:220-227
235. Iwakura A, Fujita M, Kataoka K, Tambara K, Sakakibara Y, Komeda M, Tabata Y. Intramyocardial sustained delivery of basic fibroblast growth factor improves angiogenesis and ventricular function in a rat infarct model. *Heart and vessels*. 2003;18:93-99
236. Liu Y, Sun L, Huan Y, Zhao H, Deng J. Effects of basic fibroblast growth factor microspheres on angiogenesis in ischemic myocardium and cardiac function: Analysis with dobutamine cardiovascular magnetic resonance tagging. *European journal of cardio-thoracic surgery : official journal of the European Association for Cardio-thoracic Surgery*. 2006;30:103-107
237. Bull DA, Bailey SH, Rentz JJ, Zebrack JS, Lee M, Litwin SE, Kim SW. Effect of terplex/vegf-165 gene therapy on left ventricular function and structure following myocardial infarction. Vegf gene therapy for myocardial infarction. *Journal of controlled release : official journal of the Controlled Release Society*. 2003;93:175-181
238. Heilmann CA, Attmann T, von Samson P, Gobel H, Marme D, Beyersdorf F, Lutter G. Transmyocardial laser revascularization combined with vascular endothelial growth factor 121 (vegf121) gene therapy for chronic myocardial ischemia--do the effects really add up? *European journal of cardio-thoracic surgery : official journal of the European Association for Cardio-thoracic Surgery*. 2003;23:74-80
239. Hao X, Mansson-Broberg A, Grinnemo KH, Siddiqui AJ, Dellgren G, Brodin LA, Sylven C. Myocardial angiogenesis after plasmid or adenoviral vegf-a(165) gene transfer in rat myocardial infarction model. *Cardiovascular research*. 2007;73:481-487
240. Renault MA, Losordo DW. Therapeutic myocardial angiogenesis. *Microvascular research*. 2007;74:159-171
241. Hughes C, Galea-Lauri J, Farzaneh F, Darling D. Streptavidin paramagnetic particles provide a choice of three affinity-based capture and magnetic concentration strategies for retroviral vectors. *Molecular therapy : the journal of the American Society of Gene Therapy*. 2001;3:623-630
242. Luo D, Saltzman WM. Enhancement of transfection by physical concentration of DNA at the cell surface. *Nature biotechnology*. 2000;18:893-895
243. Dai W, Wold LE, Dow JS, Kloner RA. Thickening of the infarcted wall by collagen injection improves left ventricular function in rats: A novel approach to preserve

cardiac function after myocardial infarction. *Journal of the American College of Cardiology*. 2005;46:714-719

Acknowledgements

This work was carried out in the research laboratories for cardiac tissue and organ replacement (Forschungslaboratorien für kardialen Gewebe- und Organersatz, FKGO) which was integrated into the Reference- and Translation Center for Cardiac Stem Cell Therapy (RTC), Department of Cardiac Surgery, University of Rostock, Germany, in 2009.

I appreciated Prof. Dr. Gustav Steinhoff (Director of the Department of Cardiac Surgery, University of Rostock) for his scientific supervision, crucial support, instructive advice and suggestions. I express my grateful acknowledgement to Prof. Dr. Jan Gimsa (Institute of Biosciences, University of Rostock) and Prof. Dr. Robert David (Faculty of Medicine, University of Rostock) for their co-supervision of this work. I am deeply indebted to my supervisors PD Dr. Nan Ma and Dr. Wenzhong Li (group leaders at FKGO).

I would like to extend my sincere gratitude to my previous and current colleagues: Prof. Dr. Lailiang Ou, Prof. Dr. Jun Li, Dr. Cornelia A. Lux, Dr. Koji Hirano, Dr. Dario Furlani, Dr. Ralf Gäbel, Dr. Weiwei Wang, Mr. Peter Mark, Ms. Evgenya Delyagina, Ms. Anna Schade, Mr. Erik Pittermann, Ms. Anna Skorska, Ms. Marion Ludwig and Ms. Margit Fritsche. Thanks to all of them for creating such a comfortable learning/working atmosphere in which everybody profits from the scientific discussion, efficient cooperation and warm-hearted assists.

High tribute shall be paid to Prof. Dr. Andreas Liebold, Dr. Alexander Kaminski, Dr. Peter Donndorf, Dr. Christian Klopsch, Dr. Gudrun Tiedemann, Ms. Jana Gabriel, Ms. Katrin Höfer, Ms. Jana Große, and Ms. Anke Wagner. They provided enormous help to my work and study.

The progress of this work is indispensably based on the collaboration with various other research institutes and scientists, including the Institute for Experimental Surgery, University of Rostock, Rostock, Germany. (Prof. Dr. Brigitte Vollmar), Institute of Polymer Research, GKSS Research Center, Teltow, Germany (Prof. Dr. Andreas Lendlein, Dr. Karola Lützow), and Key Laboratory of Bioactive Materials, Ministry of Education, College of Life Sciences, Nankai University, Tianjin, China (Prof. Dr. Deling Kong). I greatly acknowledge their collaboration and support.

My special thanks go to my family members. I would like to thank my parents for their encouragement. I owe a great deal of my accomplishments to my wife Mrs. Yajie Wang. Her selfless love, endless support, and meticulous care encourage me to move forward and make progress in my life.

List of publications and oral presentations

Publications

Y Zhang, W Li, L Ou, W Wang, E Delyagina, C A Lux, H Sorg, K Riehemann, G Steinhoff, N Ma. Targeted delivery of human VEGF gene via complexes of magnetic nanoparticle-adenoviral vectors enhanced cardiac regeneration. *PLoS One*. 2012; 7: e39490: 1-14.

L Ou, W Li, **Y Zhang**, W Wang, J Liu, H Sorg, D Furlani, R Gäbel, P Mark, C Klopsch, L Wang, K Lützow, A Lendlein, K Wagner, D Klee, A Liebold, R Li, D Kong, G Steinhoff, N Ma. Intracardiac injection of matrigel induces stem cell recruitment and improves cardiac functions in rat MI model. *J Cell Mol Med*. 2011; 15: 1310-1318. (Co-first author)

L Ou, W Li, Y Liu, **Y Zhang**, S Jie, D Kong, G Steinhoff, N Ma. Animal model cardiac diseases and stem cell therapy. *Open Cardiovasc Med J*. 2010; 26: 231-239. (Co-first author)

E Delyagina, N Ma, Weiwei Wang, **Y Zhang**, A Kuhlo, E Flick, H Gatzen, G Steinhoff, W Li. Magnetically guided transfection in suspension cells with PEI 25kDa conjugated to magnetic nanoparticles. *Biomed tech*. 2010 55: S37-39.

E Delyagina, N Ma, Weiwei Wang, **Y Zhang**, A Kuhlo, E Flick, H Gatzen, F Zhang, E Brukel, G Steinhoff, W Li. Titanium dioxide-mediated polyethylenimine for gene delivery. *Biomed tech*. 2010 55: S40-41.

E Delyagina, N Ma, Weiwei Wang, **Y Zhang**, A Kuhlo, E Flick, H Gatzen, G Steinhoff, W Li. PEI 600 Da conjugated to magnetic nanobeads as a non-viral vector for gene delivery. *Biomed tech*. 2010 55: S116-117.

Oral presentations

Y Zhang, N.Ma, W Li, G Steinhoff. Oral presentation “Gene Targeting with magnetic nanoparticles for cardiac regeneration”. European Society for Artificial Organs Congress (ESAO) *the 38th Annual Meeting*. October, 2012. Rostock, Germany.

Y Zhang, W Li, G Steinhoff, N.Ma. Oral presentation “*In vitro* & *in vivo* gene combined with MNBs for heart regeneration”. European Society of Cardiology Congress (ESC) *the 59th Annual Meeting*. August, 2011. Paris, France.

Y Zhang, N Ma, W Li, G Steinhoff. Oral presentation “VEGF gene combined nanoparticles for heart regeneration”. German Society Thoracic and Cardiovascular Surgery (GTS) *the 40th Annual Meeting*. February, 2010. Stuttgart, Germany.

Selbständigkeitserklärung

Ich versichere hiermit, dass ich die vorliegende Arbeit mit dem Thema: *“Development and evaluation of biotechnological techniques for myocardial angiogenesis and functional recovery”* („Entwicklung und Evaluation von biotechnologischen Techniken für myokardiale Angiogenese und funktionale Genesung“) selbstständig verfasst und keine anderen Hilfsmittel als die angegebenen benutzt habe. Die Stellen, die anderen Werken dem Wortlaut oder dem Sinn nach entnommen sind, habe ich in jedem einzelnen Fall durch Angabe der Quelle kenntlich gemacht. Ich erkläre hiermit weiterhin, dass ich meine wissenschaftlichen Arbeiten nach den Prinzipien der guten wissenschaftlichen Praxis gemäß der gültigen *“Satzungen der Universität Rostock zur Sicherung guter wissenschaftlicher Praxis”* angefertigt habe.

Rostock, den _____

(Unterschrift)